Evaluating remote sensing covariates for understanding habitat selection by boreal forest birds

by

Brendan Casey

A thesis submitted in partial fulfillment of the requirements for the degree of

Doctor of Philosophy

in

Ecology

Department of Biological Sciences
University of Alberta

Abstract

Boreal forests are changing in response to climate change and shifts in disturbance regimes. Statistical models that link distribution, abundance, and community structure to select environmental variables have been used to understand how birds respond to these changes. However, model performance is influenced by the choice of spatial covariates. Remote sensing, like Light Detection and Ranging (LiDAR), and satellite photogrammetry, can improve bird-habitat models by introducing novel biologically relevant spatial covariates at fine resolutions. This thesis presents methods to use and evaluate modern remote sensing tools to refine our understanding of species-habitat relationships. It also explores how bird communities respond to forest harvesting in the boreal. First, LiDAR can improve bird-habitat models by providing novel vegetation structure covariates. However, temporal misalignment between LiDAR acquisitions and point count surveys may influence the predictive power of models that use LiDAR predictor variables. As vegetation undergoes successional changes, LiDAR data that is temporally restricted may cease to reflect habitat conditions, thus compromising the usefulness of LiDAR predictor variables. To evaluate this, I examined how the time-lag between LiDAR acquisitions and bird surveys influenced model robustness for early-successional, mature-forest, and forest generalist birds. The results indicated that for species occupying older, more stable forests, a time difference of up to 15 years has a negligible impact on the predictive power of LiDAR based bird-habitat models. For early-successional birds, the findings suggest that a time difference of

5-13 years between LIDAR and bird data may decrease model performance. Next, I compared the suitability of covariates from LiDAR, a Landsat time series, and forest resource inventories for predicting bird response to forest harvesting in Alberta. These covariates were used to predict the abundance of twenty species associated with different foraging and nesting strata, within harvest areas across a chronosequence of recovery. The results suggest that integrating LiDAR and Landsat spectral change covariates improves model performance over models built using forest resource inventory data alone. Additionally, spectral estimates of harvest intensity and time since disturbance explained most of the variation in species abundance models. Finally, I used a spectral change detection algorithm, point count data, acoustic monitoring tools, and mixed-effects regression models to evaluate the impact of the interaction between forest harvest intensity and recovery time on the taxonomic and functional diversity of birds. The findings suggest that harvest residuals can mitigate the short-term effects of forest harvesting on bird communities. Furthermore, I demonstrate that metrics derived from a time-series of Normalized Burn Ratio (NBR) are a promising alternative to conventional categorical harvest intensity metrics included in many classified land cover maps. Collectively, this work shows that supplementing classified land cover data with LiDAR and Landsat time-series data can improve the performance of bird-habitat models while avoiding the costs of ground-based habitat surveys.

Preface

This thesis is an original work by Brendan Casey. No part of this thesis has been previously published. In chapters two through four, the contributions of my supervisor, Dr. Erin Bayne, are recognized through the use of plural pronouns. The organizations and individuals who contributed to this thesis by offering data or code are acknowledged in text or in the Acknowledgements section of this thesis.

Chapters two through four of this thesis are currently being prepared for submission to academic journals.

To Rónán and Brynn.

Acknowledgements

Thank you to my supervisor, Dr. Erin Bayne, for taking me on as a graduate student and giving me the opportunity to shift my career path. Your expertise, feedback, and support have been instrumental in shaping the direction and quality of my work. I am also grateful to the members of my doctoral committee, Dr. Greg McDermid and Dr. Jahan Kariyeva, for their valuable insights and contributions.

Thank you to the agencies and organizations that financially supported my research including the Boreal Avian Modelling (BAM) Project (borealbirds.ca), the National Science and Engineering Research Council of Canada, the University of Alberta, the Alberta Conservation Association, the UAlberta North program, and the Computational Biodiversity Science and Services ($BIOS^2$) training program. This research was also part of the Boreal Ecosystem Recovery and Assessment (BERA) project (www.bera-project.org), and was supported by a Natural Sciences and Engineering Research Council of Canada Alliance Grant (ALLRP 548285 - 19) in conjunction with Alberta-Pacific Forest Industries, Alberta Biodiversity Monitoring Institute, Canadian Natural Resources Ltd., Cenovus Energy, ConocoPhillips Canada, Imperial Oil Ltd., and Natural Resources Canada.

Thank you to all who have contributed to this thesis by sharing code, data, and expertise. Special thanks to Jennifer Hird for sharing her workflow and code for deriving NBR spectral change metrics, Chris Bater for assisting with LiDAR data, and Andrew Crosby for helping me conceptualize this research. I would also like

to thank Alex MacPhail, Natasha Annich, Cesar Estevo, Carrie Ann Adams, Justin Johnson, Jeremiah Kennedy, and all the project leads, graduate students, and field technicians from the Bioacoustic Unit who helped collect and process bird data.

Finally, thank you Brynn Bellingham and Rónán Casey for your love and support. I could not have accomplished this without you.

Contents

List of Tables

List of Figures

List of Abbreviations

AIC . . . . . Akaike's Information Criterion (AIC)

ANOVA . . . . analysis of variance

AUC . . . . . area under the receiver operating curve (ROC)

CAS-FRI . . . Common Attribute Schema for Forest Resource Inventories.

FDis . . . . . functional dispersion

FDiv . . . . . functional divergence

FEve . . . . . functional evenness

FRI . . . . . Forest resource inventory

FRic . . . . . functional richness

GEE . . . . . Google Earth Engine

GOA . . . . . Provincial government of Alberta

LandTrendr . Landsat-based detection of Trends in Disturbance and Recovery

LiDAR . . . . Light Detection and Ranging

NBR . . . . . Normalized Burn Ratio

rNBR . . . . . Relative Normalized Burn Ratio.

NDVI . . . . . Normalized Difference Vegetation Index

r . . . . . Pearson's correlation coefficients

$R^2\mathbf{c}$ . . . . . conditional R^2

$R^2\mathbf{m}$ . . . . . marginal R^2

sdm . . . . . species distribution model

1 Introduction

1.1 Disturbances in the boreal

Canada's boreal landscape is a dynamic successional mosaic driven by fire, insect disturbances, disease outbreaks, forestry, and oil and gas development (Brandt et al., 2013). Disturbance driven changes to the structural and functional elements of forests can affect the distribution and composition of bird populations (Leston et al., 2023; Norton & Hannon, 1997; Schmiegelow et al., 1997; Venier et al., 2014).

Birds play an important role in the functioning of boreal forest ecosystems (Niemi et al., 1998). In Canada's boreal forests, birds account for approximately 70% to 80% of terrestrial vertebrates, encompassing nearly 400 species (Blancher & Wells, 2005; Niemi et al., 1998). Predation by birds drive small-mammal population dynamics (Hanski et al., 2001), dampen spruce budworm (*Choristoneura fumiferana*) outbreaks (Crawford & Jennings, 1989; Venier et al., 2009), and may increase forest productivity by reducing the abundance of defoliating insects (Marquis & Whelan, 1994). Birds also play an important role in seed dispersal and nutrient cycling (Arnberg et al., 2023;

Lanner, 1996; Niemi et al., 1998). Given the strong links between birds and forest conditions, birds are often used as indicator species in sustainable forest management (Furness & Greenwood, 2013; Venier & Pearce, 2007)

Forestry practices change bird habitat by altering the structure, composition, spatial pattern, and age distribution of forests (Hobson & Schieck, 1999; Kuuluvainen & Gauthier, 2018; Schieck & Song, 2006; Venier et al., 2014). These changes directly affect the availability of food, shelter, and nesting resources for birds. Given species-specific habitat preferences, changes to habitat structure caused by natural and anthropogenic disturbances can alter the composition of bird communities. Understanding species-habitat relationships is critical for predicting how communities will respond to these changes and for effective conservation efforts (Lindermayer & Franklin, 2002; Niemi et al., 1998; Paillet et al., 2009).

1.2 Bird-habitat models

Ecologists use statistical models to estimate species abundance and distribution and to quantify community responses to environmental change (Fox et al., 2015). Many link wildlife observations (e.g. detections from point counts or bioacoustic monitoring) to environmental predictor variables (Carrillo-Rubio et al., 2014; Engler et al., 2017; Guisan & Zimmermann, 2000; He et al., 2015). Referred to as species distribution models (SDMs), this family of statistical methods combines wildlife and habitat data to infer species-habitat relationships and predict species' distributions along environmental gradients (Engler et al., 2017; Guisan & Thuiller, 2005). With advancements in modelling methods, computational power, and environmental monitoring, SDMs continue to be an important tool in ecology, conservation biology, and wildlife management (Elith & Leathwick, 2009). See reviews by Engler et al. (2017), Elith et al.

(2009), Araújo et al. (2019), and Guisan and Thuiller (2005).

SDMs are used for both explanatory and predictive modelling (Ferrier et al., 2017). Explanatory models test casual relationships between response variables (e.g. occupancy or abundance) and biologically relevant explanatory variables (Shmueli, 2010). In contrast, predictive models assume established relationships between variables and generate response values for unobserved locations, allowing for the prediction of species distributions and the creation of habitat suitability maps (Franklin, 2010b; Guisan & Thuiller, 2005). Both types of models are useful for addressing a range of ecological questions, exploring the patterns and processes that drive spatial distributions, and can inform conservation management planning. Applications include dispersal, abundance, and disturbance modelling, biodiversity assessment, global change modelling, invasive species management, identifying critical habitat, and environmental impact assessment (Araújo et al., 2019; Carrillo-Rubio et al., 2014; Franklin, 2010a; Guisan et al., 2013; Guisan & Thuiller, 2005; Randin et al., 2020).

SDMs encompass a variety of statistical approaches, including generalized linear models (Ferrier et al., 2002), resource selection functions (Boyce et al., 2002), generalized additive models (GAMs) (Brodie et al., 2020), and Bayesian models (Golding & Purse, 2016). With the increasing emphasis on predictive modelling, machine learning techniques have been applied to SDMs, such as boosted regression trees (Elith et al., 2008) and maximum entropy (Maxent) algorithms (Elith & Leathwick, 2009; Li & Wang, 2013; Phillips & Dudík, 2008). These models often use species detection data from traditional human point counts or autonomous bioacoustic monitoring as response variables (Campos-Cerqueira & Aide, 2016; Dorazio, 2014; Guisan & Thuiller, 2005), and predictors from remote sensing, classified land cover maps, or field data. The modelled relationships can be used to map predicted species distributions and

forecast distributions under different ecological scenarios (Araújo et al., 2019).

1.2.1 Predictor variables

To function, SDMs require biologically meaningful spatial covariates, often over large spatial extents, that match the scales at which ecological processes influence species (Cumming et al., 2010b; Guisan & Thuiller, 2005; Manly et al., 2002; Tattoni et al., 2012). The choice and scale of predictors play a crucial role in model performance (Fourcade et al., 2018; Franklin, 1995; Regos et al., 2019; Syphard & Franklin, 2009; Vaughn & Ormerod, 2003).

Predictor variables used in avian SDMs can exert direct or indirect effects on species and can be classified into six primary categories (Austin, 2007; Franklin, 2010a; Mackey & Lindenmayer, 2001): (1) climate variables, such as temperature, precipitation, and soil moisture (Ralston & Kirchman, 2013; Stralberg et al., 2015; Virkkala & Lehikoinen, 2014); (2) topographic variables, including elevation, slope, and topographic position (Bale et al., 2020; Franklin, 2010a; Skidmore, 1990); (3) land cover variables showing habitat type and dominant vegetation species (Büttner, 2014; Seoane et al., 2004); (4) disturbance variables indicating the type, extent, and timing of both natural and anthropogenic disturbance (Meurant, 2012); (5) vegetation structure, including vertical heterogeneity, height, cover, and density (Davies & Asner, 2014; MacArthur & MacArthur, 1961); and (6) the spatial arrangement of landscape attributes represented by proximity, complexity, and geometry metrics (Kosicki, 2018; Pearson, 1993; Vernier et al., 2002).

Many predictor variables are included in classified land cover maps, digital forest resource inventories (FRIs), digital elevation models, and interpolated climate surfaces, or gathered via direct field measurements done during wildlife surveys (Alberta

Biodiversity Monitoring Institute and Alberta Human Footprint Monitoring Program, 2019; Cosco, 2011; MacArthur & MacArthur, 1961). However, each data source has inherent limitations. For example, classified land cover maps and forest resource inventories can be temporally limited and require specialized to skills to produce. And while field measurements provide valuable data, the data is usually spatially limited and can be costly and time-consuming to collect. Some of these limitations can affect the performance of SDMs, like when predictors have coarse or limited spatiotemporal resolutions, reducing the transferability of models in space and time (Connor et al., 2018; Randin et al., 2020). Lack of transferability is often the result of misalignment between the resolution and extent of predictor and response variables (Guisan & Thuiller, 2005).

1.3 Remote sensing

Data availability can limit the choice of predictor variables in models, and the variables that are used may not capture the full range of habitat conditions that influence avian species. Avian SDMs often rely on coarse environmental covariates derived from digital maps–e.g. land cover maps and digital forest resource inventories (FRIs). These products may contain detailed information on plant species composition, disturbance history, and canopy height; and the models that use these data can make accurate broad, landscape scale predictions (Cumming et al., 2010a). However, birds respond to structural complexity and successional change, measures of which are often missing from these datasets. The inclusion of habitat structure and successional metrics, alongside habitat attributes that align with the spatiotemporal resolutions of response variables, should improve model performance (Bayne et al., 2010; Tattoni et al., 2012).

Using predictors sourced directly from remote sensing, particularly light detection

and ranging (LiDAR) and satellite imagery, can improve the capabilities of SDMs and the scale at which they operate (Elith & Leathwick, 2009). Geographic Information Systems (GIS), open-source data processing tools, and multi-petabyte geospatial catalogs have provided access to alternative sources of spatial data and new methods of analysis (Gorelick et al., 2017; Hijmans, 2021; Pebesma, 2020; Shirley et al., 2013). LiDAR can characterize three-dimensional vegetation structure (Bae et al., 2018; Davies & Asner, 2014; Kortmann et al., 2018; Lefsky et al., 2002; Renner et al., 2018), ground topography (Fritz et al., 2018; Schaffer-Smith et al., 2018), and terrain wetness (White et al., 2012). Spectral indices derived from satellite and aerial imagery can map land cover change and measure rates of post-disturbance habitat recovery (Northrup et al., 2019; Rittenhouse et al., 2010). As model covariates, such metrics can improve the capabilities of avian SDMs and overcome limitations associated with classified land cover products (Davies & Asner, 2014; Lefsky et al., 2002; Zellweger et al., 2014). Unfortunately, few have compared the value of different remote sensing predictor variables in SDMs, or assessed their differential predictive power across species.

1.3.1 LiDAR

Traditionally, vegetation structural metrics are obtained through ground-based field measurements (MacArthur & MacArthur, 1961). Field measurements are typically limited to discrete sampling regimes over relatively narrow spatial extents (Bergen et al., 2009). While valuable for explaining variation in sampled areas, such an approach has limited value in predicting where birds will or will not be in unsampled areas. Methods that directly measure the three-dimensional distribution of canopy and subcanopy structures at varying scales can dramatically increase the predictive accuracy of avian SDMs (Zellweger et al., 2014) and address limitations inherent in SDMs that only use horizontal land cover variables (Davies & Asner, 2014; Lefsky et al., 2002).

1. Introduction

Airborne LiDAR gathers structural information by measuring the elevation of surface topography and vegetation. A sensor attached to a plane or UAV repeatedly fires laser pulses towards the Earth's surface recording the echoes reflected from branches, dead woody debris, and foliage (for overviews of the LiDAR techniques used for collecting habitat structural data, see Van Leeuwen & Nieuwenhuis (2010) and Vierling et al. (2008)). The height and frequency of returned echoes can generate metrics associated with avian habitat, including those related to plant species composition (Ackers et al., 2015; Zielewska-Buettner et al., 2018), ground topography (Fritz et al., 2018; Schaffer-Smith et al., 2018), terrain wetness (White et al., 2012), and vegetation structure (Bae et al., 2018; Kortmann et al., 2018; Renner et al., 2018). Many of these variables relate to habitat structural properties selected by birds.

LiDAR is increasingly being used to characterize three-dimensional forest structures in wildlife habitat studies (Davies & Asner, 2014; Lim et al., 2003). Used as predictor variables, LiDAR metrics can improve the performance of avian SDMs (Bae et al., 2014; Clawges et al., 2008; Farrell et al., 2013; Ficetola et al., 2014). LiDAR has been used to model single species (Barnes et al., 2016; Goetz et al., 2010; Holbrook et al., 2015; Vogeler et al., 2013), guilds (Vogeler et al., 2014; Weisberg et al., 2014), and communities (Clawges et al., 2008; Lesak et al., 2011; Sheeren et al., 2014) across a range of forested habitats including boreal (Lindberg et al., 2015), montane (Müller et al., 2009), and temperate (Martinuzzi et al., 2009) forests. Though a full suite of LiDAR-derived metrics is available (Hall et al. (2005) used 39 metrics) most studies use a subset. Commonly used metrics correspond to the following categories: vegetation height, cover, structural complexity, and density of forest strata (Bae et al., 2018; Davies & Asner, 2014; Kortmann et al., 2018; Lefsky et al., 2002; Renner et al., 2018). Canopy height is a strong univariate predictor of species richness (Culbert et al., 2013;

Goetz et al., 2007), abundance (Müller et al., 2009), chick mass (Bradbury et al., 2005) and habitat selection (Seavy et al., 2009). Canopy cover can alter conditions of lower forest strata, influencing occupancy and nest selection (García-Feced et al., 2011; Swatantran et al., 2012; Vogeler et al., 2013). The relationship between structural diversity and bird communities is long established (MacArthur & MacArthur, 1961), and LiDAR measures of structural heterogeneity have been used to predict avian diversity in localized areas (Clawges et al., 2008; Goetz et al., 2007).

Despite the strong performance of LIDAR-based SDMs, LiDAR has not been fully adopted in avian ecology. Most studies continue to rely on conventional land cover products, and those that use LiDAR tend to be spatially and temporally limited. Few studies have used LiDAR to examine the effects of anthropogenic disturbances on birds. Given the cost associated with LiDAR data acquisition, it is important to know when to choose LiDAR over cheaper, more accessible products, and how much temporal misalignment between LiDAR acquisitions and bird surveys is acceptable (Wulder et al., 2012).

1.3.2 Spectral indices

Predictors from classified land cover maps can be supplemented with spectral reflectance data from space-based optical remote sensors to improve model performance (He et al., 2015). Satellites such as Landsat and Sentinel offer imagery that can be used to calculate both novel habitat metrics and ones similar to those found in classified land cover maps, but with greater temporal and spatial resolutions. For example, the normalized difference vegetation index (NDVI), a spectral measure of vegetation productivity, can indicate food availability, habitat variability, and changes in vegetation phenology (Kerr & Ostrovsky, 2003; Pettorelli et al., 2011). Studies have used NDVI to predict bird species richness, abundance, and migration timing (Bailey

et al., 2004; Evans et al., 2006, 2008; McKinnon et al., 2015; Nieto et al., 2015). Also, time series of the normalized burn ratio (NBR) have been used to measure the magnitude of spectral change between pre- and post-disturbance forest stands and estimate rates of successional recovery(Hislop et al., 2018). NBR spectral change metrics have been used to examine the relationship between fire severity and avian occupancy patterns (Rose et al., 2016). NBR spectral change metrics are a promising alternative to conventional categorical disturbance intensity metrics found in forest resource inventories and have the potential to uncover more nuanced relationships between forestry practices and bird communities.

1.4 Thesis objectives

For this thesis, I used remote sensing, point count databases, and bioacoustic tools to examine the response of bird communities to human-driven environmental changes in boreal forests. The research described had two overarching objectives: (1) Use, evaluate and compare the suitability of LiDAR, Landsat, and classified habitat data from forest resource inventories (FRIs) and land cover maps for modelling species-habitat relationships in boreal forests. (2) Evaluate the impacts of different retention regimes on boreal bird communities over a successional gradient. Over three chapters, this thesis presents various methods to use and evaluate modern remote sensing tools to refine our understanding of species-habitat relationships, and explores how bird communities respond to forestry in the boreal.

In Chapter 2, I evaluated the influence of temporal misalignment between LiDAR acquisitions and bird surveys on model robustness for early-successional, mature-forest, and forest generalist birds across a gradient of 0 to 15 years misalignment. I also assessed how differences in resultant predictive distribution maps correlate with forest

age. The primary aim of Chapter 3 was to identify variables that best predicted the post-harvest abundance of twenty bird species associated with different foraging and nesting strata. Towards this, I compared the predictive power of three sources of variables characterizing harvested forest areas: classified land cover data from forest resource inventories, airborne LiDAR, and a time series of optical satellite data. In Chapter 4, I investigated the long-term effects of retention forestry on bird communities. An annual time series of NBR was used to assess the intensity and recovery of forest harvests. NBR change metrics were then used to predict the taxonomic and functional diversity of birds within harvested areas. Finally, Chapter 5 serves as a synthesis of the findings from the preceding chapters. It explores the implications of these findings for bird research and wildlife management practices, discusses the potential of remote sensing in species habitat modelling, and outlines avenues for future research.

2

The influence of time-lag between LiDAR and wildlife survey data on species distribution models

2.1 Introduction

The composition and structure of forests are changing in response to climate change, shifts to natural disturbance regimes, and increasing industrial development (Brandt et al., 2013). Predictive models linking field observations to environmental variables can reveal how birds respond to these changes (Carrillo-Rubio et al., 2014; Engler et al., 2017; Guisan & Zimmermann, 2000; He et al., 2015). Broadly known as species distribution models (SDMs), this family of statistical methods predict bird distributions by comparing habitat where individuals were observed against habitat where they were absent (Guisan & Thuiller, 2005). SDMs and resulting predictive distribution maps are used to understand bird habitat preferences and the drivers of broad scale population declines and have applications in conservation management planning and environmental impact assessments (Engler et al., 2017; Franklin, 2010a).

2. The influence of LiDAR time-lag on SDMs

Many factors influence the predictive capacity of SDMs, but the inclusion of ecologically relevant spatial covariates are key drivers of model accuracy (Fourcade et al., 2018; Franklin, 1995; Vaughn & Ormerod, 2003). Bird SDMs often rely on categorical predictors derived from digital maps delineating land cover, vegetation composition, and human footprint. While useful, they often miss key forest features affecting habitat selection, namely those related to vegetation structure.

Vegetation structure influences the abundance, distribution, and behavior of birds (Davies & Asner, 2014; MacArthur & MacArthur, 1961). The height and density of vegetation influence where birds perch, feed, and reproduce (Bradbury et al., 2005) by mediating microclimates, providing shelter from weather (Carrascal & Diaz, 2006), concealment from predators (Gotmark et al., 1995), and creating habitat for insect prey (Halaj et al., 2000). Light Detection and Ranging (LiDAR) can characterize these three-dimensional forest structures (Lim et al., 2003). Common LiDAR derived metrics correspond with vegetation height, cover, structural complexity, and density of forest strata (Bae et al., 2018; Davies & Asner, 2014; Kortmann et al., 2018; Lefsky et al., 2002; Renner et al., 2018). Used as predictor variables, LiDAR metrics can improve the predictive power of bird SDMs (Bae et al., 2014; Clawges et al., 2008; Farrell et al., 2013; Ficetola et al., 2014).

Publicly funded regional LIDAR data and space-based sensors like NASA's Ice, Cloud and Land Elevation Satellite-2 (ICESat-2) and Global Ecosystem Dynamics Investigation (GEDI), have made large amounts of wall-to-wall structural data available to researchers (Abdalati et al., 2010; Coops et al., 2016; Dubayah et al., 2020). However, LiDAR continues to be under-used in bird ecology. The limited temporal resolution of most LiDAR products may be a factor. LiDAR is often limited to a single season, with long multiyear gaps between repeat surveys. Temporal misalignment

between wildlife surveys and LiDAR is common (Babcock et al., 2016).

Temporal misalignment occurs when wildlife surveys and LiDAR acquisitions are done at different times (Babcock et al., 2016; Vierling et al., 2014). It is unclear how much temporal misalignment influences the performance of LiDAR based SDMs. Disturbance-succession cycles drive changes in vegetation structure, and eventually, LiDAR gathered in one year will no longer reflect ground conditions in another year. Temporal misalignment can occur when the surveyed forest transitions between stages of stand development (e.g. from stand initiation to stem exclusion) (Babcock et al., 2016; Brassard & Chen, 2010). Thus, temporal misalignment can impact the power of bird SDMs as successional changes in forest structure influence habitat selection by birds (Sitters et al., 2014).

Consider Alberta's boreal forests. It is a dynamic successional mosaic driven by forestry, fire, and energy exploration (Brandt et al., 2013; Gauthier et al., 2015). The landscape is a patchwork of early to late-successional stands with distinct structural characteristics (Bergeron & Fenton, 2012; Brassard & Chen, 2010) and bird communities (Schieck & Song, 2006). In early-successional forests, bird communities are dominated by species that nest and forage in open vegetation, wetlands, and shrubs, along with some habitat generalists. As trees regenerate and the stand's structural properties change, open habitat avian species give way to species associated with closed canopy forests that vary in underlying vertical structure over time (Leston et al., 2018; Schieck & Song, 2006).

Thus, succession occurring between LiDAR and wildlife surveys may influence SDM performance. Consequently, LiDAR's usefulness as a source of explanatory variables can degrade as temporal misalignment increases. For researchers pairing LiDAR covariates with long-term wildlife survey data, this can lead to a trade-off:

(1) minimize temporal misalignment by reducing the sample size to survey data gathered near the time of the LiDAR acquisition, or (2) maximize sample size and risk sacrificing model accuracy.

To inform this trade-off, we addressed the question of how much temporal misalignment is acceptable in LiDAR based SDMs. Our objectives were to (1) evaluate how temporal misalignment between LiDAR acquisitions and bird surveys influence the performance of SDMs across a gradient of 0 to 15 years, (2) compare the influence of temporal misalignment on models for early-successional, mid-successional, mature-forest, and forest generalist birds, and (3) assess how differences in resultant predictive distribution maps correlate with forest age.

The effects of temporal misalignment on SDMs will likely vary by habitat type (e.g. forest age, disturbance history, and dominant vegetation) and the life history characteristics of the study species. We predicted that the performance of SDMs will decrease with increased temporal misalignment and that the magnitude of change will vary according to the habitat associations of the focal species. We predicted that (1) SDMs for early-successional associates, Mourning Warbler (*Geothlypis philadelphia*) and White-throated Sparrow (*Zonotrichia albicollis*), would be most affected by temporal misalignment because of faster vertical growth rates of establishment trees and loss of dense shrub layers (Falls & Kopachena, 2020; McCarthy, 2001; Pitocchelli, 2020). (2) SDMs for mid-seral species like American Redstart (*Setophaga ruticilla*) that are associated with dense midstory vegetation, would see moderate declines in performance as temporal misalignment increases due to self-thinning during the stem exclusion stage of succession (Brassard & Chen, 2010; Sherry et al., 2020). And (3) mature forest associates, Black-throated Green Warbler (*Setophaga virens*), will be least effected by temporal misalignment as the processes effecting mature forest canopy structure

(insect defoliation and windthrow) happen at too small a scale to effect overall model performance (Morse & Poole, 2020; Vierling et al., 2014). For all species, we predicted that differences in distribution maps will be negatively correlated with forest age.

2.2 Methods

Our methodological workflow is illustrated in Figure 2.1. Analyses were done using R statistical software (R Core Team, 2020). We built SDMs using bird data from the Calling Lake Fragmentation project (Schmiegelow et al., 1997).

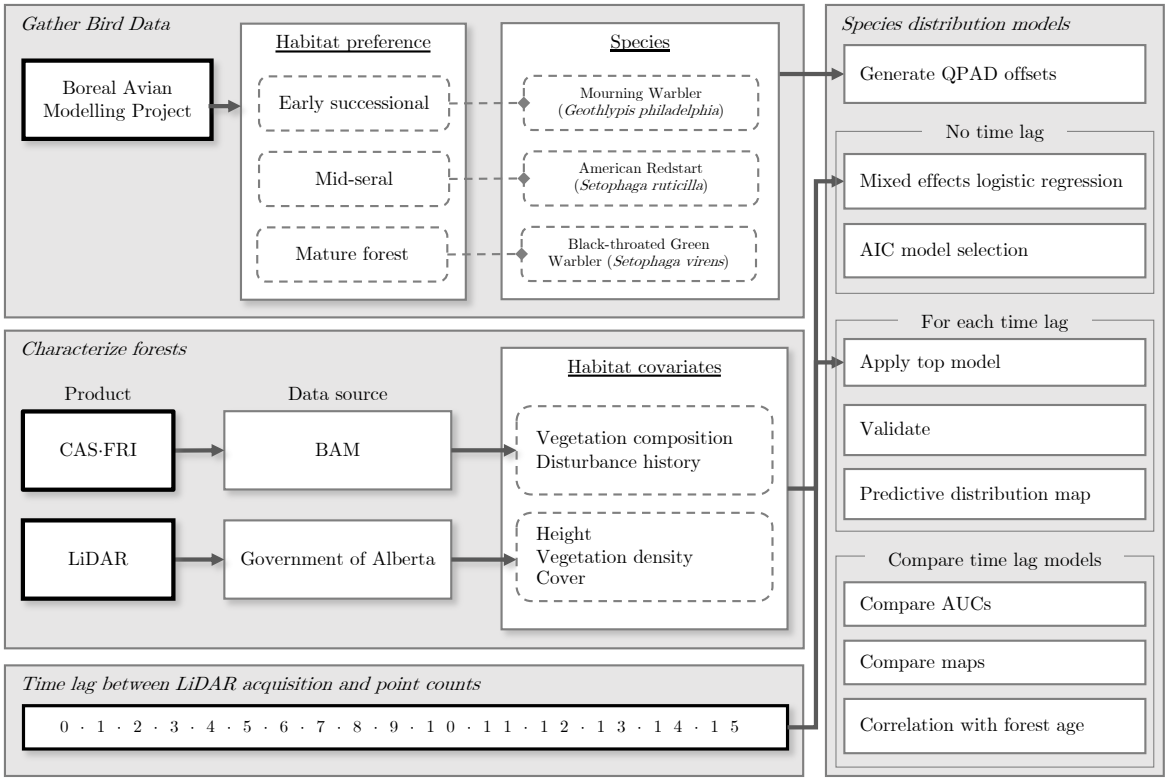

Figure 2.1: Conceptual diagram of our methodology. SDM methods were repeated at every time lag for each species. SDMs were compared using AUC and correlation between predictive maps.

2.2.1 Study area

We used bird survey data from the Calling Lake Fragmentation Experiment (Schmiegelow et al., 1997). Surveys were conducted across ≈ 14,000 ha of boreal mixedwood forests near Calling Lake, in northern Alberta, Canada (55°14′51″N 113°28′59″W) (Figure 2.2). The experiment was designed to study the long-term impacts of forest harvesting on birds (Hannon & Schmiegelow, 2002; Leston et al., 2018; Schmiegelow et al., 1997). The study's experimental harvest treatments have led to a landscape patchwork of early- to mid- successional stands surrounded by tracts of unharvested mature forests. When the experiment began in 1994, the landscape was dominated by older mixedwood forests composed of trembling aspen (*Populus tremuloides*), balsam poplar (*Populus balsamifera*), and white spruce (*Picea glauca*), and treed bogs containing black spruce (*Picea mariana*) and larch (*Larix laricina*). Understory vegetation in the mixedwood forests was composed mostly of alder (*Alnus* spp.) and willow species (*Salix* spp.).

2.2.2 Bird data

The Calling Lake Fragmentation Experiment included long term bird monitoring via annual repeated point counts. Point counts used in this study came from 20 consecutive breeding seasons (from 1995-2015). As the experiment's study area overlapped spatially with government wall-to-wall LiDAR coverage, there was an opportunity to study the impacts of temporal misalignment between point counts and LiDAR on bird SDMs.

We used detection data from 187 stations where consecutive annual point counts were conducted within sixteen years of the LiDAR acquisition date. Stations were spaced ≈ 200 m apart. At each station, three to five morning point count surveys were conducted over each breeding season (May 16 to July 7) between sunrise and 10:00 h. Observers recorded the species detected during each five minute point count

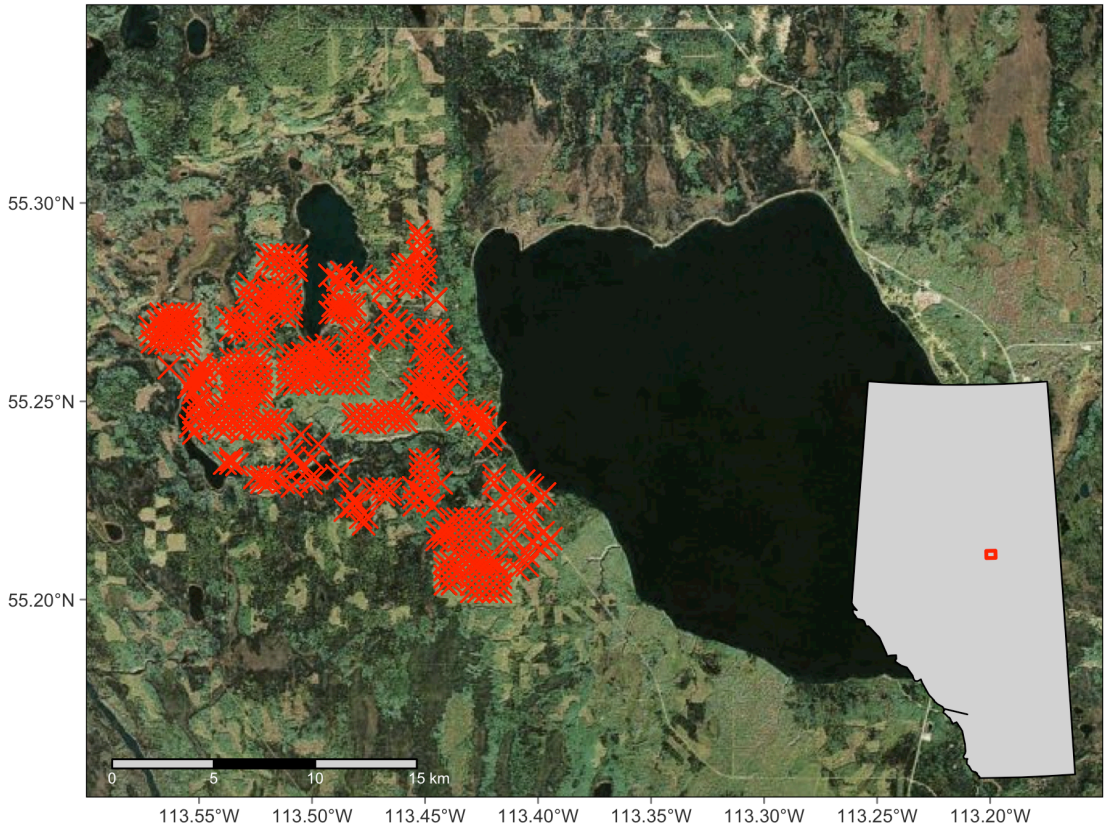

Figure 2.2: Locations of point count survey sites from the Calling Lake Fragmentation Study near Calling Lake, Alberta (Schmiegelow et al., 1997). Repeat point counts were conducted during the breeding seasons from 1993 and 2015.

interval within sampling radii of 50 and 100 m. See Schmiegelow et al. (1997) for further information on the Calling Lake Fragmentation Experiment's study design and point count protocols. To minimize the influence of forest edges on model predictions, we limited point count stations to those conducted within a single forest stand age (SD *<5 yrs* within a 100 m buffer of the station). We accessed point count data using the Boreal Avian Modelling Project's avian database; available on request from www.wildtrax.ca (Boreal Avian Modelling Project, 2018).

2. The influence of LiDAR time-lag on SDMs

We tested the effects of LiDAR temporal misalignment on six bird species common to the study area (detected in $\geq 10\%$ of all point count events) that were associated with different forest age classes: American Redstart, Black-throated Green Warbler, Mourning Warbler, Swainson's Thrush (*Catharus ustulatus*), White-throated Sparrow, and Winter Wren (*Troglodytes hiemalis*). The focal species showed low variability in the total number of detections each year across the 16 years modelled ($CV < 0.5$).

2.2.3 Predictor variables

Habitat covariates included LiDAR vegetation metrics provided by the Provincial Government of Alberta (GOA), forest stand attributes from the Common Attribute Schema for Forest Resource Inventories (CAS-FRI) (Cosco, 2011), and mean summer NDVI calculated from a time series of Landsat images (Survey, 2018) (Table 2.1).

Airborne LiDAR was gathered between 2008-2009 by Alberta Agriculture and Forestry, Government of Alberta. The data was part of a larger provincial broad scale LiDAR mapping effort. For an overview of the LiDAR specifications and collection protocols see Alberta Environment and Sustainable Resource Development (2013). The Government of Alberta provided us with 30m LiDAR raster layers representing vegetation height, cover, and density metrics. The rasters were calculated from point cloud data using FUSION software (McGaughey, 2018). For each raster, we calculated the mean pixel value within a 100 m radius of point count stations using the *raster* package in R (Hijmans, 2020).

Forest stand attributes were extracted from the Common Attribute Schema for Forest Resource Inventories (CAS-FRI). CAS-FRI is a standardized collection of 2 ha forest inventory geospatial data (Cosco, 2011). CAS-FRI stand attributes were interpreted using 1:10,000 to 1:40,000 aerial photography flown between 1987 and

Table 2.1: Spatial covariates included in the analysis.

Metric	Source	Description
elev_mean	LiDAR	Mean height
elev_maximum	LiDAR	Maximum height
elev_cv	LiDAR	Height coefficient of variation
canopy_relief_ratio	LiDAR	Canopy relief ratio (mean - min)/(max-min)
elev_p50	LiDAR	50th percentile of canopy height
elev_kurtosis	LiDAR	Height kurtosis
elev_p99	LiDAR	99th percentile of canopy height
elev_stddev	LiDAR	Height standard deviation
percentage_first_returns_above_2pnt00	LiDAR	Percentage of first returns above 2 m
percentage_first_returns_above_mean	LiDAR	Percentage of first returns above the mean return height
total_all_returns	LiDAR	Total all returns
elev_p95	LiDAR	95th percentile of canopy height
strata_0pnt15_to_2pnt00	LiDAR	Proportion of points between 0.15 and 2 m
strata_2pnt00_to_4pnt00	LiDAR	Proportion of points between 2 and 4 m
strata_4pnt00_to_6pnt00	LiDAR	Proportion of points between 4 and 6 m
strata_6pnt00_to_8pnt00	LiDAR	Proportion of points between 6 and 8 m
strata_8pnt00_to_10pnt00	LiDAR	Proportion of points between 8 and 10 m
strata_10pnt00_to_15pnt00	LiDAR	Proportion of points between 10 and 15 m
strata_15pnt00_to_20pnt00	LiDAR	Proportion of points between 15 and 20 m
strata_20pnt00_to_25pnt00	LiDAR	Proportion of points between 20 and 25 m
strata_25pnt00_to_30pnt00	LiDAR	Proportion of points between 25 and 30 m
strata_30pnt00_to_50pnt00	LiDAR	Proportion of points between 30 and 50 m
forest_age	CAS-FRI	Mean age of the forest stand
NDVI	Landsat 5, 7, and 8	Mean NDVI

2010. For each point-count station location we determined the disturbance history and mean forest age. As there was not much variation in the dominant vegetation species at survey locations, we excluded vegetation composition as a covariate in our models.

We used the Normalized Difference Vegetation Index (NDVI) as an indicator of vegetation cover (Pettorelli et al., 2011). We generated 30 m composite NDVI rasters from 1995 to 2015 using surface reflectance imagery from the Landsat 5 Thematic Mapper (bands 3 and 4), the Landsat 7 Enhanced Thematic Mapper (bands 3 and 4), and the Landsat 8 Operational Land Imager (bands 4 and 5) (Survey, 2018). Satellite images were accessed and processed using the Google Earth Engine (GEE) Code Editor (Gorelick et al., 2017). As all of the point counts occurred during summer breeding season, we limited Landsat images to those taken between June and September. Images were masked to exclude snow, cloud, and cloud shadow pixels using the CFMask algorithm (Foga et al., 2017). We generated annual median composites of masked Landsat images and calculated NDVI rasters from the composites ($NDVI = \frac{NIR-R}{NIR+R}$) (USGS, 2020). For each survey year we calculated the mean values of NDVI pixels within a 100 m buffer of point count locations.

2.2.4 Analyses

We evaluated the effects of LiDAR temporal misalignment on model performance by comparing mixed effects logistic regression models. We built models using the *glmer* function in the R package *lme4* (Bates et al., 2015).

To accommodate the influence of survey methods and nuisance parameters on detection probabilities, we included statistical offsets in the models generated using QPAD (Sólymos et al., 2013). The QPAD method integrates removal and distance models to generate detectability offsets for individual point count events. In the

QPAD framework, distance models account for the effects of environmental conditions on the decreasing probability of observing a bird the further it is from the observer (Buckland et al., 2001). Removal models estimate the probability that an available bird will be observed vocalizing within a given point count duration (Alldredge et al., 2007). Distance and removal models were combined to get point count specific detectability offsets that were used in GLMMs. We modelled bird abundance using Poisson GLMMs with log-link functions.

We used the following multi-step process for each focal species. In Step 1, we grouped point count data according to the amount of temporal misalignment with LiDAR. There were 16 groups, one group for each year of time-lag between LiDAR and point count surveys (zero through fifteen years).

In Step 2, we built and evaluated models for the zero time-lag group of point counts. We first computed a global model with all candidate predictor variables as fixed effects and station location as a random effect. We checked for nonlinear relationships between response and predictors by separately evaluating, linear, quadratic, and cubic functions of each variable. To avoid multicollinearity between predictors, we used Pearson correlation coefficients and VIF scores to iteratively remove highly correlated predictors from the global model. We kept metrics with low correlation ($r < 0.5$ and VIF < 3) that were associated with different vegetation structure categories: height, cover, and complexity (Valbuena et al., 2020). For correlated metrics associated with the same category, we selected the variable with the lowest P value. We evaluated models consisting of the remaining predictors using the *dredge* function in the R package *MuMIn* (Barto, 2020). We defined the top model as that with the lowest Akaike's Information Criterion (AIC)(Burnham & Anderson, 2002). We calculated pseudo-R^2 as a measure of explanatory power (Nakagawa & Schielzeth, 2013). For

models with similar AIC values (a difference less than two) we selected the model with the largest pseudo-R^2.

In Step 3, we applied the Step 2 model to the remaining groups of time-lag point counts. For each group, we used the fitted model and a raster stack of covariates to map species occurrence probability using the *predict* function in the R package *raster* (Hijmans, 2021).

In Step 4, we compared the performance of different time-lag models. We compared their predictive accuracy using the area under the receiver operating curve (ROC) (AUC) calculated using the *auc* function in the *pROC* package in R (Robin et al., 2011). Models with an AUC >0.7 were considered moderately predictive of species occurrence (Vanagas, 2004) We tracked the amount of LiDAR time-lag necessary for models to have an AUC <0.7. The contribution of individual fixed effects were estimated by calculating semi-partial R^2 values using the *r2beta* function from the *r2glmm* package using standardized general variances (Jaeger, 2017). We compared the predictive maps for different time-lag groups by calculating the per pixel differences between them (i.e., we subtracted the zero time lag map from the map of each subsequent time lag group, resulting in 15 "difference" rasters). We used Pearson's correlations to examine the relationship between differences in species occurrence probability and forest age.

2.3 Results

The LiDAR variables used in top performing models varied by species (Table 2.2). The most common predictor variables across species were maximum vegetation height (used in all top models), and mean summer NDVI (used in top models for five out of six species). The rates and magnitude by which AUC was effected by LiDAR-bird survey temporal misalignment varied by species (Figure 2.3).

Table 2.2: The fixed effects and summary statistics for top models for each species. Marginal R^2 (R^2m) is a measure of the variance explained by the fixed effects. Conditional R^2 (R^2c) is a measure of variance explained by the full model, both fixed and random effects (Nakagawa & Schielzeth, 2013) .

Species	Fixed effects	R^2m	R^2c	AUC
American Redstart (*Setophaga ruticilla*)	ndvi + elev_2pnt00_to_4pnt00_return_proportion + elev_cv+ elev_maximum + elev_p50	0.46	0.62	0.78
Black-throated Green Warbler (*Setophaga virens*)	elev_p50 + elev_maximum + total_all_returns	0.48	0.63	0.80
Mourning Warbler (*Geothlypis philadelphia*)	ndvi^2 + elev_0pnt15_to_2pnt00_return_proportion+ elev_2pnt00_to_4pnt00_return_proportion + elev_maximum *elev_stddev+ percentage_first_returns_above	0.49	0.50	0.78
Swainson's Thrush (*Catharus ustulatus*)	ndvi^2 + elev_maximum + elev_p50	0.13	0.16	0.67
White-throated Sparrow (*Zonotrichia albicollis*)	ndvi + elev_cv + elev_maximum + percentage_first_returns_above_2pnt00	0.20	0.33	0.70
Winter Wren (*Troglodytes hiemalis*)	ndvi + canopy_relief_ratio+ elev_4pnt00_to_6pnt00_return_proportion+ elev_maximum + percentage_first_returns_above	0.42	0.45	0.70

2.3.1 American Redstart

Occupancy probability for American Redstart increased with NDVI, the coefficient of variation of vegetation height, and the 50th percentile vegetation height, and decreased with maximum vegetation height, and the proportion of LiDAR returns 2-4 m high. The model built using temporally aligned covariates explained 46% of the variance in American Redstart occupancy and had an AUC of 0.784. The coefficient of variation of vegetation height contributed most to predicting occupancy ($b = 3.149$, SE $= 0.691$, $p < 0.001$, semi-partial $R^2 = 0.065$), followed by NDVI ($b = 0.92$, SE $= 0.267$, $p <$

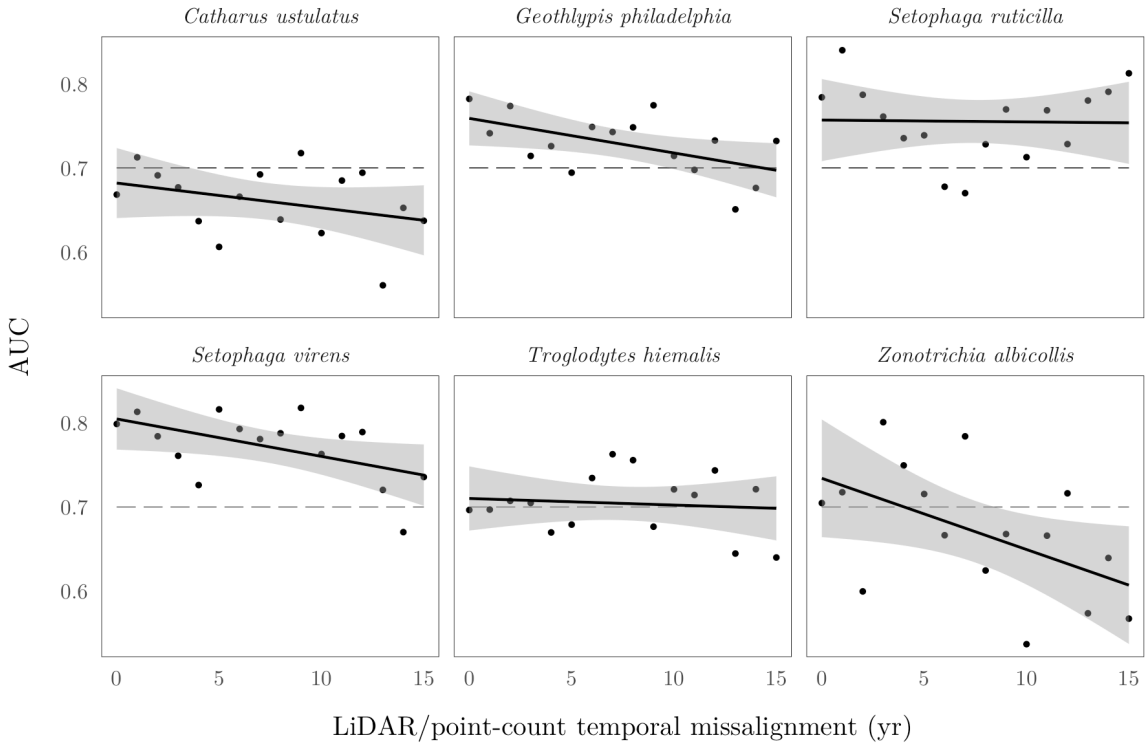

Figure 2.3: Plot showing the relationship between model AUC and LiDAR temporal misalignment with bird surveys for each species.

0.001, semi-partial R^2 = 0.051), and maximum elevation (b = -3.633, SE = 0.861, p < 0.001, semi-partial R^2 = 0.046) (Table 2.3). The percentage of explained variance did not decline with temporally misaligned LiDAR. For American Redstart, temporal misalignment did not lead to a decrease in model performance as measured by AUC.

2.3.2 Black-Throated Green Warbler

Occupancy probability for Black-Throated Green Warbler increased with maximum vegetation height and decreased with the 50th percentile of canopy height and the total of all LiDAR height returns. The model built using temporally aligned covariates explained 48% of the variance in Black-Throated Green Warbler occupancy and had an AUC of 0.799. Maximum vegetation height contributed the most to model performance

Table 2.3: Predictor variables ranked according to their semi-partial R^2. AMRE = American Redstart (*Setophaga ruticilla*); BTNW = Black-throated Green Warbler (*Setophaga virens*); MOWA = Mourning Warbler (*Geothlypis philadelphia*); SWTH = Swainson's Thrush (*Catharus ustulatus*); WIWR = Winter Wren (*Troglodytes hiemalis*); WTSP = White-throated Sparrow (*Zonotrichia albicollis*).

Predictor	AMRE	BTNW	MOWA	SWTH	WIWR	WTSP
strata_2pnt00_to_4pnt00	4		3			
elev_cv	1					4
elev_maximum	3	1	8	1	1	1
elev_p50	4	2		2		
ndvi_lag_0	2				5	2
total_all_returns		3				
strata_0pnt15_to_2pnt00			2			
elev_maximum:elev_stddev			5			
elev_stddev			6			
percentage_first_returns_above_mean			4		4	
poly(ndvi_lag_0, 2)1			1	3		
poly(ndvi_lag_0, 2)2			7	4		
canopy_relief_ratio					2	
strata_4pnt00_to_6pnt00					3	
percentage_first_returns_above_2pnt00						3

(b = 2.743, SE = 0.559, $p < 0.001$, semi-partial R^2 = 0.138) followed by the 50th percentile of canopy height (b = -1.439, SE = 0.351, $p < 0.001$, semi-partial R^2 = 0.035). There was no discernible trend in the explained variance with increasing LiDAR temporal misalignment. However, we observed a significant decrease in model performance (R^2=0.28, p<0.05). The AUC statistic for the zero-time lag model was < 0.7 with 14 years of LiDAR-bird survey time lag.

2.3.3 Mourning Warbler

Mourning Warbler occupancy responded positively to the percentage of first returns above the mean vegetation height, NDVI, the density of vegetation <2 m, and maximum vegetation height at low standard deviation of vegetation height. Mourning Warbler occupancy decreased with increased vegetation density between two and four meters. The model built using temporally aligned covariates explained 49% of the variance in Mourning Warbler occupancy and had an AUC of 0.782. NDVI contributed the most to model predictions (b = 25.81, SE = 0.354, $p < 0.001$, semi-partial R^2 = 0.074) followed by the proportion of vegetation returns below two meters (b = 0.797, SE = 0.215, $p < 0.001$, semi-partial R^2 = 0.028). For Mourning Warbler, we found that increased LiDAR-point count temporal misalignment led to reductions in the amount of explained variance (r^2=0.29, p<0.05) and model performance (r^2=0.29, p<0.05). AUC statistics were <0.7 with >13 years of LiDAR temporal misalignment.

2.3.4 Swainson's Thrush

Swainson's Thrush occupancy probability responded non-linearly to NDVI (the probability of occupancy increased with increasing low NDVI values and decreased with higher values). Occupancy probability responded negatively to the 50th percentile of vegetation returns and positively to the maximum vegetation height. The model

built using temporally aligned covariates explained 13% of the variance in Swainson's Thrush occupancy and had an AUC of 0.668. The maximum vegetation height contributed the most to model performance (b = 0.955, SE = 0.163, $p < 0.001$, semi-partial R^2 = 0.067) followed by the 50th percentile of vegetation height (b = -0.944, SE = 0.166, $p < 0.001$, semi-partial R^2 = 0.063). The percentage of explained variance did not decline with temporally misaligned LIDAR, nor was there a decrease in model performance as measured by AUC. AUC values were < 0.70 for all Swainson's Thrush models.

2.3.5 Winter Wren

Winter Wren occupancy was positively influenced by NDVI, the maximum vegetation height, and the percentage of first vegetation returns above the mean vegetation height. Winter Wren occupancy responded negatively to the canopy relief ratio and the density of vegetation returns between four and six meters in height. The model built using temporally aligned covariates explained 42% of the variance in Winter Wren occupancy and had an AUC of 0.696. Maximum vegetation height contributed the most to model performance ($b = 1.024$, SE = 0.27, $p < 0.001$, semi-partial $R^2 = 0.047$) followed by the canopy relief ratio (b = -1.666, SE = 0.518, $p < 0.01$, semi-partial R^2 = 0.024). The percentage of explained variance did not decline with temporally misaligned LIDAR, nor was there a significant decrease in model performance as measured by AUC.

2.3.6 White-Throated Sparrow

The top White-Throated Sparrow model predicted that occupancy probability responds positively to NDVI, the coefficient of variation of vegetation height, and the maximum vegetation height, and negatively to the percentage of LiDAR vegetation returns above two meters. The model built using temporally aligned covariates ex-

plained 20% of the variance in White-Throated Sparrow occupancy, and had an AUC of 0.705. Maximum vegetation height contributed the most to model performance (b = 0.813, SE = 0.155, $p < 0.001$, semi-partial $R^2 = 0.064$) followed by NDVI (b = 0.477, SE = 0.151, $p < 0.01$, semi-partial $R^2 = 0.022$). There was no discernible trend in the explained variance with increasing LiDAR temporal misalignment. However, we observed a significant decrease in model performance (R^2=0.28, $p < 0.05$). AUC statistics were < 0.7 with over five years of temporal misalignment.

2.3.7 Forest age

For American Redstart and Black-throated Green Warbler, we found a significant relationship between forest age and the pixel-wise differences between predictive maps ($p < 0.001$). Comparing the zero and fifteen year time lag models, we found that models using 15-year-old LiDAR data overestimated the occupancy probability of American Redstart in stands <25 years old. The 15-year-old LiDAR data overestimated the probability of Black-throated Green Warbler occupancy in forests of all ages (Figure 2.4). Forest age explained 23% and 30% of the variance between predictive maps for American Redstart and Black-throated Green Warbler, respectively.

For Mourning Warbler, Swainson's Thrush, Winter Wren, and White-Throated Sparrow, we found significant but weak relationships between forest age and the differences between predictive maps built with increasing amounts of LiDAR-point count temporal misalignment (p<001). For these species, forest age explained $< 5\%$ of the variance between predictive maps.

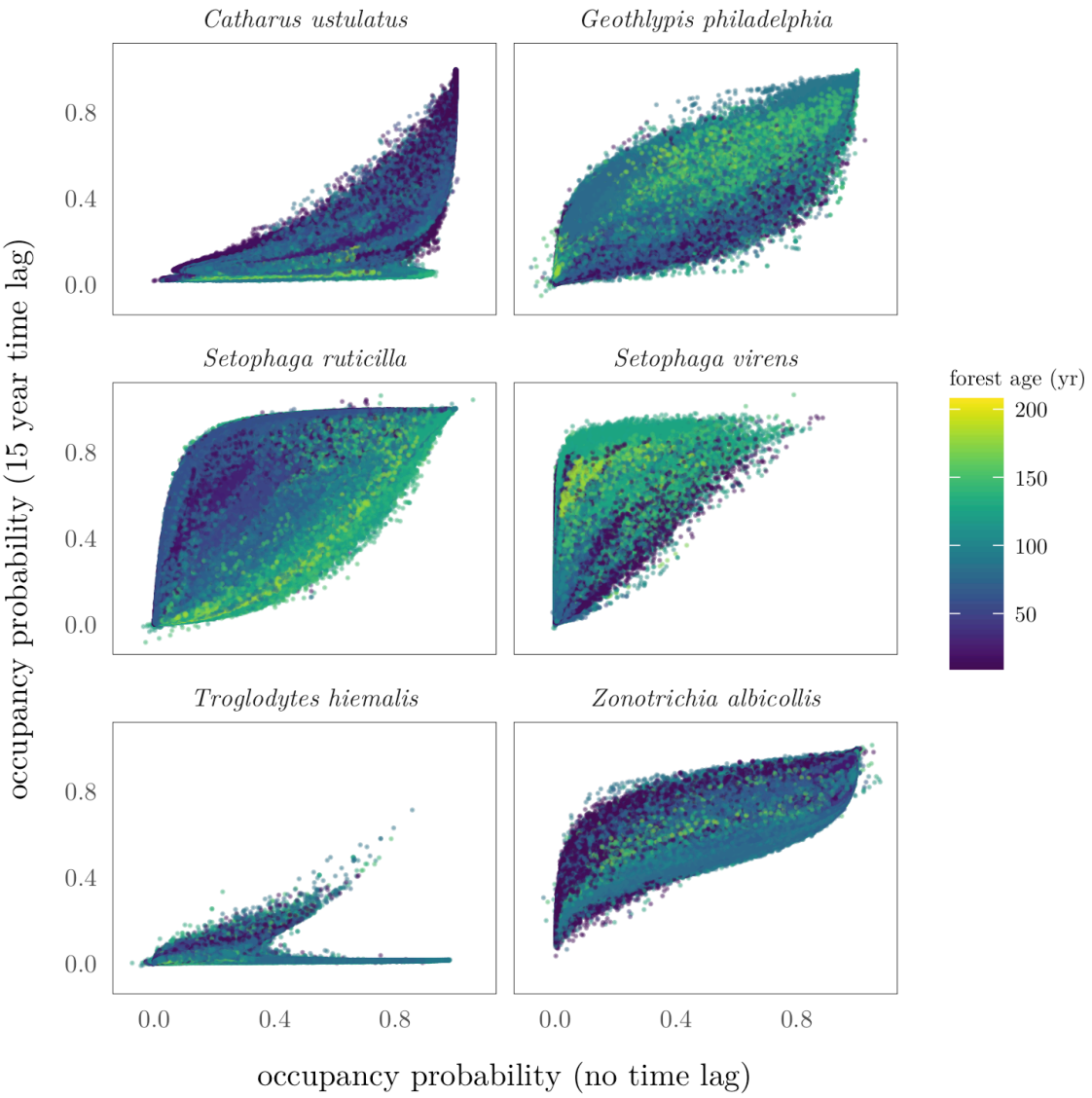

Figure 2.4: Scatter plots of per-pixel occupancy probability for predictive distribution maps representing zero and 15 years of time-lag between LIDAR and bird data. Scatter plots are coloured according to the forest age of each mapped pixel.

2.4 Discussion

2.4.1 Model performance

We found LiDAR based models were moderately predictive of occupancy probability (0.7<AUC<0.9) for four of the six focal species: American Redstart, Black-Throated

Green Warbler, Mourning Warbler, and White-throated Sparrow. The influence of LiDAR time-lag with bird observations on SDM performance varied.

As predicted, SDMs for Mourning Warbler, an early-successional associate, saw significant declines in model performance with increased LiDAR temporal misalignment. Mourning Warbler nest and feed near the ground in dense shrub vegetation and colonize clearings opened by forestry and oil and gas exploration (Atwell et al., 2008; Pitocchelli, 2020). As forests regenerate, and canopy closing trees replace early-successional vegetation, Mourning Warbler abundance declines (as early as 10 years post-disturbance) (Brawn et al., 2001). The proportion of LiDAR vegetation returns < 2 m, an indicator of dense shrub understory vegetation, was the LiDAR variable that contributed the most to the explained variation in Mourning Warbler occupancy. This may help explain the declines in model performance with increased LiDAR temporal misalignment. As shrub density decreases through succession, LiDAR metrics indicating shrub becomes less useful. For Mourning Warbler, we found models became less predictive (AUC < 0.70) with 13 years between LIDAR and bird surveys.

Temporal misalignment also strongly influenced the performance of SDMs for the White-throated Sparrow. The White-throated Sparrow is one of the most abundant species in Alberta's boreal mixed-wood forests (Schmiegelow et al., 1997). They occur along forested edges, in early-successional stands or mature forest canopy gaps (Falls & Kopachena, 2020). White-throated Sparrows nest and feed near the ground with low dense vegetation cover (Falls & Kopachena, 2020). Similar to Mourning Warbler, it's feeding and nesting preferences likely impact the amount of acceptable time lag between LiDAR and bird survey data in predictive models because of changes in shrub layer vegetation occurring between the LiDAR acquisition and point-counts. The White-throated sparrow SDMs became less predictive (AUC < 0.70) after five

years of time lag between LiDAR and point-count data.

We predicted that increasing the temporal lag between LiDAR and point-count data would lead to moderate declines in the performance of American Redstart SDMs. Our findings did not bear this out. Temporal misalignment had no discernible impact on model performance. American Redstart SDMs remained moderately predictive of occupancy with 15 years temporal misalignment between LIDAR and bird detections. American Redstart occurs in a range of successional stands and mixed-age plots (Sherry et al., 2020). In Alberta, they are associated with structurally complex deciduous forests (Leston et al., 2018; Mahon et al., 2016). Our results support this. LiDAR measures of structural complexity were more predictive of American Redstart occupancy than other LiDAR variables. Two things may account for the American Restart models' resilience to LIDAR temporal misalignment. (1) The structurally complex, uneven-aged forests that American Redstart are associated with change over decades (Brassard & Chen, 2010). The rate of change may not be captured with 15 years of time lag between LiDAR and point-counts. (2) Near Calling Lake, AB., the American Redstart decreased in abundance after harvesting (Norton & Hannon, 1997). Given that we controlled for natural and human disturbances occurring between LiDAR acquisition and bird surveys, American Redstart declines caused by harvesting were not captured by our models.

Contrary to our predictions, we observed a significant negative influence of LiDAR temporal misalignment on the performance of Black-throated Green Warbler SDMs. However, the SDMs were still moderately predictive of occupancy with fifteen years of time-lag between LIDAR and bird surveys. Canopy height was the biggest predictor of Black-throated Green Warbler occupancy. Black-throated Green Warbler is a forest interior species associated with older deciduous and mixed-wood forests (Mahon et al.,

2016; Morse & Poole, 2020; Schieck & Song, 2006). Declines in SDM performance were likely the result of changes in canopy height caused by natural gap opening events like individual tree fall or insect defoliation (Brassard & Chen, 2010). However, canopy changes that occurred during our 15 year study period were not large enough to reduce AUC to <0.70.

2.4.2 Recommendations

We identified two studies examining the influence of temporal misalignment between LiDAR and wildlife data on the performance of species-habitat models. Vierling et al. (2014) studied the effect of six years of LiDAR time-lag with wildlife surveys on Brown Creeper (*Certhia americana*) SDMs. They found that the six-year time-lag had a small influence on model performance (a 5% decrease in mapped occupancy probability). Similarly, Hill and Hinsley (2015) examined how LiDAR data with a time-lag of up to 11 years with field data influenced breeding habitat models for the Great Tit (*Parus major*). When comparing time-lags of one, four, and 11 years, they found only a small impact (< 1%) on model predictions. Both studies cautiously suggested that for mature and stable forests, temporal misalignment did not play a major role in the performance of predictive bird models. Brown Creeper occupies late-successional mature forests (Poulin et al., 2020) and the Great Tit is a habitat generalist (Van Balen, 1973). We found similar results for Black-throated Green Warbler and American Redstart. However, our results for early-successional species suggest that, for birds strongly associated with dense shrubs and open canopies, over five years of time-lag between LiDAR and wildlife surveys may erode model performance.

With its ability to capture vegetation structural attributes often missing from classified land-cover data, LiDAR is increasingly being used in bird studies (Davies & Asner, 2014; Lefsky et al., 2002). Despite the increasing availability of LiDAR,

multitemporal LiDAR data remains limited (Lesak et al., 2011). Consequently, most studies modelling bird-habitat relationships include some temporal misalignment between LiDAR and bird data (Moudrý et al., 2021): e.g., 3 years (Hinsley et al., 2006), 4 years (Goetz et al., 2010; Vogeler et al., 2014), 5 years (Weisberg et al., 2014), and 10 years (Huber et al., 2016). Our results suggest researchers should consider temporal misalignment when applying LiDAR to bird-habitat models. For species associated primarily with mid- to late-successional boreal forests, coincident bird and LiDAR data may not be necessary. But caution should be taken with early-successional species occupying burned and harvested areas, and those that nest and feed near the ground with dense shrub vegetation. For these, we recommend limiting temporal misalignment to <5 years. If multi-temporal LiDAR is unavailable, other remote sensing may be better for characterizing post-disturbance vegetation, like time-series of spectral indices from optical satellites (Kennedy et al., 2018). Spectral change detection can be used to identify disturbance events and can play a crucial role in determining the suitability of LiDAR data. For instance, in areas of significant spectral change, extra care should be taken to minimize temporal misalignment between LiDAR acquisitions and point counts.

2.5 Conclusion

We evaluated how time lag between LiDAR acquisitions and bird surveys influenced model robustness for early-successional, mature forest, and forest generalist birds. We found that LIDAR-based SDMs are moderately predictive of occupancy for American Redstart, Black-throated Green Warbler, Mourning Warbler, and White-throated Sparrow. The influence of temporal misalignment on SDMs varied across species with the greatest impact on models for early-successional associates. For species occupying

older, more stable forests, temporal misalignment between LiDAR and bird surveys had only a small impact on the predictive power of SDMs. For early-successional birds, our findings suggest that a time difference of 5-13 years between LIDAR and bird data may reduce model performance.

3

Predicting the effects of forestry on birds using forest resource inventories, LiDAR, and Landsat

3.1 Introduction

Canada's boreal forests span 270 million ha and provide breeding habitat for close to 400 bird species (Blancher & Wells, 2005; Natural Resources Canada, 2017). The composition and structure of boreal forests are changing in response to climate change, shifts to natural disturbance regimes, and industrial development (Brandt et al., 2013). In recent decades, timber production and energy exploration have altered the successional mosaic of the boreal landscape (Brandt et al., 2013), impacting bird communities (Norton & Hannon, 1997; Schmiegelow et al., 1997; Venier et al., 2014). Recently, forest management has shifted away from single-use timber production towards strategies that balance economic and environmental objectives, and reduce the impact of timber production on biodiversity (Fedrowitz et al., 2014; Galetto et al., 2019). Variable retention forestry–focused on preserving some vegetation structure within harvest

blocks–is a prevailing approach (Galetto et al., 2019).

Retention has well-established benefits–see reviews by Fedrowitz et al. (2014), and Mori and Kitagawa (2014). However, most studies on the impacts of retention only compare the effects of different amounts of harvest residuals (e.g., 50% retention vs clearcut), and ignore variability in their arrangement, structural composition, and regeneration rates. Also, few have examined the long-term effects of retention on bird communities (>15 years).

Predictive models linking distribution, abundance, and community structure to environmental variables are often used to understand how birds respond to forestry (Carrillo-Rubio et al., 2014; Engler et al., 2017). Many factors influence their predictive power, but ecologically relevant covariates are important drivers of model accuracy (Fourcade et al., 2018; Franklin, 1995; Vaughn & Ormerod, 2003). With an emphasis on volume over quality of residuals, studies modelling bird response to forestry often rely on classified habitat data from land cover maps and digital forest inventories. These products often include useful harvest related disturbance metrics for most forest tenures across Canada. However, they are slow to update and poorly describe harvest residuals. Instead, they provide rough estimates of the percent of the harvest area disturbed. The reliance on these categorical variables to characterize harvests may limit the predictive power of models describing bird response to retention forestry. It is unclear how well such estimates predict birds compared to other measures of post-harvest structure and regeneration.

Expanding covariates beyond discrete harvest intensity classifications to those derived directly from modern remote sensors may reveal relationships between the structure of within-block post-harvest residuals and bird communities. Satellite image times series' and Light Detection and Ranging (LiDAR) have the potential to improve

model predictions by providing high resolution structural and spectral change metrics rarely included in forest inventories and classified maps, and over larger areas than can be obtained from ground-based field surveys (He et al., 2015; Turner et al., 2003). For example, LiDAR can directly measure the three-dimensional distribution of vegetation structure and is increasingly used to explore bird-habitat relationships (Davies & Asner, 2014; Lefsky et al., 2002) in a range of forested habitats, including boreal (Lindberg et al., 2015), montane (Müller et al., 2009), and temperate (Martinuzzi et al., 2009) forests. While useful, LiDAR is often limited to a single acquisition year and thus unsuited to characterize stand conditions over long periods. Alternatively, time series of optical satellite data can be used to both estimate harvest intensity and track post-disturbance forest recovery (Frolking et al., 2009).

The availability of country-wide bird monitoring and remote sensing data provide opportunities to improve on existing research by (a) enabling the study of large numbers of harvest blocks over wide spatial extents; (b) providing novel covariates related to the vertical structure of harvests; and (c) allowing monitoring of post-disturbance forest regeneration. But the expansion of potential model covariates comes with uncertainty. Which covariates best predict bird response to harvesting? Here, we used point count data and modern remote sensors to predict the within-block effects of harvesting on birds. We simultaneously compared the predictive power of three sources of variables characterizing harvests: traditional forest resource inventory data, airborne LiDAR, and a time series of Landsat normalized burn ratio (NBR).

3.2 Methods

See Figure 3.1 for an illustration of our methodological workflow. Analyses were done using R statistical software (R Core Team, 2020) and Google Earth Engine

(Gorelick et al., 2017).

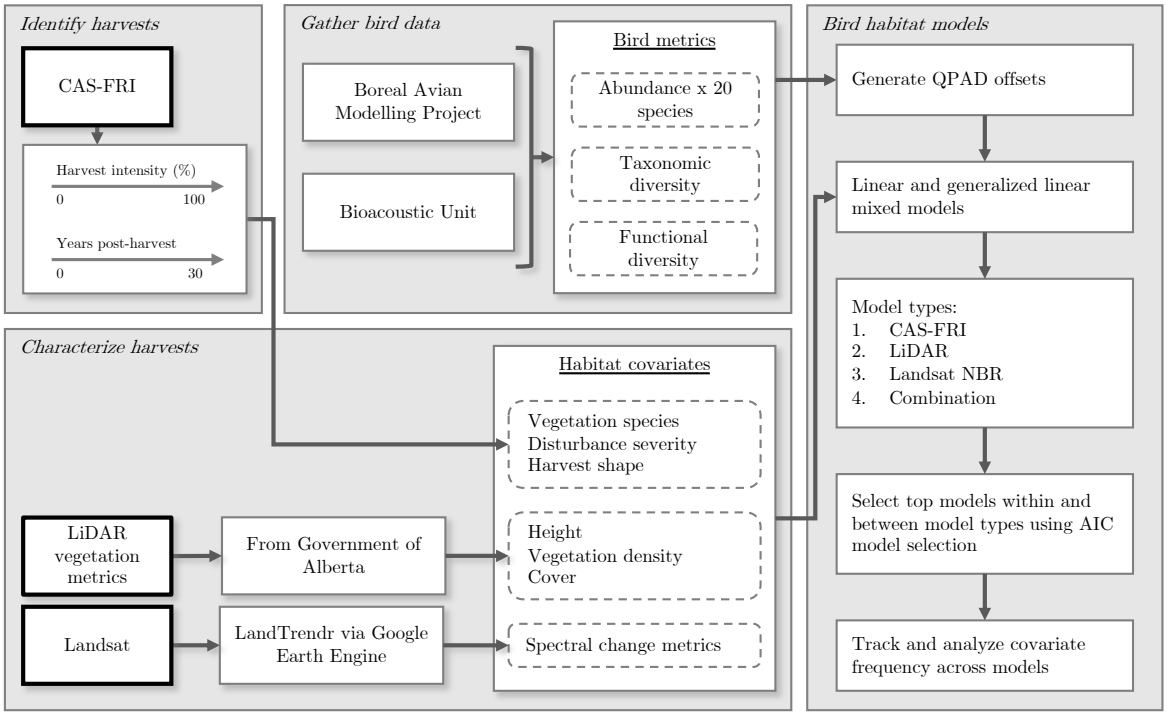

Figure 3.1: Conceptual diagram of our methodological workflow. We identified harvests using the Common Attribute Schema for Forest Resource Inventories (CAS-FRI), a standardized compilation of forest resource inventory data.

3.2.1 Study Area

We studied forestry harvest blocks distributed across 50,190 km^2 of the Boreal Central Mixedwood Natural Subregion of Northern Alberta, Canada (Figure 3.2). The availability of LiDAR data and locations of corresponding bird surveys from point count databases informed the spatial extent of the study area. Alberta's Central Mixedwood Natural Subregion is composed of a mosaic of aspen (*Populus tremuloides*) and white spruce (*Picea glauca*) mixed wood forests, white spruce and jack pine (*Pinus banksiana*) upland stands, aspen dominated deciduous forests, and shrubby black spruce (*Picea mariana*) fens (Natural Regions Committee, 2006). Aspen and conifer harvesting and

energy exploration occur across the study area.

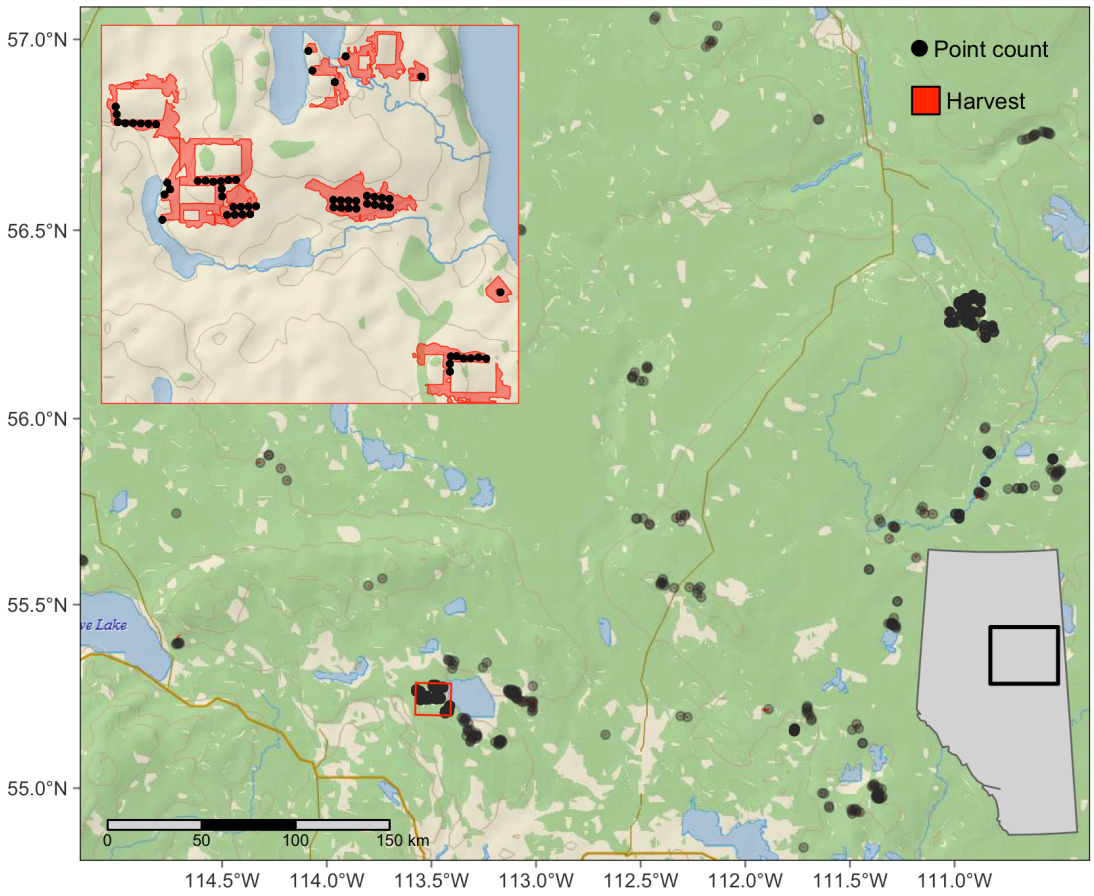

Figure 3.2: Locations of point counts in the Boreal Central Mixedwood Natural Subregion of Northern Alberta.

3.2.2 Site selection

We selected harvest blocks using the forest inventory and GIS data from CAS-FRI (Cosco, 2011). CAS-FRI spatial data included harvest polygons from across Canada and their associated attributes. Selected harvests represented a range harvest of intensities (100-95, 95-75, 75-50, 50-25, and 25-1% disturbed) and were surveyed for

birds across a chronosequence of recovery from 5 to 25 years post-harvest. The mean area of a harvest block was 105 ha. To control for the effect of subsequent harvests and wildfires on birds, we selected harvest blocks that had no recorded overlapping secondary disturbances.

3.2.3 Bird data

We gathered bird detection data from avian point count databases managed by the Boreal Avian Modelling Project (BAM) (Boreal Avian Modelling Project, 2018) and the University of Alberta's Bioacoustic Unit (http://bioacoustic.abmi.ca/). Data used in our analysis came from 2198 point counts performed across 243 locations between 2002 and 2016. Point counts were conducted by both human observers (graduate students and trained field technicians) and autonomous recording units. Surveys lasted between three and ten minutes at sampling radii ranging from 50 to 150 m. We limited point counts to those conducted over the course of a breeding season (May-July). At each location, point counts were repeated between three and eight times in a season. We only included data from point counts done in harvest blocks < 5 years of the corresponding LiDAR acquisition date. More than five years of temporal misalignment between LIDAR acquisitions and point counts can reduce the accuracy of predictive models for early-successional birds associated with dense shrub vegetation (Casey & Bayne, 2022c).

For each site, we calculated bird species richness (the sum of species detected over multiple visits in a season) and Shannon's diversity. While species diversity has long been used in forestry research, functional diversity (i.e. the value and range of species traits present in a community) are better linked with the underlying processes driving communities (Petchey & Gaston, 2006). Towards this, we calculated multidimensional functional diversity indices based on the diet, foraging, and nesting traits

Table 3.1: Descriptions of the functional diversity indices included in the analysis.

Functional diversity index	Description
Functional divergence (FDiv)	The extent to which the distribution of individual species abundances maximizes differences between functional traits found in a community (Mason et al., 2005)
Functional evenness (FEve)	The regularity of the distribution of abundance along the minimum spanning tree which links all species in a functional trait space (Villeger et al., 2008)
Functional richness (FRic)	The minimum convex hull volume that includes all species in a functional trait space (Villeger et al., 2008)

of detected species using the *FD* package in R (Laliberté et al., 2014). Traits of detected species, such as foraging strata, diet, and body size, were extracted using the *traitdata* package in R (RS-eco, 2021; Wilman et al., 2014). Indices represented three components of functional diversity: functional richness (FRic), functional evenness (FEve), and functional divergence (FDiv) (Laliberté & Legendre, 2010; Mason et al., 2005; Villeger et al., 2008). See Table 3.1 for definitions of included functional diversity indices. For all bird diversity indices, we limited species to those with known breeding ranges in the Boreal Central Mixedwood Natural Subregion of Northern Alberta, Canada that were detected at a minimum of three survey locations. Besides community metrics, we modeled the abundance of twenty species associated with different foraging and nesting strata (Wilman et al., 2014): Alder Flycatcher (*Empidonax alnorum*), American Redstart (*Setophaga ruticilla*), Black-throated Green Warbler (*Setophaga virens*), Chipping Sparrow (*Spizella passerina*), Common Yellowthroat (*Geothlypis trichas*), Hermit Thrush (*Catharus guttatus*), Least Flycatcher (*Empidonax minimus*), LeConte's Sparrow (*Ammospiza leconteii*), Lincoln's Sparrow (*Melospiza lincolnii*), Mourning Warbler (*Geothlypis philadelphia*), Ovenbird (*Seiurus aurocapilla*), Philadelphia Vireo (*Vireo philadelphicus*), Red-eyed Vireo (*Vireo goli-*

vaceus), Ruby-crowned Kinglet (*Corthylio calendula*), Swainson's Thrush (*Catharus ustulatus*), Warbling Vireo (*Vireo gilvus*), White-throated Sparrow (*Zonotrichia albicollis*), Winter Wren (*Troglodytes hiemalis*), Yellow Warbler (*Setophaga petechia*), and Yellow-rumped Warbler (*Setophaga coronata*).

3.2.4 Spatial variables

We characterized harvest blocks using LiDAR, Landsat time series, and CAS-FRI. See Table 3.2 for a detailed list of metrics and definitions.

Table 3.2: Spatial covariates included in the analysis.

Metric	Source	Description
elev_mean	LiDAR	Mean height
elev_cv	LiDAR	Coefficient of variation of LiDAR return heights
canopy_relief_ratio	LiDAR	Canopy relief ratio (mean - min)/(max-min)
elev_p50	LiDAR	50th percentile of canopy height
elev_p95	LiDAR	95th percentile height of canopy height
strata_0pnt15_to_2pnt00	LiDAR	Proportion of points between 0.15 and 2 m
strata_2pnt00_to_4pnt00	LiDAR	Proportion of points between 2 and 4 m
strata_4pnt00_to_6pnt00	LiDAR	Proportion of points between 4 and 6 m
strata_6pnt00_to_8pnt00	LiDAR	Proportion of points between 6 and 8 m
strata_8pnt00_to_10pnt00	LiDAR	Proportion of points between 8 and 10 m
strata_10pnt00_to_15pnt00	LiDAR	Proportion of points between 10 and 15 m
strata_15pnt00_to_20pnt00	LiDAR	Proportion of points between 15 and 20 m
strata_20pnt00_to_25pnt00	LiDAR	Proportion of points between 20 and 25 m
strata_25pnt00_to_30pnt00	LiDAR	Proportion of points between 25 and 30 m
strata_30pnt00_to_50pnt00	LiDAR	Proportion of points between 30 and 50 m
crown_closure_upper	CAS-FRI	Upper bound of crown closure

Table 3.2: *(continued)*

Metric	Source	Description
height_upper	CAS-FRI	Upper bound of height class
disturbance_extent_upper	CAS-FRI	Upper estimate for the proportion of the polygon affected by the disturbance
PercentConif	CAS-FRI	Percent of forest comprised of conifer species
forsest_type	CAS-FRI	Deciduous, conifer, or mixed forest
pa_ratio	CAS-FRI	Ratio of the perimeter to the area of the harvest polygon
distance_edge	CAS-FRI	Distance of bird survey to polygon edge
polygon_area	CAS-FRI	Area of the polygon (m)
ss_dst_timelag	CAS-FRI	Number of years between harvest year and bird survey year
$\Delta NBR_{disturbance}$	Landsat NBR	Difference between pre-disturbance NBR and the NBR at the start of regeneration
$\Delta NBR_{recovery}$	Landsat NBR	Percent of $\Delta NBR_{disturbance}$ values regained at the year of the bird survey
NBR_{survey}	Landsat NBR	NBR values at the time of the survey

CAS-FRI

CAS-FRI is a standardized compilation of forest resource inventory data from across Canada. The included 2 ha resolution forest stand maps were interpreted from 1:10,000 to 1:40,000 scale aerial photography taken between 1987 and 2010 (Cosco, 2011; Cumming et al., 2010b). CAS-FRI contains common vegetation and disturbance attributes used in bird habitat models, including forest composition and disturbance history (Cosco, 2011). We used the following CAS-FRI attributes as model covariates in our analysis: post-harvest forest type (coniferous, deciduous, or mixed-wood stand), vegetation composition, and harvest intensity. We calculated geometry metrics from CAS-FRI harvest polygons using the *sf* package in R (Pebesma, 2020)

including harvest area, the perimeter-area (PA) ratio of harvest polygons as a measure of shape complexity and relative edge amounts, and the Euclidian distance between point count locations and the nearest edge of the original harvest polygon.

LiDAR

Between 2003 and 2014, the Government of Alberta, Canada acquired airborne LiDAR covering 33 million ha of forested land using multiple contractors. Over 70% of the LiDAR was gathered between 2006 and 2008. Pulse density ranged between 1 and 4 returns per m^2 (Alberta Environment and Sustainable Resource Development, 2013). The Government of Alberta provided 34 LiDAR vegetation metric raster layers produced at a 30 m resolution using FUSION software (McGaughey, 2018).

For each LiDAR vegetation metric, we summarized the mean value of pixels within each CAS-FRI harvest polygon using the *raster* package in R (Hijmans, 2020). Many of the metrics were highly correlated and associated with similar structural categories. To minimize multicollinearity in models, we calculated Pearson's correlation coefficients (r) between LiDAR metrics. We retained metrics with low correlation ($r < 0.5$), and that corresponded to different vegetation structure categories: height, cover, and structural complexity (variability in the arrangement of vegetation) (Valbuena et al., 2020). For highly correlated metrics belonging to the same structural category, we selected the metric most predictive of species richness in univariate linear models. After removing highly correlated metrics, 15 LiDAR metrics remained for candidate bird habitat models.

Landsat time series

Leveraging recent advances in cloud computing, spectral change detection algorithms, and the free public availability of the Landsat archive, we calculated recovery

metrics for all sampled harvest polygons using an annual time series of NBR. We followed the workflow developed by Hird et al. (2021) to calculate spectral change metrics using the LandTrendr (Landsat-based Detection of Trends in Disturbance and Recovery) algorithm via Google Earth Engine (Gorelick et al., 2017; Kennedy et al., 2018). The workflow details methods for atmospheric corrections, cloud, shadow, and water detection and masking, the generation of annual NBR image composites, and the extraction of NBR change metrics.

NBR is calculated using the near-infrared (NIR) and shortwave-infrared (SWIR) reflectance bandwidths (Key & Benson, 2006b):

$$NBR = \frac{NIR - SWIR}{NIR + SWIR}$$

NBR change metrics were first used to map burn severity (Key & Benson, 2006a). NBR leverages the difference in spectral reflectance of NIR and SWIR to differentiate between healthy green vegetation and bare soil. Following a disturbance, NBR decreases with the loss of green vegetation and moisture content. As forests regenerate, NBR rebounds with increasing forest structure and vegetation water content (Hislop et al., 2018; Veraverbeke et al., 2011; White et al., 2018). We generated annual NBR rasters from 1984 to 2016 using Bands 4 and 7 of the Landsat 5 Thematic Mapper and the Landsat 7 Enhanced Thematic Mapper and bands 5 and 7 of and the Landsat 8 Operational Land Imager (Survey, 2018). Raster resolution was 30 m.

We calculated the following metrics using LandTrendr via the Google Earth Engine JavaScript API: mean NBR values prior to disturbance ($NBR_{pre\text{-}disturbance}$), the mean NBR values at the time of the bird point count (NBR_{survey}), the mean NBR values in the year post-harvest ($NBR_{disturbance}$), the change in NBR values between pre-harvest and harvest ($\Delta\text{NBR}_{\text{disturbance}}$), and the amount of spectral recovery ($\Delta\text{NBR}_{\text{recovery}}$=$\text{NBR}_{\text{survey}}$-$\text{NBR}_{\text{harvest}}$).

3.2.5 Analysis

We used linear and generalized linear mixed models to evaluate the predictive power of CAS-FRI, NBR time series, and LiDAR covariates on abundance and diversity metrics in harvest blocks. We built the mixed models using the *lme4* package in R (Bates et al., 2015).

In single species models, we used the QPAD method developed by Sólymos et al. (2013) to accommodate the influence of differential detection error in sampling methods on detection probabilities. See Section 2.3.4 for details on QPAD. We approached the community models differently. Because community metrics were based on cumulative detections across repeated point counts in a season, QPAD (which calculates offsets for individual point count events) was inappropriate. Instead, we used the $\log_{10}$ of survey days as an offset term to reduce the influence of different sampling efforts on bird detections. We modelled community metrics using linear mixed models.

For each response variable, we built four groups of models corresponding to the source of covariates: (1) CAS-FRI, (2) LiDAR, (3) Landsat NBR, and (4) multiple sources. Harvest ID and survey year were included as nested random effects in all models. Top models within and among covariate groups were ranked using Akaike's Information Criterion (AIC) and the explained variance (R^2_{GLMM}) (Burnham & Anderson, 2002; Nakagawa & Schielzeth, 2013). We tracked the frequency of use of individual model covariates across all top models, and evaluated their relative contribution within top models by calculating the semi-partial R^2 for all fixed effects using the *r2glmm* package (Jaeger, 2017). We compared the semi-partial R^2 of fixed effects across top models using a one-way analysis of variance (ANOVA). Finally, we compared the relative performance of models grouped by covariate source using an ANOVA of rank transformed AIC scores as the response variable.

3.3 Results

3.3.1 Source of covariates in top models

Most of the highest AIC ranked models used metrics from multiple sources (48%) while 24% used only Landsat NBR, 12% were LiDAR-based, and 16% used CAS-FRI. Of models that used multiple sources of metrics, 50% used both CAS-FRI and Landsat NBR, 17% used CAS-FRI and LiDAR, and 33% used metrics from all sources. Among top single species and community models (Table 3.3), an ANOVA showed significant variation in AIC model fit between those built using CAS-FRI, LiDAR, Landsat NBR, and multiple sources of metrics ($F=14.47_{(3,96)}$, $p < 0.001$). Tukey's HSD Test for multiple comparisons found integrating metrics from a variety of sources improved model performance. Models that supplemented CAS-FRI metrics with LIDAR or Landsat NBR predictors had lower AIC scores than those built with only CAS-FRI ($p = 0.04$) or LiDAR ($p < .001$). For models using predictors from a single source: Landsat NBR-based models ranked higher than LiDAR-based ones ($p < .001$); and CAS-FRI models tended to perform better than LiDAR models ($p = 0.002$). We found no significant difference in the mean explained variance (R^2_{GLMM}) of models built using CAS-FRI, LiDAR, Landsat NBR, or multiple sources ($F=0.33_{(3,96)}$, $p = 0.8$).

Table 3.3: Top models for each response variable and corresponding R^2_{GLMM} (marginal R^2 (R^2m) and conditional R^2 (R^2c). R^2m is a measure of the variance explained by the fixed effects. R^2c is a measure of variance explained by the full model, including random effects (Nakagawa & Schielzeth, 2013) .

Response	Fixed effects	df	R^2m	R^2c	Source
functional divergence	ss_dst_timelag^2 * $\Delta NBR_{disturbance}{}^2$	12	0.224	0.423	multiple

Table 3.3: *(continued)*

Response	Fixed effects	df	R^2m	R^2c	Source
functional evenness	ss_dst_timelag^2	6	0.03	0.449	cas-fri
functional richness	ΔNBR$_{disturbance}{}^2$:ss_dst_timelag^2	8	0.016	0.357	multiple
richness	ΔNBR$_{disturbance}{}^2$ + ss_dst_timelag^2 + elev_p50 + elev_cv	9	0.304	0.587	multiple
shannon diversity	ss_dst_timelag^2 * ΔNBR$_{disturbance}{}^2$ + ΔNBR$_{recovery}{}^2$	14	0.219	0.706	multiple
Empidonax alnorum	elev_cv + elev_p50 + strata_0pnt15_to_2pnt00 + strata_10pnt00_to_15pnt00 + strata_15pnt00_to_20pnt00 + elev_mean	9	0.522	0.606	lidar
Setophaga ruticilla	ΔNBR$_{disturbance}$ + NBR$_{survey}$	5	0.034	0.331	nbr
Setophaga virens	elev_p50 + elev_cv + ss_dst_time	6	0.015	0.996	multiple
Spizella passerina	PercentConif + Shape_Area + ss_dst_timelag^3 + dist_to_edge	9	0.129	0.207	cas-fri
Geothlypis trichas	ss_dst_timelag * ΔNBR$_{disturbance}$ + NBR$_{survey}{}^2$	8	0.39	0.54	multiple
Catharus guttatus	ΔNBR$_{disturbance}$	4	0	0.094	nbr
Ammospiza leconteii	elev_p50 + ss_dst_timelag + ΔNBR$_{disturbance}$	6	0.009	1	multiple
Empidonax minimus	ss_dst_timelag * ΔNBR$_{disturbance}$ + ΔNBR$_{recovery}$	7	0.028	0.477	multiple
Melospiza lincolnii	elev_p50 + elev_cv + ss_dst_time	6	0.138	0.226	multiple
Geothlypis philadelphia	ΔNBR$_{recovery}$	4	0.006	0.13	nbr
Seiurus aurocapilla	PercentConif + Shape_Area + ss_dst_timelag^2 + dist_to_edge	8	0.214	0.275	cas-fri
Vireo philadelphicus	strata_0pnt15_to_2pnt00 + strata_10pnt00_to_15pnt00 + strata_15pnt00_to_2	5	0.008	0.108	lidar
Corthylio calendula	ΔNBR$_{disturbance}{}^2$ + ΔNBR$_{recovery}$ + NBR$_{survey}$	7	0.137	0.27	nbr

Table 3.3: *(continued)*

Response	Fixed effects	df	R^2m	R^2c	Source
Vireo olivaceus	PercentConif + Shape_Area + ss_dst_timelag^2 + dist_to_edge	8	0.059	0.123	cas-fri
Catharus ustulatus	elev_p50 + ss_dst_timelag^2 + ΔNBR$_{disturbance}$	7	0.004	0.049	multiple
Vireo gilvus	ΔNBR$_{disturbance}$ * ss_dst_timelag + elev_p50 * elev_cv	9	0.074	0.167	multiple
Troglodytes hiemalis	elev_cv + elev_p50 + strata_0pnt15_to_2pnt00 + strata_2pnt00_to_4pnt00 + strata_15pnt00_to_20pnt00 + dist_to_edge	9	0.025	0.057	lidar
Zonotrichia albicollis	ΔNBR$_{disturbance}{}^2$ + ΔNBR$_{recovery}{}^2$ + NBR$_{survey}$	8	0.072	0.119	nbr
Setophaga petechia	ss_dst_timelag * ΔNBR$_{disturbance}$ + ΔNBR$_{recovery}{}^2$	8	0.187	0.775	multiple
Setophaga coronata	ΔNBR$_{disturbance}$ * ΔNBR$_{recovery}$	6	0.06	0.24	nbr

3.3.2 Frequency of covariate use

Covariate use varied in top models (Figure 3.3). The most frequently used metrics were the time since disturbance (64%), ΔNBR$_{\text{disturbance}}$ (60%), ΔNBR$_{\text{recovery}}$ (28%), the 50th percentile of canopy height (elev_p50) (32%), and the coefficient of variation of LiDAR return heights (elev_cv) (24%). Time since disturbance and ΔNBR$_{\text{disturbance}}$ were paired together in 46% of top models. We performed Fisher exact tests to compare metric use across top models. We found no difference between the metrics used in single species and community models ($p = 0.94$), and none between those used to predict ground, understory, mid-canopy, and upper-canopy associated birds ($p = 0.99$).

Of the 27 candidate variables used in model selection, 13 were absent from top models. Missing were CAS-FRI-based estimates of crown closure, upper canopy height,

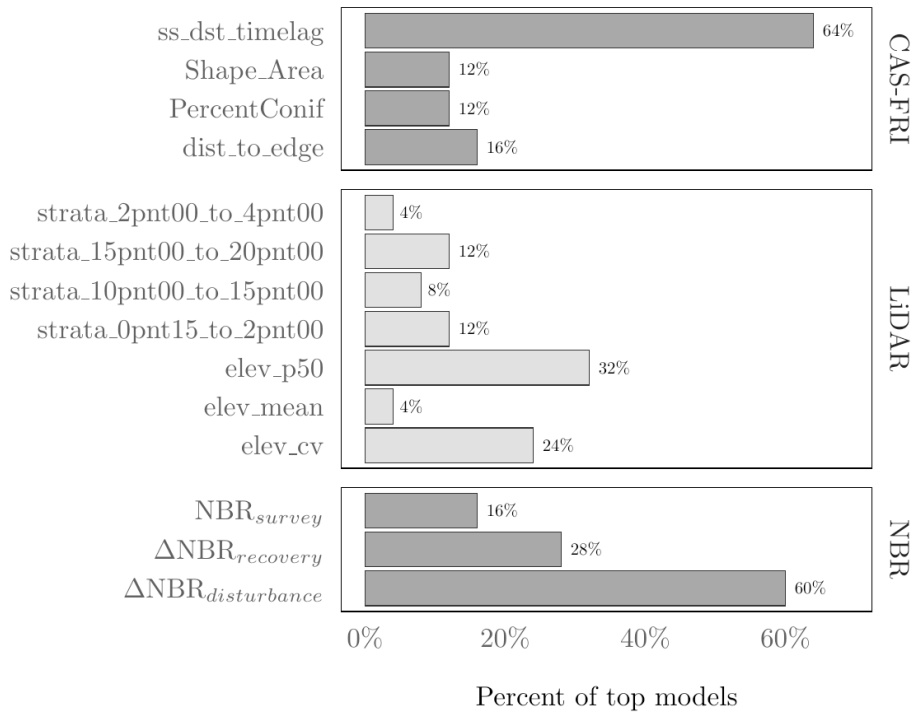

Figure 3.3: The frequency of metrics used in top models.

disturbance severity, and the perimeter area ratio of harvest polygons.

3.3.3 Contribution of covariates

While the partial effect size of individual metrics varied across top models (Figure 3.4), we found differences in their relative contribution to explained variance ($F=4.311_{(3,115)}$, $p = 0.002$). Tukey's HSD Test found that $\Delta NBR_{disturbance}$ explained more variance than the two top LiDAR metrics; 19% ± 9% more than elev_cv ($p < 0.001$), and 22% ± 9% more than elev_p50 ($p < 0.001$). Time since harvest also explained more variance than LiDAR metrics; 14% ± 9% more than elev_cv ($p = 0.001$), and 17% ± 9% more than elev_p50 ($p < 0.001$). We found no significant difference between the contribution of $\Delta NBR_{disturbance}$, $\Delta NBR_{recovery}$, and time since harvest. There was no evidence that the contribution of individual metrics varied between community and

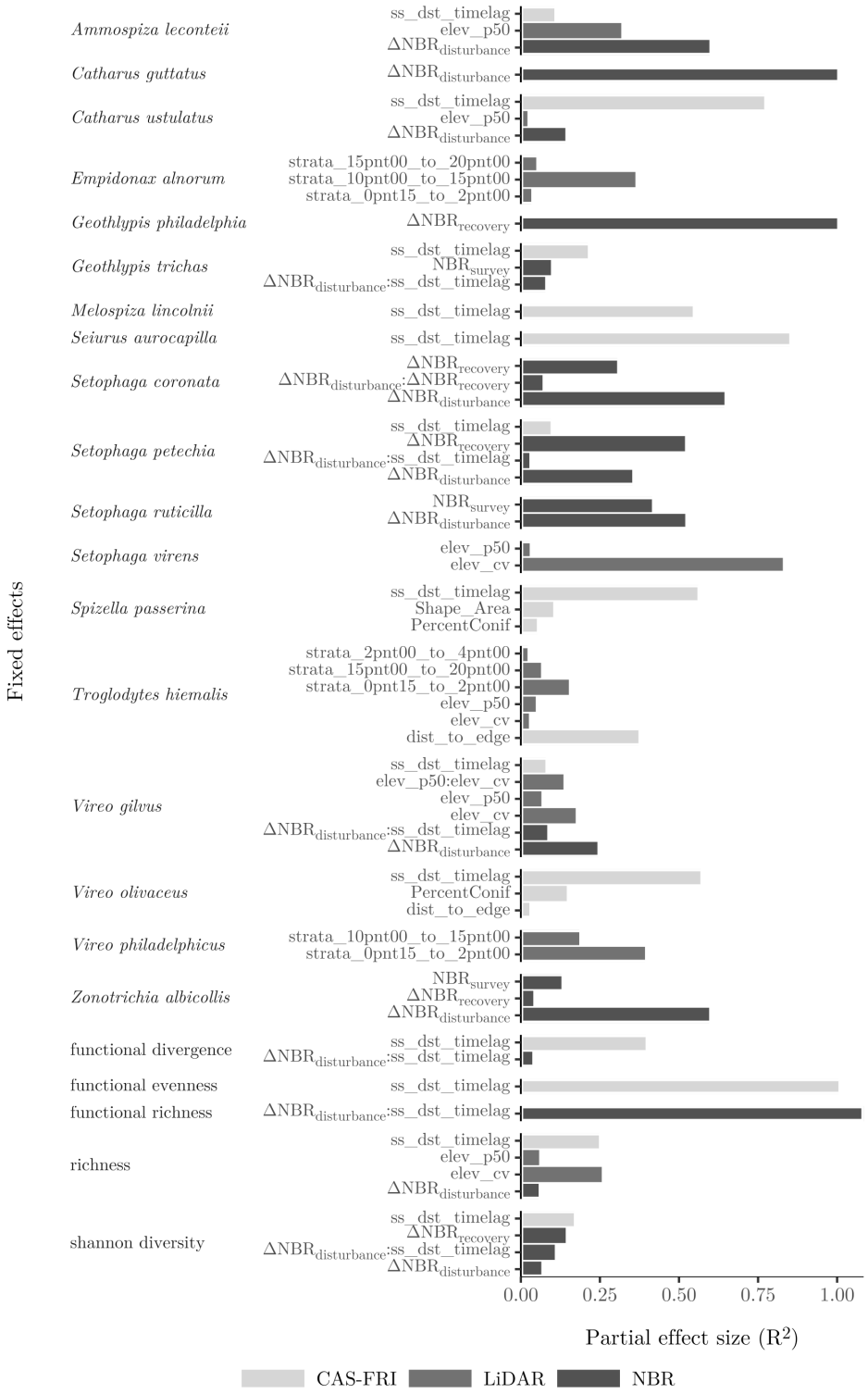

Figure 3.4: The contribution of fixed effects in top models defined by their partial effect size (R^2).

species models, or between species grouped by their associated nesting strata. Grouped by source, there were differences in the total contribution of CAS-FRI, LiDAR, Landsat NBR metrics ($F=3.41_{(2,69)}$, $p = 0.03$). Specifically, NBR metrics contributed more to model performance than LiDAR metrics ($p = 0.03$).

3.4 Discussion

We assessed the usefulness of three sources of model covariates (CAS-FRI, LiDAR, and Landsat NBR) for predicting the within block response of birds to harvesting. We found that (1) model performance improves with integrating LiDAR and ΔNBR metrics over models built using forest inventory data alone. (2) Of the initial set of thirty candidate variables, $\Delta NBR_{disturbance}$, time since disturbance, elev_p50, and elev_cv contributed the most to community and species abundance models. While LiDAR metrics improved some predictions, they contributed less overall to model performance than $\Delta NBR_{disturbance}$ and time since harvest. (3) Metrics related to harvest intensity, regeneration, and structure contribute more to model performance than the specific tree species present. And (4) contrary to our expectations, metric use did not vary between species belonging to different nesting guilds. The differential predictive power of metrics may result from different habitat requirements of the birds studied. Our results correspond with a growing body of literature showing the value of unclassified remote sensing predictors in species distribution models (Davies & Asner, 2014; Gottschalk et al., 2005; Swatantran et al., 2012).

3.4.1 CAS-FRI

Benefits of using forest inventory data in bird distribution models include their ecological interpretability and inclusion of conventional forestry terms. However, our results

show these benefits may come at the cost of reduced model performance. Overall, models only using CAS-FRI data were less predictive than those that used unclassified remote sensing data. Of the nine candidate CAS-FRI predictors included in our analyses, only four appeared in the top models: time since disturbance, harvest area, forest composition, and the distance between the point count location and the nearest harvest polygon edge. Except for time since disturbance, these variables contributed less to the predictive power of top models than ΔNBR and LiDAR metrics. Expectedly, the time elapsed between harvest and bird survey was the most useful and common metric for predicting bird and community response to harvesting. Notably, top models did not use CAS-FRI harvest intensity categories. Instead, $\Delta NBR_{disturbance}$ was more predictive in all instances. CAS-FRI's overly broad harvest intensity categories likely explain its reduced performance against ΔNBR metrics. CAS-FRI defines five categories of harvest intensity: 1-25%, 26-50%. 51-75%, 76-95%, and 96-100% disturbed. While similar disturbance categories have been useful for examining the impacts of forestry on birds (Craig & Macdonald, 2009; Odsen et al., 2018), it excludes a lot of variation between harvests.

These results correspond with other comparisons of classified and continuous remote sensing predictors (Koma et al., 2022; Sheeren et al., 2014). For example, Thuiller et al. (2004) found that while classified land cover data adds thematic detail and interpretability to species distribution models, they did not improve models' predictive power. The reduced predictive power of CAS-FRI metrics may be inherent to classified data. Reducing continuous remote sensing metrics into discrete land cover categories can remove important information on the structures and processes influencing birds (Bradley & Fleishman, 2008)

3.4.2 ΔNBR

We found that ΔNBR derived from a Landsat time series was more useful for predicting how birds respond to harvesting than the disturbance severity categories in forest resource inventories. $\Delta NBR_{disturbance}$ and $\Delta NBR_{recovery}$ were used in 60% and 28% of top models and contributed more to model performance than LiDAR metrics. While $\Delta NBR_{recovery}$ performed well compared to predictors from forest resource inventories, it performed less well then ΔNBR. This is likely due to saturation of the spectral signal over time (Pickell et al., 2016).

While the efficacy of ΔNBR to characterize harvests and burns is well documented (Hislop et al., 2018; Kennedy et al., 2010; Miller & Thode, 2007), few have integrated ΔNBR into bird species distribution models. Examples include Rose et al. (2016), who used ΔNBR to model how passerines respond to fire severity; and Russel et al. (2007), who supplemented field collected vegetation data with ΔNBR to model suitable habitat for cavity-nesting birds. However, similar spectral indices, particularly the normalized difference vegetation index (NDVI), are used widely (Gottschalk et al., 2005). Comparisons have shown NDVI-based bird models to perform as well or better than those using classified land cover maps (Hopkins et al., n.d.; Sheeren et al., 2014). We determined that ΔNBR is a viable alternative to forest inventory disturbance classifications for modelling how birds respond to harvests. Landsat change detection can obtain continuous measures of forest change over time, in contrast to the limited temporal and spatial availability of classified land cover products (Bartels et al., 2016).

3.4.3 LiDAR

LiDAR metrics were used in 36% of top models, often in conjunction with ΔNBR or CAS-FRI covariates. While LiDAR metrics contributed to some bird models (Alder

Flycatcher, Black-throated Green Warbler, LeConte's Sparrow, Lincoln's Sparrow, Philadelphia Vireo, Swainson's Thrush, Warbling Vireo, Winter Wren), the magnitude of those contributions were not generalizable across species and community response variables. Similarly, Tattoni et al. (2012) and Koma et al. (2022) found that the model improvements gained from LiDAR covariates varied by species. Different structural requirements of species may explain the lack of generalization (MacArthur & MacArthur, 1961). While we did not detect any differences in the response to LiDAR predictors between birds associated with different forest strata, others have suggested that the utility of LiDAR metrics varies by functional guild (Davies & Asner, 2014; Lesak et al., 2011).

Within block measures of vegetation structure and height were less predictive of bird abundance and diversity than the successional stage of the recovering harvest block (indicated by time since harvest and ΔNBR metrics). This lends support to the many studies that rely solely on percent disturbed and time since harvest categories to study the impacts of different harvest regimes. LiDAR performed well against other CAS-FRI predictors. The 50th percentile of canopy height and the coefficient of variation of LiDAR return heights explained more model variance than all other CAS-FRI candidate variables, including vegetation composition and the shape and area of harvest polygons. This aligns with a growing body of research that suggests LiDAR height and complexity metrics perform better than classified land cover data in bird models (Farrell et al., 2013; Ficetola et al., 2014). For example, Müller et al. (2010) found that LiDAR structure metrics are more predictive of bird distributions than plant species composition.

3.4.4 Multiple sources

While the performance of CAS-FRI, LiDAR, and ΔNBR metrics varied, we found that most top models used metrics from multiple sources. CAS-FRI, LiDAR, and ΔNBR complement each other by capturing different habitat characteristics influencing birds (i.e. successional stage, vertical structure, and vegetation resources). Others have highlighted the usefulness of integrating different sources of remote sensing data in bird models. Bae et al. (2014) built Hazel Grouse (*Tetrastes bonasia*) models using a variety of covariates from LiDAR, aerial photography, and ground-based vegetation surveys. Swatantran et al. (2012) found that bird models incorporating LiDAR, Synthetic Aperture Radar, and multispectral data were more predictive than those using any one sensor alone. Similarly, Koma et al. (2022) determined that species distribution models using LiDAR, NDVI, and Synthetic Aperture Radar explained the habitat preferences of wetland birds better than those made using detailed land cover maps. Furthermore, in bird SDMs, vegetation structure covariates from remote sensing are viable alternatives to similar ones from ground-based field surveys (Bae et al., 2014; Chaparro et al., 2022; Clawges et al., 2008). However, when LiDAR is not available, integrating satellite imagery or classified land cover data with habitat structure variables gathered from field surveys can improve model performance compared to using either alone (Bayne et al., 2010; Gottschalk et al., 2007).

3.4.5 Limitations

Limitations inherent to CAS-FRI and LIDAR may have influenced the predictive power of their corresponding metrics. The time lag between forest inventory acquisitions and bird surveys may have reduced the performance of vegetation composition metrics because of floristic changes driven by succession. As many studies rely on

irregularly updated land cover maps, future research should explore the influence of time lag between classified vegetation predictors on bird models. There were also large time lags between harvest and LiDAR acquisition dates. The temporal resolution of the LiDAR was far more limited than that of Landsat. Most of the LiDAR data was acquired between 2006 and 2008, often years after harvest. This temporal lag presented a challenge, as the efficacy of LiDAR predictor variables can diminish with increasing temporal misalignment (Vierling et al., 2014). While the influence of LiDAR temporal misalignment on mature-forest bird-habitat models is limited, it can lead to significant reductions in the predictiveness of LiDAR variables used in early-successional bird-habitat models (Casey & Bayne, 2022c). To minimize these effects, LiDAR was used to characterize conditions near the time of the bird survey, not the conditions immediately post-harvest. Conversely, with its large temporal resolution, we used Landsat to characterize harvests at both the time of harvest and the time of the bird survey. The temporal resolution of the LiDAR also reduced the amount of bird data we could use in our analyses. As we only included point counts completed within five years of LiDAR acquisition dates, our final data set was too small to split into training and evaluation data sets. As LiDAR becomes more widely available and less of a constraint on existing bird data, future studies can take advantage of more robust model fitting techniques (Guisan & Zimmermann, 2000).

Unclassified LiDAR and Landsat can be used in place of classified habitat data and ground-based measurements, but their improved predictions can come at the cost of interpretability (Li & Wu, 2004). While this work focused on the relative predictive power of ΔNBR, LiDAR, future work should aim to increase their ecological interpretability. LiDAR and ΔNBR metrics should be linked back to specific harvest residuals and understandable forestry terms to better inform adaptive management

and implementation monitoring.

3.4.6 Moving Forward

A challenge to the improvement of bird distribution models is the lack of comprehensive time series of bird observation data that can be paired in space and time with corresponding land cover variables (Rose et al., 2015). However, large-scale long-term bird monitoring data are increasingly available and can be combined with publicly accessible remote sensing data to monitor how birds respond to anthropogenic disturbances. But while unclassified remote sensing data can improve model performance, cost, availability, and training in their use and interpretation have limited their adoption in ecological research (Neumann et al., 2015). Now, provincial and continental scale remote sensing products and cloud-based computing platforms provide opportunities to model species-habitat relationships using novel remote sensing metrics over large spatial extents. Through cloud computing platforms like Google Earth Engine, Microsoft Azure, and Amazon Web Services (AWS), users can remotely access and process multi-petabyte catalogs of Earth observation data (Gomes et al., 2020), and include computationally demanding geospatial tasks in their modelling workflow. As we showed, researchers can produce usable forest change metrics using products like Landsat. This is especially useful when available classified data is limited or when studying birds in a successional mosaic.

Currently, most bird-habitat studies that use LiDAR are spatially constrained by the costs of acquiring LiDAR. But inexpensive wider coverage products are increasingly available. Government funded LiDAR acquisitions and the deployment of space-based sensors and can broaden the scale of LiDAR-based species distribution models moving forward while avoiding the costs of acquiring LiDAR internally (Burns et al., 2020; Coops et al., 2016). The increased availability of quality broad-scale remote sensing

data can help us better understand how birds respond to changing forests globally and aid in real-time monitoring efforts (Casey & Bayne, 2022a; Marvin et al., 2016; Roy et al., 2019).

3.5 Conclusion

To accurately predict how birds respond to forestry, we need covariates that fully describe post-harvest conditions. While useful, classified predictors like those in forest inventories can be temporally limited, require specialized technical training to produce, and often lack important components of bird habitat (Foody, 2002). Here we show an alternative. Unclassified metrics from optical remote sensing and LiDAR can be useful alternatives to those in traditional forest inventories. We found that, in addition to time since harvest, LiDAR height and complexity metrics and spectral measures of harvest intensity are more predictive of birds than the discrete harvest intensity and habitat classes often used in predictive models. We recommend supplementing forest resource inventory data with LiDAR and Landsat time-series to improve the accuracy of bird models while avoiding the costs of ground-based vegetation surveys.

4

Predicting avian response to forest harvesting using the Normalized Burn Ratio

4.1 Introduction

Forestry companies are increasingly adopting sustainable practices, such as retention harvesting, to reduce the effects of forestry on biodiversity and emulate natural disturbance regimes (Fedrowitz et al., 2014; Galetto et al., 2019). Variable retention forestry is used to promote multifunctional landscapes by maintaining pre-harvest legacy structures, such as patches of live standing trees, dead woody debris, and understory vegetation, throughout the harvest cycle (Franklin et al., 2000; Lindenmayer et al., 2012). Retention accelerates the recovery of harvest blocks by increasing structural complexity relative to clear cuts, emulates natural disturbances like fire and insect outbreaks, and optimizes habitat for "keystone" or protected species (Galetto et al., 2019; Lindermayer & Franklin, 2002; Serrouya & D'Eon, 2004). By maintaining legacy structures, retention can improve the continuity of ecological processes and organisms

across forest generations by maintaining habitat for species with low dispersal and/or small home ranges, enhancing ecological connectivity via residual stepping stones, accelerating stand recolonization by late successional species, moderating changes to microclimate, and maximizing niche availability through the maintenance of structural complexity (Baker & Read, 2011; Baker et al., 2014, 2016; Chan-Mcleod & Moy, 2007; Fedrowitz et al., 2014; Franklin et al., 2000; Heithecker & Halpern, 2007; Tews et al., 2004).

Researchers have found that retention forestry can accelerate post-harvest ecological recovery (Fedrowitz et al., 2014; Mori & Kitagawa, 2014). However, the nonlinear effects of the interaction between forest harvest intensity and recovery time on the functional attributes of bird communities remain unclear. Furthermore, it is uncertain the duration needed for post-harvest bird communities in different retention treatments to reach parity with those of undisturbed, mature forests.

Studies assessing the impacts of retention on bird communities often use ANOVA-style study designs and broad categorical harvest intensity metrics based on basal area or percent canopy coverage (e.g., 1-25%, 26-50%, 51-75%, 75-95%, 96-100% disturbance) to compare the short-term (<15 years) effects of harvesting on taxonomic diversity or the abundance of specific indicator species (Gustafsson et al., 2010; Rosenvald & Lohmus, 2008). While categorical harvest intensity metrics can predict post-harvest bird communities (Odsen et al., 2018; Price et al., 2020), they bring limitations. They are often obtained from intensive fieldwork or from digital land cover maps that can be slow to update, require specialized knowledge to produce, and may not capture the full range of harvest intensities present in the landscape. Furthermore, common harvest intensity variables do not differentiate between possible retention treatments, including understory protection, structural retention, dispersed

single-tree retention, and aggregated retention.

Remote sensing can provide detailed, up-to-date information on the magnitude and recovery of harvests, offering a promising alternative to categorical harvest intensity metrics, without intensive field-based vegetation surveys. Continuous measures of disturbance magnitude from remote sensing may reveal subtler relationships between forestry practices and bird communities. The Landsat program has collected a continuous 50-year archive of global land surface imagery, making it well-suited for monitoring long-term vegetation change (Cohen & Goward, 2004; Wulder et al., 2008). A growing body of image processing and change detection methods, along with the public availability of the full Landsat archive, are providing new ways to analyze optical time series data (Gomez et al., 2016; Tewkesbury et al., 2015; Zhu, 2017). For example, algorithms such as Landsat-based detection of Trends in Disturbance and Recovery (LandTrendr) (Kennedy et al., 2018), Breaks For Additive Seasonal and Trend (BFAST) (Verbesselt et al., 2010), and the Continuous Change Detection and Classification (CCDC) (Zhu & Woodcock, 2014) can produce spectral recovery and disturbance metrics using Google Earth Engine.

A time series of normalized burn ratio (NBR) can be used to assess changes in forest structure and vegetation following disturbances. NBR is a spectral index that is calculated using near-infrared (NIR) and shortwave-infrared (SWIR) reflectance bandwidths (Key & Benson, 2006b). The index can be used to differentiate between undisturbed forests and harvested or burned stands by leveraging differences in the way healthy green vegetation and bare soil reflect light. NBR is calculated by subtracting SWIR from NIR and then dividing the result by the sum of SWIR and NIR:

$$NBR = \frac{NIR - SWIR}{NIR + SWIR}$$

A decrease in NBR indicates a loss of green vegetation structure and moisture

content. When harvest areas regenerate, NBR increases with the return of green vegetation and forest structure (Hislop et al., 2018; Veraverbeke et al., 2011; White et al., 2018). For measuring harvest intensity, NBR offers several advantages over other indices calculated from Landsat imagery such as the Normalized Difference Vegetation Index (NDVI), Tasseled Cap Greenness (TCG), and the Normalized Difference Moisture Index (NDMI) (Schultz et al., 2016)). First, the Short-Wave Infrared (SWIR) reflectance band used in NBR is sensitive to forest structure and vegetation moisture, making it well-suited for assessing the characteristics of regenerating stands (Hislop et al., 2018). Second, NBR has a slower saturation rate than other indices, allowing for more accurate measurement of long-term forest changes, and may allow researchers to study forestry impacts at later stages of succession (Pickell et al., 2016). And third, NBR can outperform other SWIR-based indices for forest disturbance monitoring (Cohen et al., 2018; Veraverbeke et al., 2012). The spatial and temporal resolution of the Landsat archive makes it well suited for measuring long-term changes in vegetation cover from forestry over broad extents (Bost et al., 2019; Kennedy et al., 2009). This is an advantage over classified habitat maps that are more temporally limited. In addition, NBR measures of harvest intensity tend to be more predictive of post-harvest species abundance than LiDAR-derived vegetation height and structure metrics (Casey & Bayne, 2022b).

Here, we used continuous NBR measures of harvest intensity to explore the impacts of retention forestry on bird communities and estimate the time for communities to reach parity with mature forest reference areas. However, choice of community response variables can influence whether a harvest is considered "recovered". Taxonomic diversity metrics (e.g. richness and the Shannon diversity index) are common response variables in forestry. Alternatively, functional diversity (i.e. the diversity of species

niches), quantifies the distribution of traits within a community and is more directly connected with underlying ecological phenomenon (Cadotte et al., 2011; Gagic et al., 2015; Petchey & Gaston, 2006). By prioritizing the "types" of species over species richness and abundance, trait-based measures of diversity can offer a more generalizable understanding of the mechanisms shaping post-harvest communities (Lelli et al., 2018) and enable researchers to compare forestry treatments across broader spatial scales (Aubin et al., 2013).

Given these advantages, functional diversity response variables have been used to study forest structure and productivity (Bae et al., 2018), ecosystem processes (Gagic et al., 2015; Lavorel et al., 2013), land cover change (Becik et al., 2020; Bregman et al., 2016; Mouillot et al., 2013a), and forest management (Aubin et al., 2013; Curzon et al., 2020; Leaver et al., 2019).

In this study, we used bird point count data, acoustic monitoring tools, and a 25 year time series of Landsat NBR to examine effects of the interaction between forest harvest intensity and successional age on bird communities compared against mature forest reference areas. Our objectives were to (1) quantify the influence of variable retention on the functional and taxonomic diversity of birds along a successional gradient of 0-25 years, (2) evaluate the time required for bird communities to recover to mature forest reference conditions following different harvest treatments, and (3) assess the efficacy of NBR as a measure of harvest intensity in predictive bird models.

4.2 Methods

4.2.1 Study area

Human and acoustic point counts were conducted within harvested forest areas across 413,161 km^2 of the Foothills and Boreal Forest Natural Regions of Alberta, Canada

(Natural Regions Committee, 2006) (Figure 4.1). The Foothills Natural Region is situated at the eastern edge of the Rocky Mountains and is dominated by mixedwood forests comprising lodgepole pine (*Pinus contorta*), white spruce (*Picea glauca*), trembling aspen (*Populus tremuloides*), and balsam poplar (*Populus balsamifera*) at lower elevations. Lodgepole pine forests are typical of higher elevations (Natural Regions Committee, 2006). The Boreal Forest Natural Region, which spans across most of northern Alberta, comprises coniferous forests dominated by black spruce (*Picea mariana*), white spruce, and jack pine (*Pinus banksiana*), mixedwood forests with trembling aspen and balsam poplar, and shrubby black spruce fens (Natural Regions Committee, 2006). Despite the differences in vegetation and topography, there is a significant overlap of bird species between the foothills and boreal. In both regions, energy production and the harvesting of aspen and conifer are common.

4.2.2 Forest harvest data

We used two sources of data to identify forest harvest areas: the Common Attribute Schema for Forest Resource Inventories (CAS-FRI) (Cosco, 2011) and the Wall-to-Wall Human Footprint Inventory (HFI) (Alberta Biodiversity Monitoring Institute and Alberta Human Footprint Monitoring Program, 2019). CAS-FRI provides standardized 2 ha forest attributes derived from 1:10,000 to 1:40,000 aerial photography flown between 1987 and 2010 (Cosco, 2011). HFI contains human footprint attributes interpreted from aerial and SPOT satellite imagery acquired between 1950 and 2019 (Alberta Biodiversity Monitoring Institute and Alberta Human Footprint Monitoring Program, 2019). We selected harvests with a range of CAS-FRI defined categorical harvest intensities (100-95, 95-75, 75-50, 50-25, and 25-1%). The mean area of individual harvests was 115.4 ha (SD=110.2). Unharvested mature forest reference areas (stand age >60 years) were identified using CAS-FRI, HFI, and historical wildfire data

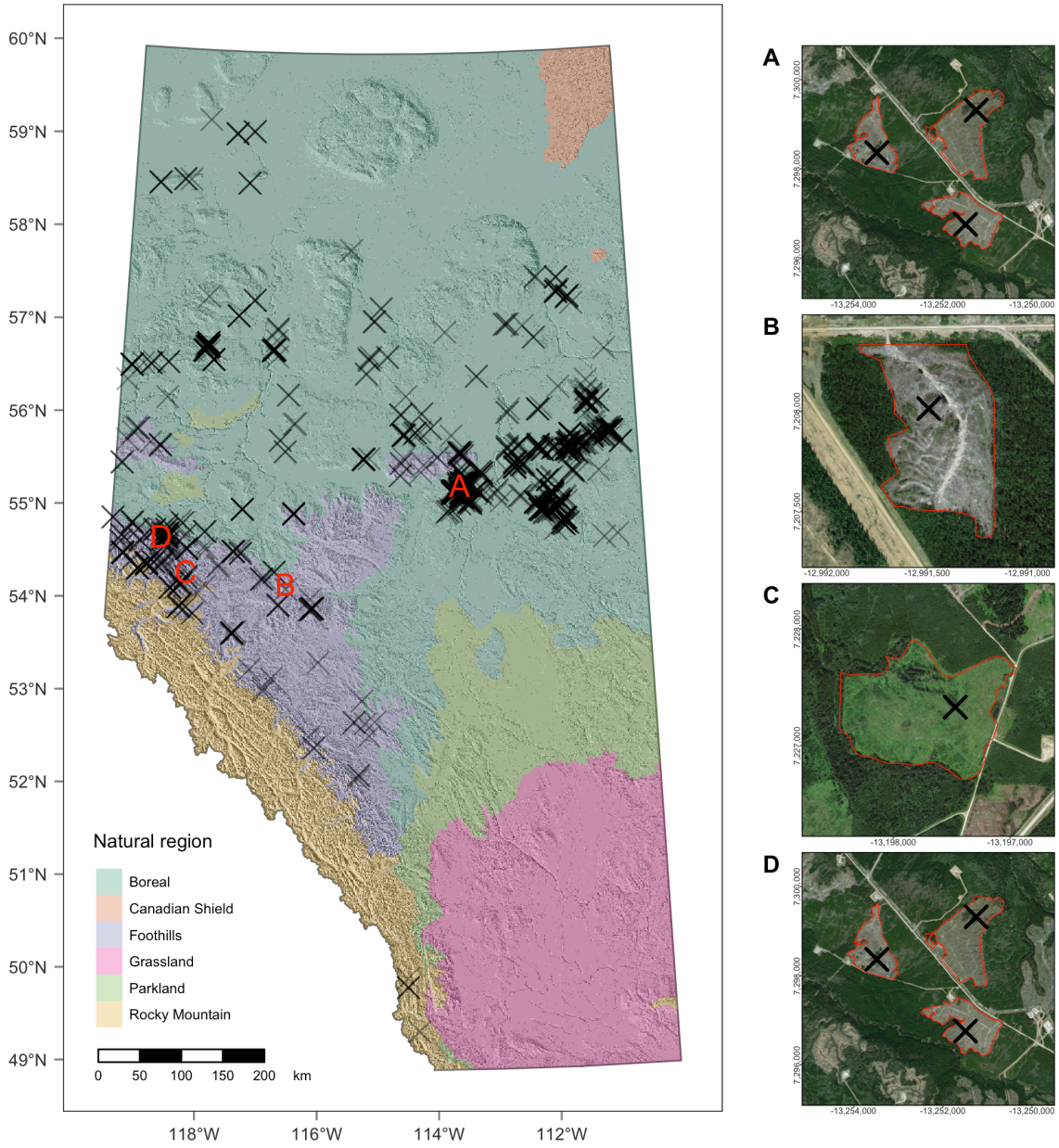

Figure 4.1: Locations of point counts in the Boreal Central Mixedwood Natural Subregion of Northern Alberta. The right-hand column shows examples of point count locations (black x) in forest harvest areas (red polygons). Boxes A to D show close up images of surveyed harvest blocks.

(Alberta Biodiversity Monitoring Institute and Alberta Human Footprint Monitoring Program, 2019; Alberta, 2022; Cosco, 2011). Reference areas were within 500 to 1000 m of sampled harvest areas.

4.2.3 Bird data

Avian point counts were conducted in harvested areas ranging from 5 to 25 years post-harvest. We used bird detection data from databases managed by the Boreal Avian Modelling Project (BAM) (Boreal Avian Modelling Project, 2018) and the University of Alberta's Bioacoustic Unit (`http://bioacoustic.abmi.ca/`). Our study included data from 9700 individual point counts conducted in or within 1000 meters of 1181 harvest blocks between 1995 and 2021. These point counts were conducted by human observers and autonomous recording units. Surveys were conducted within sampling radii ranging from 50-150 m and lasted 1-10 minutes. We included point counts conducted during the breeding season (May 16 to July 7) between sunrise and 10:00 h. Each location was surveyed 3-10 times approximately three days apart. To account for differences in bird detections resulting from varying sampling effort, we used the $\log_{10}$ of sampling effort (i.e., the number of survey days multiplied by point count durations) as an offset term in bird-habitat models.

For each point count location, we computed site-level bird species richness, Shannon diversity, and functional diversity indices based on the diet, foraging, and nesting traits of species (Wilman et al., 2014) (Table 4.1). We calculated functional divergence (FDiv), functional evenness (FEve), functional richness (FRic), and functional dispersion (FDis) using the *dbFD* function in the *FD* package in R (Laliberté et al., 2014; Laliberté & Legendre, 2010; Mason et al., 2005; Villeger et al., 2008). Shannon diversity was calculated using the *diversity* function in the *vegan* package in R (Oksanen et al., 2020). Our analysis was limited to bird species with known breeding

ranges in the Foothills and Boreal Forest Natural Regions of Alberta, Canada and that were observed at > 3 point count locations.

Table 4.1: Response variables included in the analysis.

Response variable	Description
Functional dispersion (FDis)	The mean distance in a functional trait space between individual species and the centroid of all species present in a community weighted according relative species abundance (Laliberté & Legendre, 2010)
Functional divergence (FDiv)	The extent to which the distribution of individual species abundances maximizes differences between functional traits found in a community (Mason et al., 2005)
Functional evenness (FEve)	The regularity of the distribution of abundance along the minimum spanning tree which links all species in a functional trait space (Villeger et al., 2008)
Functional richness (FRic)	The minimum convex hull volume that includes all species in a functional trait space (Villeger et al., 2008)
Richness	The sum of species detected over multiple visits in a season
Shannon diversity index (shan)	$H' = -\sum_i p_i \ln p_i$, where p_i is the proportion of a community comprised of species i (Oksanen et al., 2020)

4.2.4 Model covariates

To calculate harvest intensity metrics using NBR, we used methods developed by Hird et al. (2021) (Figure 4.2). First, we pre-processed harvest polygons using the *sf* package in R (Pebesma, 2020). We repaired errors in polygon geometries, dissolved "doughnut shaped" polygons, buffered polygons by -30 m to minimize the influence of harvest edges on NBR estimates, and simplified polygons using a tolerance of 5 m. Once processed, we uploaded the harvest polygons as a shapefile to Google Earth Engine (Gorelick et al., 2017). Next, we generated 30 m summer (June-September) composite NBR rasters from 1984 to 2021 using images from the Landsat 5 Thematic

Mapper (bands 4 and 7), Landsat 7 Enhanced Thematic Mapper (bands 4 and 7), and Landsat 8 Operational Land Imager (bands 5 and 7) via Google Earth Engine's JavaScript API (Survey, 2018). Snow, cloud, and cloud shadow pixels were masked and removed using the CFMask algorithm (Foga et al., 2017). Finally, we applied the LandTrendr algorithm to NBR composites to generate the following spectral change metrics for each forest harvest area: the mean NBR value for the five years pre-harvest ($NBR_{pre\text{-}disturbance}$), the lowest NBR post-harvest value ($NBR_{post\text{-}disturbance}$), NBR spectral change ($\Delta NBR$=$NBR_{pre\text{-}disturbance}$-$NBR_{post\text{-}disturbance}$), and relative spectral change (Miller & Thode, 2007):

$$R\Delta NBR = \frac{NBR_{pre-disturbance} - NBR_{post-disturbance}}{\sqrt{|NBR_{pre-disturbance}/1000|}}$$

In addition to spectral change metrics, we calculated the Euclidean distance between point count locations and the nearest harvest edge using the *sf* package in R (Pebesma, 2020). We also calculated fractional land cover (% cover of habitat types) for the year of the point count, mean canopy height, and the standard deviation of canopy height within a 300 m circular buffer of point count locations using Google Earth Engine (Hermosilla et al., 2022; Lang et al., 2022). Model covariates and their definitions can be found in Table 4.2.

Table 4.2: Spatial covariates included in the analysis.

Predictor	Description
canopy_height	Mean canopy height (Lang et al., 2022)
canopy_standard_deviation	Standard deviation of canopy height (Lang et al., 2022)
Coniferous	Percent of coniferous species (Hermosilla et al., 2022)
dist_to_edge	Distance of bird survey to nearest harvest edge

Table 4.2: *(continued)*

Predictor	Description
Exposed_Barren_land	Percent exposed barren land (Hermosilla et al., 2022)
Herbs	Percent herbs (Hermosilla et al., 2022)
lat	Latitude of point count location
Mixedwood	Percent mixedwood (Hermosilla et al., 2022)
RdNBR	Relative dNBR (Miller & Thode, 2007)
Shrubs	Percent shrubs (Hermosilla et al., 2022)
ss_dst_timelag_nbr	The time between the harvest event and point count survey (yr)
Water	Percent water (Hermosilla et al., 2022)

4.2.5 Analyses

We employed mixed-effects regression models to investigate the impact of NBR harvest intensity indices on bird community metrics over time using the *glmer* package in R *lme4* (Bates et al., 2015). We used a Poisson generalized linear mixed model with a log link to predict species richness. To predict Shannon diversity, functional divergence, functional evenness, functional richness, and functional dispersion, we employed Gamma generalized linear mixed models with a log link. As mentioned, log(survey days * point count durations) was used as an offset to correct for differential sampling effort.

We followed the same modelling process for each response variable. First, we fit a global model that included all potential predictor variables as fixed effects, and nested random effects for harvest ID and survey year. Second, we assessed the linearity of predictor-response relationships by fitting separate models using linear, quadratic, and

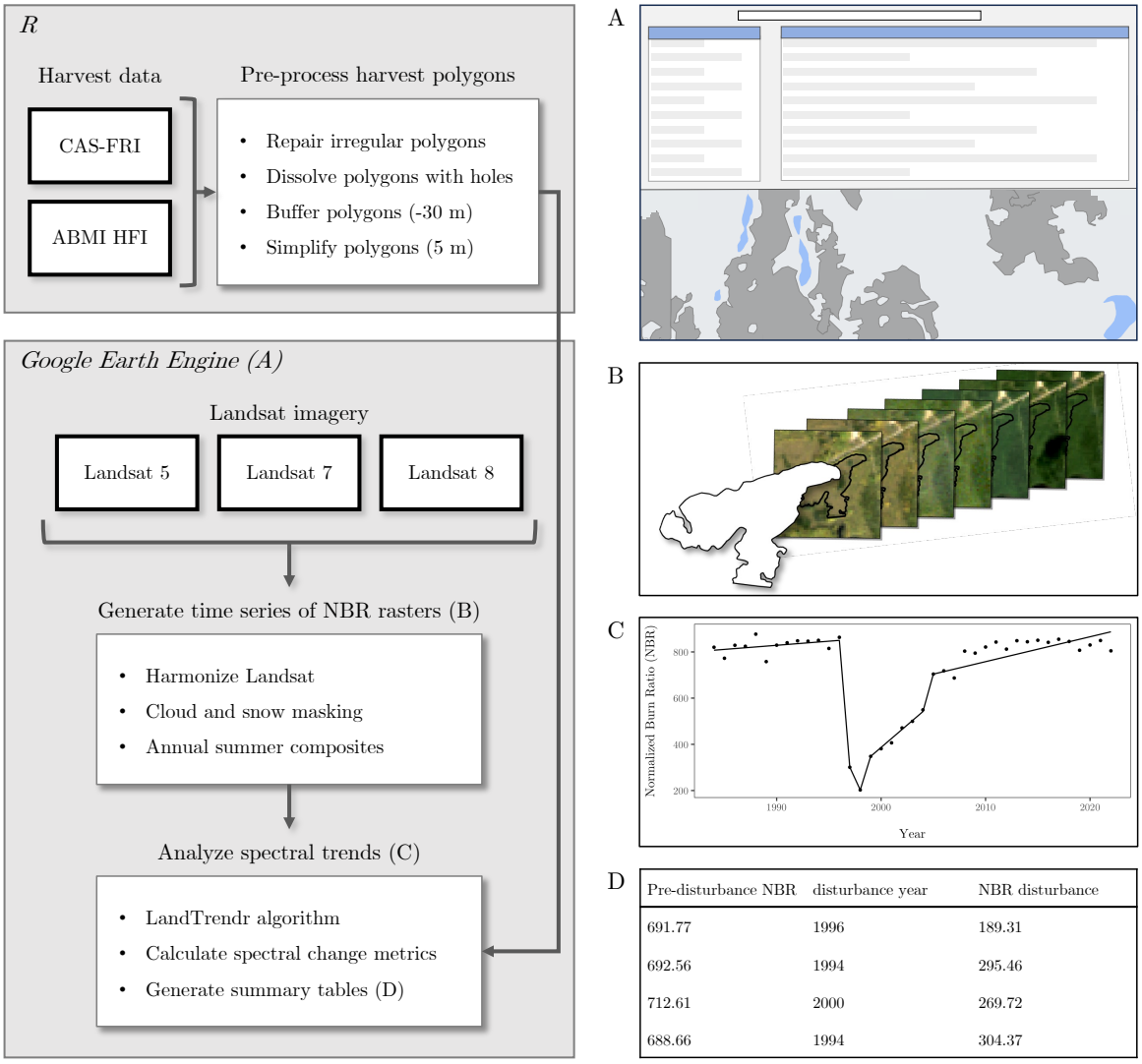

Figure 4.2: The workflow we used to calculate NBR spectral change metrics. We identified harvests using the Common Attribute Schema for Forest Resource Inventories (CAS-FRI) (Cosco, 2011) and the Wall-to-Wall Human Footprint Inventory (HFI) (Alberta Biodiversity Monitoring Institute and Alberta Human Footprint Monitoring Program, 2019). Harvest polygons were preprocessed using R statistical software (R Core Team, 2020) and NBR spectral change metrics were calculated using Google Earth Engine (Gorelick et al., 2017)

cubic terms. Third, we addressed multicollinearity by calculating pairwise Pearson correlation coefficients and VIF scores for all predictors, and iteratively removed highly correlated predictors from the global model. We kept only predictors with low correlation ($r < 0.5$ and VIF < 3). Fourth, we used the *dredge* function from the R package *MuMIn* to assess the performance of models containing combinations of the remaining predictors (Barto, 2020). For each model we calculated pseudo-R2 as an indicator of model fit (Nakagawa & Schielzeth, 2013). The model with the lowest Akaike's Information Criterion (AIC) was selected as the top model (Burnham & Anderson, 2002). Where models had similar AIC values (differing by less than two) we chose the one with the highest pseudo-R^2. Finally, we calculated semi-partial R^2 values for predictor variables using the *r2beta* function from the *r2glmm* R package with standardized general variances.

4.3 Results

Several fixed effects were common across the top models (Table 4.3). Time since harvest and RΔNBR were applied to all the top models, and the interaction between these two variables were included in the top models for richness, functional richness, functional divergence, functional dispersion, and functional evenness. Standard deviation of canopy height and fractional water and shrub cover were common fixed effects that were top contributors to model performance across response variables. In contrast, tree species composition was not predictive of bird communities.

4.3.1 Species diversity

Results show that species richness was negatively associated with the percentage of shrub cover, and positively associated with fractional water and herb cover, and the

Table 4.3: The fixed effects and R^2_{GLMM} (marginal R^2 (R^2m) and conditional R^2 (R^2c) for the top model of each response variable. R^2m is a measure of the variance explained by the fixed effects. R^2c is a measure of variance explained by the full model, both fixed and random effects (Nakagawa & Schielzeth, 2013) .

Response variable	Fixed effects	R^2c	R^2m
Functional dispersion (FDis)	ss_dst_timelag_nbr^2 * RdNBR + dist_to_edge + Exposed_Barren_land	0.55	0.09
Functional divergence (FDiv)	ss_dst_timelag_nbr * RdNBR + dist_to_edge + Shrubs + canopy_standard_deviation	0.44	0.08
Functional evenness (FEve)	ss_dst_timelag_nbr^2:RdNBR + Shrubs + Water + canopy_standard_deviation + lat	0.56	0.05
Functional richness (FRic)	ss_dst_timelag_nbr^2 * RdNBR + Herbs + Water + Shrubs	0.59	0.15
Richness	ss_dst_timelag_nbr^2 * RdNBR + Exposed_Barren_land + Herbs + Shrubs + Water + canopy_standard_deviation	0.40	0.24
Shannon diversity index (shan)	ss_dst_timelag_nbr^2 + RdNBR^2 + Shrubs +Exposed_Barren_land + Water + canopy_standard_deviation	0.71	0.22

standard deviation of canopy height. The top model for species richness included the interaction between RΔNBR and time since harvest as a fixed effect (Figure 4.3). The interaction led to an inverted U-shaped effect curve at levels of RΔNBR <85% with maximum species richness occurring 15 to 20 years post-harvest. At high levels of harvest intensity (>85%) maximum species richness occurred 20 to 25 years post-harvest. After 20 years post-harvest, the top model predicted that species richness in all harvest intensities would converge with the mean species richness of unharvested stands. The linear term for time since harvest was the strongest predictor of species richness (b = 0.197, SE = 0.023, $p < 0.001$, semi-partial R^2 = 0.037), followed by fractional cover of water (b = 0.093, SE = 0.008, $p < 0.001$, semi-partial R^2 = 0.034), and the quadratic term for time since harvest (b = -0.083, SE = 0.016, $p < 0.001$, semi-partial R^2 = 0.014).

4. Bird response to NBR harvest intensity

Shannon diversity index decreased with the percentage of exposed barren land and shrubs, and increased with the standard deviation of canopy height and the fractional cover of water. The response of Shannon diversity to time since harvest was nonlinear and followed an inverted U-shaped effect curve, with maximum Shannon diversity occurring after ≈ 20 years post-harvest for all harvest intensities. The top model for Shannon diversity included a quadratic term for RΔNBR, resulting in a shallow U-shaped effect curve with a minimum harvest intensity of ≈ 45%. However, we found no significant interaction between time since harvest and RΔNBR. After 20 years post-harvest, Shannon diversity in areas with harvest intensities below 75% was predicted to converge with the mean Shannon diversity of unharvested forests. The quadratic term for time since harvest was the strongest predictor of Shannon diversity (b = -0.046, SE = 0.015, $p < 0.01$, semi-partial $R^2 = 0.099$), followed by the proportion of water(b = 0.038, SE = 0.004, $p < 0.001$, semi-partial $R^2 = 0.016$), the linear term for time since harvest ($b = 0.118$, SE = 0.026, $p < 0.001$, semi-partial $R^2 = 0.013$), and the proportion of exposed barren land(b = -0.040, SE = 0.008 , $p < 0.001$, semi-partial $R^2 = 0.002$).

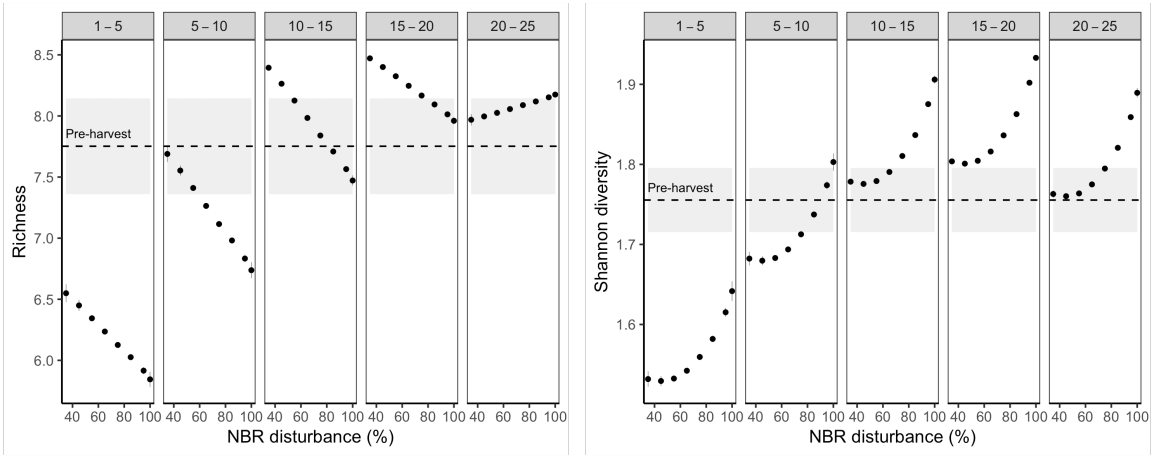

Figure 4.3: Richness and Shannon diversity estimates for all time periods and NBR derived harvest intensities with 95% confidence intervals.

4.3.2 Functional diversity

Functional richness had a negative response to shrub cover and a positive response to fractional cover of water and herbs. Our findings revealed a mild interaction between time since harvest and RΔNBR, leading to an inverted U-shaped curve at harvest intensities > 60%. Peak functional richness was observed 15 to 20 years post-harvest (Figure 4.4. Functional richness approached the mean pre-harvest functional richness level 15 to 20 years post-harvest across all harvest intensities. Among the predictors, fractional cover of water was the strongest predictor of functional richness (b = 0.123, SE = 0.016, $p < 0.001$, semi-partial R^2 = 0.024), followed by the linear term of time since harvest (b = 0.295, SE = 0.065, $p < 0.001$, semi-partial R^2 = 0.020), and fractional shrub cover (b = -0.125, SE = 0.028, $p < 0.001$, semi-partial R^2 = 0.014).

Functional divergence decreased with time since harvest, shrub cover, and the distance to the nearest forested edge, and increased with RΔNBR. The top model for functional divergence included the interaction between time since harvest and RΔNBR. For harvest intensities < 50%, functional divergence converged with the mean functional divergence of unharvested stands after 20 years. Time since harvest was the strongest predictor of functional divergence (b = -0.021, SE = 0.007, $p <$ 0.001, semi-partial R^2 = 0.038), followed by RΔNBR (b = 0.028, SE = 0.006, $p <$ 0.001, semi-partial R^2 = 0.038), and the distance to the nearest forested edge (b = -0.022, SE = 0.002, $p < 0.001$, semi-partial R^2 = 0.028).

Functional dispersion was negatively associated with the percentage of exposed barren land and the distance to the nearest forested edge, and positively associated with RΔNBR. The top model for functional dispersion included a quadratic term for time since harvest, revealing a U-shaped response curve with the highest functional dispersion occurring 10 to 15 years post-harvest. Functional dispersion approached

the levels observed in unharvested stands 20 to 25 years post-harvest. We found no significant interaction effect between time since harvest and RΔNBR on functional dispersion. The linear term of time since harvest was the strongest predictor of functional dispersion (b = 0.070, SE = 0.017, $p < 0.001$, semi-partial R^2 = 0.017), followed by the quadratic term of time since harvest (b = -0.039, SE = -.010, $p <$ 0.001, semi-partial R^2 = 0.017), and the distance to the nearest forested edge (b = -0.021, SE = 0.003, $p < 0.001$, semi-partial R^2 = 0.008)

Functional evenness responded negatively to water, shrubs, and the standard deviation of canopy height. The top model for functional evenness included an interaction between time since harvest and RΔNBR which led to an inverted U-shaped curve for harvest intensities > 50%, with maximum functional evenness observed 15 to 20 years post-harvest. Functional evenness at all harvest intensities approached mean pre-harvest functional evenness 20 to 25 years post-harvest. The interaction between the linear term of time since harvest and RΔNBR was the strongest predictor of functional evenness (b = 0.017, SE = 0.007, $p < 0.01$, semi-partial R^2 = 0.010), followed by the interaction between the quadratic term of time since harvest and RΔNBR (b = -0.008, SE = 0.003, $p < 0.05$, semi-partial R^2 = 0.005), and the standard deviation of canopy height (b = -0.007, SE = 0.004, $p < 0.075$, semi-partial R^2 = 0.001).

4.4 Discussion

Our results suggest that spectral measures of harvest intensity, post-harvest recovery time, and fractional land cover variables associated with low-lying vegetation and water are important drivers of variation in post-harvest bird communities. Our study suggests that harvest residuals can mitigate the impacts of forest harvesting on birds over time. In the short term, i.e., < five years after harvesting, we observed significant

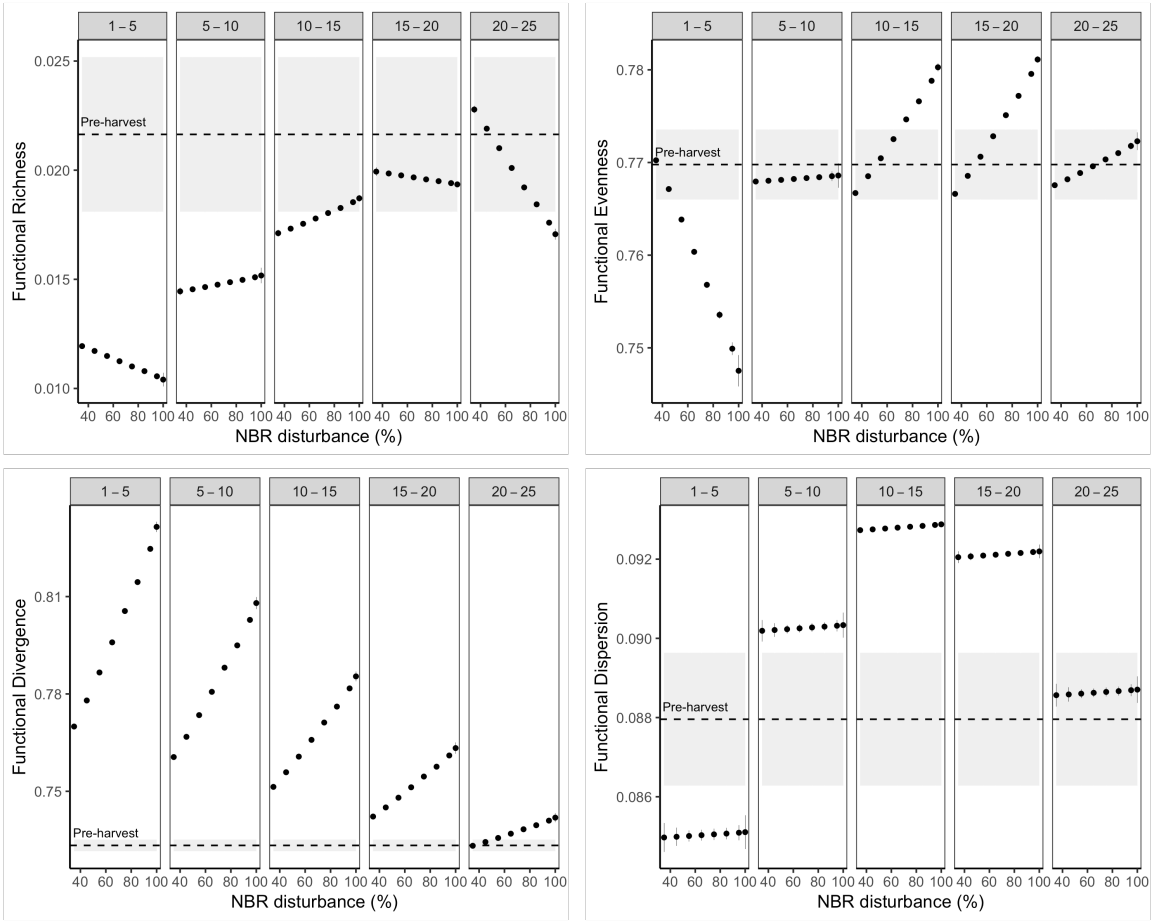

Figure 4.4: Functional diversity estimates for all time periods and NBR derived harvest intensities with 95% confidence intervals.

changes in bird community metrics for harvest intensities ranging from 35% to 100%. However, the rates of community recovery varied depending on the intensity and extent of harvesting. Our analysis revealed strong evidence that harvest residuals accelerated the recovery of bird species richness, functional evenness, and functional divergence. Additionally, across all harvest intensities, taxonomic richness, functional richness, functional dispersion, and functional evenness converged with levels of unharvested reference areas in less than 25 years.

4.4.1 The influence of harvest intensity on diversity

Our study provides evidence that reducing harvest intensity (i.e., spectral change) can hasten the recovery of species diversity in post-harvest stands. We found that the response curves for both richness and Shannon diversity followed an inverted U-shape in relation to time since harvest, with immediate declines observed across all harvest intensities. However, we noted opposing trends between richness and Shannon diversity in response to harvest intensity. Specifically, 1 to 20 years post-harvest, increasing harvest intensity negatively impacted richness, but resulted in higher Shannon diversity. The opposing trends between richness and Shannon diversity we observed may indicate increased evenness in the distribution of species abundances post-harvest (Hill, 1973).

Retention promoted the recovery of species richness. Harvest intensities of less than 60% led to convergence of mean richness with un-harvested mature forest reference areas within 10 years. Shannon diversity at all harvest intensities converged with non-harvested areas within 10 years. However, between 10 and 20 years post-harvest, areas with harvest intensities >75% showed increased Shannon diversity beyond the mean Shannon diversity in un-harvested areas before eventually converging with unharvested areas 25 years post-harvest.

Our findings are consistent with studies that have reported a decrease in species richness following harvests and higher levels of richness in areas with high retention compared to clear-cuts (Fedrowitz et al., 2014; Odsen et al., 2018; Price et al., 2020; Twedt, 2020). This is likely due to harvest residuals increasing the horizontal and vertical vegetation heterogeneity of regenerating stands. Increases in vegetation heterogeneity can expand the niche space, leading to higher bird species richness (Culbert et al., 2013; Tews et al., 2004).

4. Bird response to NBR harvest intensity

Our study revealed complex and contrasting trends between functional diversity indices and harvest intensity over time. Specifically, we found that functional richness exhibited a similar response to that of species richness, with an immediate decline in the size of the communities' functional trait space after harvest, followed by a rapid recovery and convergence with the mean functional richness of unharvested areas after approximately 20 years. However, although our models suggested a mild negative effect of harvest intensity on functional richness, this effect was negligible and did not significantly contribute to the overall model performance. Therefore, our findings suggest that the size of the post-harvest functional trait space is similar across different harvest intensities.

Similar to the results of Leaver et al. (2019) and Edwards et al. (2013), we observed short-term declines in functional evenness (the regularity of the abundance distribution of species with different traits (Villeger et al., 2008)) in areas with harvest intensities $> 50\%$. This could be due to short-term increases in species dominance of cavity-nesting birds and birds that nest and forage in shrubs, as new recruits out-compete other species (Schieck & Song, 2006). In areas with $< 50\%$ harvest intensity, functional evenness did not deviate from the mean functional evenness of unharvested areas across all stages of recovery. This suggests that high amounts of harvest residuals can maintain the relative abundance of functional traits that would otherwise decline with greater harvest intensities.

Conversely, our models showed an increase in functional divergence post-harvest. Functional divergence refers to the extent to which the distribution of individual species abundances maximizes differences between functional traits (Mason et al., 2005). We found that harvest intensity had a positive linear relationship with functional divergence, providing further evidence of the increased dominance of a few

functionally distinct species at higher harvest intensities. While functional divergence decreased across all harvest intensities with time, it did not fully converge with the mean functional divergence of unharvested areas within 25 years post-harvest.

Functional dispersion, a measure of community heterogeneity that estimates the mean distance of species to the centroid of all species in the functional trait space (Laliberté & Legendre, 2010), declined immediately post-harvest, followed by an inverted U-shaped response curve that peaked after 10-15 years and converged with the functional dispersion of unharvested areas after 20 years. Our models suggest that, following an initial decline, functional heterogeneity of communities increases relative to that of unharvested areas before converging after 20 years post-harvest. The increase in functional dispersion we found between 5 and 15 years post-harvest could be associated with the establishment of early-seral specialists as also noted by Swanson et al.(2011).

4.4.2 Convergence with reference areas

The differential response of community metrics to harvest intensity suggests that minimum retention recommendations may depend on the community indices used and the optimal timeline for recovery. Our study found that in the first 10 years after harvesting, harvest intensities of $< 50\%$ reduced changes to species richness, functional richness, functional evenness, and functional dispersion. However, differences between harvest treatments shrank over time and for all harvest intensities, these metrics recovered to non-harvest levels within 25 years. With functional divergence and Shannon diversity, recovery took longer to reach baseline levels. For Shannon diversity, harvest intensities $> 75\%$ did not reach unharvested levels within 25 years. Among the metrics assessed, functional divergence was the slowest to recover, and harvest intensities $> 50\%$ were not predicted to reach baseline levels within 25 years post-

harvest. Our findings align with a growing body of forestry research that shows that even small amounts of retention can reduce community change and accelerate post-harvest recovery (Craig & Macdonald, 2009; Gustafsson et al., 2010; Halpern et al., 2012; Odsen et al., 2018).

4.4.3 Moving forward

Our research shows that spectral measures of disturbance derived from Landsat Time Series (LTS) data, particularly the differences in NBR between pre- and post-disturbance forests, can serve as a useful substitute for common harvest intensity metrics from ground-based stem volume and canopy cover measurements or photo-interpretation of canopy cover; metrics that are often temporally and spatially limited (Bartels et al., 2016; White et al., 2018).

However, while ΔNBR is a useful measure of harvest intensity, it does not distinguish between the various silvicultural treatments present in the landscape. Furthermore, spectral saturation may limit the ability of ΔNBR to detect subtle differences between high-intensity disturbances (Allen & Sorbel, 2008; Delcourt et al., 2021; French et al., 2008). Our study included a variety of treatments, such as understory protection, structural retention, dispersed single-tree retention, and aggregated retention, but we could not differentiate between these treatments when estimating harvest intensity. This is a common limitation in retention studies (Gustafsson et al., 2010; Rosenvald & Lohmus, 2008). Because of its 30m resolution, Landsat alone is insufficient to overcome this challenge. At this resolution, it is hard to identify dispersed residual trees and make precise measurements related to the shape and spatial arrangement of residual patches. However, canopy closure and the availability of large trees are closely linked to percent retention and may compensate for the lack of differentiation between treatments (Vanderwell et al., 2007).

4. Bird response to NBR harvest intensity

Nevertheless, distinguishing between treatments in future research could inform managers about the optimum density and spatial configuration of retained vegetation. For example, aggregated retention may create different habitat conditions than dispersed single tree retention, influencing tree mortality, edge habitat, vegetation heterogeneity, microclimate, and the persistence of mature forest and early successional bird species (Curzon et al., 2020; Fedrowitz et al., 2014; Price et al., 2020; Vanderwell et al., 2007; Venier et al., 2015).

Retention forestry should aim to provide suitable conditions for a range of species representing different functional guilds (Gustafsson et al., 2012). Taxonomic and functional diversity models can be useful for detecting broad patterns and informing forestry management strategies that benefit multiple species simultaneously (Lindenmayer et al., 2007). However, for managing specific taxa, single-species models are often needed to understand the mechanisms driving changes in abundance. Even species with similar functional traits may have unique response patterns to stand age and harvest intensity (Akresh et al., 2021). To gain a more comprehensive understanding of the impact of forestry on birds, future research could take a combined approach that incorporates both single-species and functional diversity response variables.

To better address the needs of forestry managers, future research should also target specific federally listed species at risk or those representative of important functional guilds. Furthermore, comparing natural disturbance regimes like fire with retention forestry is crucial to understanding whether the variability of post-harvest bird communities falls within natural bounds.

4.5 Conclusion

To effectively conserve boreal birds and their habitats, it is crucial to understand the impact of forestry activities on bird populations. Our study used an annual time series of Landsat normalized burn ratio to measure the intensity of forest harvesting and assess its impact on bird functional and taxonomic diversity within recovering harvested areas. While previous studies have used categorical harvest intensity metrics to assess the impacts of retention on bird communities, ours is the first to use continuous spectral measures of harvest intensity. Our findings indicate that retention forestry can mitigate the impacts of forest harvesting on bird communities. Also, including functional indices as response variables provides a more comprehensive understanding of community response compared to relying on taxonomic diversity alone (Mouillot et al., 2013b). Furthermore, we demonstrated the value of LandTrendr, a cloud-based change detection algorithm, as a tool for assessing harvest intensity and recovery in boreal forests. Landsat change metrics derived using LandTrendr are useful alternatives to those from traditional classified land cover maps. The findings show that methods incorporating novel remote sensing algorithms and community functional indices can reveal subtle relationships between forestry practices and bird communities over time.

5
Discussion

In this thesis, I evaluated and compared different sources of predictor variables for SDMs. Additionally, I investigated the response of bird communities to forestry across a range of harvest intensities and successional ages in the boreal region. In Chapter 2, I examined the influence of temporal misalignment between LiDAR acquisitions and bird surveys on the performance of SDMs for early-successional, mature forest, and forest generalist birds. The influence of temporal misalignment on SDMs varied across species, with early-successional associates being the most affected. In Chapter 3, I evaluated the effectiveness of CAS-FRI, LiDAR, and Landsat NBR data for predicting the response of birds in regenerating forest harvest areas. I found that spectral measures of harvest intensity and structural metrics from LiDAR were better predictors of species abundance and diversity compared to commonly used vegetation and disturbance classifications. In Chapter 4, I evaluated the impact of the interaction between forest harvest intensity and recovery time on the taxonomic and functional diversity of birds. I found that harvest residuals can mitigate the impacts of forest harvesting on birds and accelerate the recovery of bird species richness, functional

evenness, and functional divergence within harvest areas. Together, this work shows that bird-habitat models can be improved by including LiDAR and Landsat time-series predictor variables. The findings align with the growing body of literature that applies remote sensing to investigate the abundance and distribution of wildlife (Davies & Asner, 2014; Goetz et al., 2010; He et al., 2015; Sheeren et al., 2014; Simonson et al., 2014; Swatantran et al., 2012; Tattoni et al., 2012; Turner et al., 2003).

In Chapters 2 and 3, I showed the value and limitations of LiDAR predictor variables in bird-habitat models. In Chapter 2, I found that LIDAR-based SDMs are moderately predictive of occupancy for American Redstart (*Setophaga ruticilla*), Black-throated Green Warbler (*Setophaga virens*), Mourning Warbler (*Geothlypis philadelphia*), and White-throated Sparrow (*Zonotrichia albicollis*). Chapter 3 used LIDAR to characterize conditions within harvest blocks, leading to improved model performance for eight of the twenty focal species including Alder Flycatcher (*Empidonax alnorum*), Black-throated Green Warbler (*Setophaga virens*), LeConte's Sparrow (*Ammospiza leconteii*), Lincoln's Sparrow (*Melospiza lincolnii*), Philadelphia Vireo (*Vireo philadelphicus*), Swainson's Thrush (*Catharus ustulatus*), Warbling Vireo (*Vireo gilvus*), Winter Wren (*Troglodytes hiemalis*).

The top-performing LiDAR predictors varied among species, but frequently included maximum vegetation height, the 50th percentile of canopy height, and the coefficient of variation of LiDAR return heights. These variables explained more model variance compared to variables derived from land cover maps, such as vegetation composition and the shape, area, and perimeter-area ratio of harvest polygons. Similar findings by Farrell et al. (2013), Ficetola et al. (2014), and Muller et al. (2010) have shown that LiDAR metrics outperform plant species composition and other classified land cover metrics for predicting bird response.

LiDAR metrics corresponding to vegetation density, such as the proportion of LiDAR vegetation returns below two meters, were highly variable in their contribution to model performance. These variables were most valuable in modeling the response of bird species closely associated with dense shrub vegetation, including the Mourning Warbler, Alder Flycatcher, and Winter Wren. Also, the effectiveness of specific predictor variables was not generalizable across species, consistent with the findings of Koma et al. (2022) and Tattoni et al. (2012).

Chapter 2 showed that the influence of LiDAR-point count temporal misalignment on the performance of SDMs varied across species. For early-successional birds, temporal misalignment had a strong negative influence on model performance, indicating that LiDAR-point count time lag should be limited to less than five years. Conversely, temporal misalignment had little impact on SDMs for forest generalists. Regarding mature forests birds, although LiDAR temporal misalignment had a significant impact on models for Black-throated Green Warbler, they remained moderately predictive, even with fifteen years between LiDAR and bird surveys. These findings are consistent with previous studies conducted by Hill and Hinsley (2015) and Vierling et al. (2014).

While the findings indicated that the impact of LiDAR temporal misalignment varies depending on the nesting and feeding characteristics of the focal species, Chapter 3 of this thesis revealed no consistent pattern in the performance of LiDAR predictor variables across different feeding and nesting guilds. This was unexpected and contrasts with studies suggesting that the applicability of LiDAR metrics is generalizable to the habitat guild of the study species (Davies & Asner, 2014; Lesak et al., 2011).

Chapters 3 and 4 provided evidence that spectral change metrics from NBR can serve as a proxy for the disturbance intensity categories found in forest resource inventories. In Chapter 3, I found that for most response variables, LiDAR vege-

tation metrics were less predictive of bird abundance and diversity than successional indicators like time since harvest and ΔNBR. This suggests that studies relying solely on percent disturbed and time since harvest categories to assess the impacts of different harvest regimes would not significantly benefit from incorporating LiDAR predictors. Alternatively, studies would benefit from replacing harvest categories with measures of disturbance derived from Landsat Time Series (LTS) data, particularly the NBR differences between pre- and post-disturbance forest (Bartels et al., 2016; White et al., 2018).

In Chapter 4, when NBR was used to explore the impacts of retention forestry, I found complex and contrasting trends between functional diversity indices and the interaction between harvest intensity and time since harvest. Here I found evidence that harvest residuals can mitigate the impacts of forest harvesting on birds. Within the initial five years following harvesting, the presence of residuals reduced changes in taxonomic richness, functional richness, functional evenness, and functional dispersion. Moreover, the rates of recovery for these metrics were positively associated with higher amounts of harvest residuals. Across all harvest intensities, taxonomic richness, functional richness, functional dispersion, and functional evenness converged with the levels observed in unharvested reference areas in a timeframe of less than 25 years.

These findings are consistent with a growing body of research highlighting the positive contribution of retention forestry to the recovery of bird communities following harvests (Craig & Macdonald, 2009; Gustafsson et al., 2010; Halpern et al., 2012). For example, studies have reported that retention harvesting promotes greater species richness in post-harvest communities compared to clear-cut areas (Fedrowitz et al., 2014; Odsen et al., 2018; Price et al., 2020; Twedt, 2020). However, the application of functional diversity response variables in studying the effects of forestry in the boreal region remains limited, with most studies focusing on taxonomic richness or

the abundance of specific focal species. Given the findings from Chapter 4, functional diversity indices have the potential to provide a more nuanced understanding of post-harvest bird communities compared to the commonly used taxonomic diversity indices. How one measures a community matters (Becik et al., 2020; Meynard et al., 2011), and I observed that different aspects of the post-harvest community, as indicated by the seven taxonomic and functional diversity response variables included in the study, exhibited varying recovery rates and response curves. For example, while species richness recovered within 25 years after harvesting, functional divergence remained higher than baseline levels during the same period.

While we found NBR change metrics useful for evaluating the stand level impacts of forestry on birds, the improved predictions of unclassified NBR metrics come at the cost of ecological interpretability (Li & Wu, 2004). While ΔNBR is a useful measure of harvest intensity, it does not distinguish between specific silvicultural treatments, like dispersed single-tree retention, aggregated retention, structural retention, and understory protection (Groot et al., 2005). This issue is not unique to the use of ΔNBR. Retention studies that use classified disturbance metrics rarely distinguish between specific forestry practices (Gustafsson et al., 2010; Rosenvald & Lohmus, 2008).

Unfortunately, failing to account for treatment types makes it harder to produce actionable recommendations on the optimum density and spatial configuration of retained vegetation. Future work should reference specific treatment types to better inform sustainable forest management practice.

Regarding LiDAR, future research should assess the differential strength of LiDAR predictor variables across avian feeding and nesting guilds. While LiDAR is increasingly being used in avian SDMs (Davies & Asner, 2014), the generality of LiDAR for modelling birds is unclear. The type and number of LiDAR metrics included in

avian models varies between studies. Many use LiDAR to more precisely measure variables already available from other sources (i.e. tree height), while others use novel metrics to describe structural elements not available from traditional photogrammetry (i.e. strata density). The importance of including novel versus more precise measures of structural variables likely depends on a species niche and life history. For example, Vogeler et al. (2014) examined the relationships between richness of nesting guilds and a suite of height and density metrics and found understory vegetation density was far more important for understanding ground nesters than tree height, and Weisberg et al. (2014) found that measures of habitat heterogeneity are stronger predictors of richness of foliage foragers than ground foragers. This contrasts with my findings from Chapter 3, where I did not observe any generalizable trends in metric use by guild. More research is needed and would help inform variable selection in future studies.

In Chapter 3, the inclusion of remote sensing predictor variables from various sources improved the predictive models for eight out of the twenty focal species. This makes sense as each source (CAS-FRI, LiDAR, and a time-series of Landsat NBR) captures different habitat characteristics that influence birds, such as successional stage, vertical structure, and vegetation resources. Previous studies, as discussed in Chapter 3, have also emphasized the benefits of integrating a variety of remote sensing data in species ecology (Hill & Thomson, 2005; Koma et al., 2022; Swatantran et al., 2012). By incorporating multiple technologies, researchers can expand the spatial and temporal scales at which they study ecological patterns and processes (Marvin et al., 2016). For future studies, I recommend supplementing classified land cover data with unclassified remote sensing data that matches the spatiotemporal resolution of the response variable and captures essential habitat features often overlooked by traditional sources. This can enhance the predictive capabilities of models while also

reducing the per-area costs of analyses (Asner et al., 2014; Marvin et al., 2016).

In recent years, wildlife biologists have advanced bird habitat models by reducing errors in response variables. Wildlife biologists have improved automated species recognition (Knight et al., 2020), developed methods for addressing imperfect detections (Sólymos et al., 2013; Yip et al., 2019), and improved acoustic localization (Wilson & Bayne, 2018). However, my work shows that greater attention is needed to enhance habitat covariates, including their accuracy, spatiotemporal resolution, and ecological relevance. The reliance on classified land cover maps is outdated, and biologists should use modern resources like cloud computing and multi-source multi-temporal remote sensing data.

Fine scale data at continental extents are often necessary to fully understand the mechanisms driving bird distributions. (Rose et al., 2015). With the availability of broad scale wall-to-wall remote sensing products and advances in cloud-based computing, SDMs can now be built using multi-source spatial data over large spatial extents. Publicly funded data like Landsat, Sentinel, and, increasingly, wall-to-wall LiDAR, have removed some of the spatial and cost constraints that once limited the use of remote sensing in SDMs (Burns et al., 2020; Coops et al., 2016).

Advancements in GIS and cloud computing have improved the analytical capabilities of researchers (Randin et al., 2020). For example, cloud computing platforms like Google Earth Engine, have given users cost-efficient ways to access and process high resolution remote sensing data over large areas and time-frames (Gomes et al., 2020; Randin et al., 2020). These platforms enable researchers to perform the computationally intensive tasks necessary for extracting important predictors related to climate, topography, land cover, disturbance history, and vegetation structure (He et al., 2015; Roy et al., 2019). By combining these predictors with large-scale, long-

term bird monitoring data, researchers can develop models that better describe how birds respond to habitat change.

References

Abdalati, W., Zwally, H. J., Bindschadler, R., Csatho, B., Farrell, S. L., Fricker, H. A., Harding, D., Kwok, R., Lefsky, M., Markus, T., Marshak, A., Neumann, T., Palm, S., Schutz, B., Smith, B., Spinhirne, J., & Webb, C. (2010). The ICESat-2 Laser Altimetry Mission. *Proceedings of the IEEE*, *98*(5), 735–751. https://doi.org/10.1109/jproc.2009.2034765

Ackers, S. H., Davis, R. J., Olsen, K. A., & Dugger, K. M. (2015). The evolution of mapping habitat for northern spotted owls (*Strix occidentalis caurina*): A comparison of photo-interpreted, Landsat-based, and lidar-based habitat maps. *Remote Sensing of Environment*, *156*, 361–373. https://doi.org/10.1016/j.rse.2014.09.025

Akresh, M. E., King, D. I., Lott, C. A., Larkin, J. L., & D'Amato, A. W. (2021). A meta-analysis of the effects of tree retention on shrubland birds. *Forest Ecology and Management*, *483*, 118730. https://doi.org/10.1016/j.foreco.2020.118730

Alberta Biodiversity Monitoring Institute and Alberta Human Footprint Monitoring Program. (2019). *Wall-to-Wall Human Footprint Inventory 2019*.

Alberta Environment and Sustainable Resource Development. (2013). *General specifications for acquisition of LiDAR data*. Government of Alberta.

Alberta, G. of. (2022). *Historical Wildfire Perimeter Data: 1931 – 2021*. https://www.alberta.ca/wildfire-maps-and-data.aspx

Alldredge, M. W., Pollock, K. H., Simons, T. R., Collazo, J. A., & Shriner, S. A. (2007). Time-of-detection method for estimating abundance from point-count surveys. *The Auk*, *124*(2), 653–664. https://doi.org/10.1642/0004-8038(2007)124%7B%

5B%7D653:TMFEAF%5D2.0.CO;2

Allen, J. L., & Sorbel, B. (2008). Assessing the differenced Normalized Burn Ratio's ability to map burn severity in the boreal forest and tundra ecosystems of Alaska's national parks. *International Journal of Wildland Fire*, *17*(4), 463–475. https://doi.org/10.1071/WF08034

Araújo, M. B., Anderson, R. P., Márcia Barbosa, A., Beale, C. M., Dormann, C. F., Early, R., Garcia, R. A., Guisan, A., Maiorano, L., Naimi, B., et al. (2019). Standards for distribution models in biodiversity assessments. *Science Advances*, *5*(1). https://doi.org/10.1126/sciadv.aat4858

Arnberg, M. P., Patten, M. A., Klanderud, K., Haddad, C., Larsen, O., & Steyaert, S. M. (2023). Perfect poopers; passerine birds facilitate sexual reproduction in clonal keystone plants of the boreal forest through directed endozoochory towards dead wood. *Forest Ecology and Management*, *532*, 120842. https://doi.org/10.1016/j.foreco.2023.120842

Asner, G. P., Knapp, D. E., Martin, R. E., Tupayachi, R., Anderson, C. B., Mascaro, J., Sinca, F., Chadwick, K. D., Higgins, M., Farfan, W., et al. (2014). Targeted carbon conservation at national scales with high-resolution monitoring. *Proceedings of the National Academy of Sciences*, *111*(47), E5016–E5022. https://doi.org/10.1073/pnas.1419550111

Atwell, R. C., Schulte, L. A., & Palik, B. J. (2008). Songbird response to experimental retention harvesting in red pine (*Pinus resinosa*) forests. *Forest Ecology and Management*, *255*(10), 3621–3631. https://doi.org/10.1016/j.foreco.2008.02.049

Aubin, I., Venier, L., Pearce, J., & Moretti, M. (2013). Can a trait-based multi-taxa approach improve our assessment of forest management impact on biodiversity? *Biodiversity and Conservation*, *22*(12), 2957–2975. https://doi.org/10.1007/s10531-013-0565-6

Austin, M. (2007). Species distribution models and ecological theory: A critical assessment and some possible new approaches. *Ecological Modelling*, *200*(1-2),

1–19. https://doi.org/10.1016/j.ecolmodel.2006.07.005

Babcock, C., Finley, A. O., Cook, B. D., Weiskittel, A., & Woodall, C. W. (2016). Modeling forest biomass and growth: Coupling long-term inventory and LiDAR data. *Remote Sensing of Environment*, *182*, 1–12. https://doi.org/10.1016/j.rse.2016.04.014

Bae, S., Müller, J., Lee, D., Vierling, K. T., Vogeler, J. C., Vierling, L. A., Hudak, A. T., Latifi, H., & Thorn, S. (2018). Taxonomic, functional, and phylogenetic diversity of bird assemblages are oppositely associated to productivity and heterogeneity in temperate forests. *Remote Sensing of Environment*, *215*(June), 145–156. https://doi.org/10.1016/j.rse.2018.05.031

Bae, S., Reineking, B., Ewald, M., & Mueller, J. (2014). Comparison of airborne lidar, aerial photography, and field surveys to model the habitat suitability of a cryptic forest species – the hazel grouse. *International Journal of Remote Sensing*, *35*(17), 6469–6489. https://doi.org/10.1080/01431161.2014.955145

Bailey, S.-A., Horner-Devine, M., Luck, G., Moore, L., Carney, K., Anderson, S., Betrus, C., & Fleishman, E. (2004). Primary productivity and species richness: Relationships among functional guilds, residency groups and vagility classes at multiple spatial scales. *Ecography*, *27*(2), 207–217. https://doi.org/10.1111/j.0906-7590.2004.03631.x

Baker, S. C., & Read, S. M. (2011). Australian forestry variable retention silviculture in Tasmania's wet forests: Ecological rationale, adaptive management and synthesis of biodiversity benefits. *Australian Forestry*, *74*(3), 218–232. https://doi.org/10.1080/00049158.2011.10676365

Baker, T. P., Jordan, G. J., & Baker, S. C. (2016). Microclimatic edge effects in a recently harvested forest: Do remnant forest patches create the same impact as large forest areas? *Forest Ecology and Management*, *365*, 128–136. https://doi.org/10.1016/j.foreco.2016.01.022

Baker, T. P., Jordan, G. J., Steel, E. A., Fountain-Jones, N. M., Wardlaw, T. J., & Baker, S. C. (2014). Microclimate through space and time: Microclimatic

variation at the edge of regeneration forests over daily, yearly and decadal time scales. *Forest Ecology and Management*, *334*, 174–184. https://doi.org/10.1016/j.foreco.2014.09.008

Bale, S., Beazley, K. F., Westwood, A., & Bush, P. (2020). The benefits of using topographic features to predict climate-resilient habitat for migratory forest landbirds: An example for the Rusty Blackbird, Olive-sided Flycatcher, and Canada Warbler. *The Condor*, *122*(1), duz057. https://doi.org/10.1093/condor/duz057

Barnes, K. W., Islam, K., & Auer, S. A. (2016). Integrating LIDAR-derived canopy structure into cerulean warbler habitat models. *Journal of Wildlife Management*, *80*(1), 101–116. https://doi.org/10.1002/jwmg.995

Bartels, S. F., Chen, H. Y. H., Wulder, M. A., & White, J. C. (2016). Trends in post-disturbance recovery rates of Canada's forests following wildfire and harvest. *Forest Ecology and Management*, *361*, 194–207. https://doi.org/10.1016/j.foreco.2015.11.015

Barto, K. (2020). *MuMIn: Multi-model inference* [Manual]. https://CRAN.R-project.org/package=MuMIn

Bates, D., Mächler, M., Bolker, B., & Walker, S. (2015). Fitting linear mixed-effects models using lme4. *Journal of Statistical Software*, *67*(1), 1–48. https://doi.org/10.18637/jss.v067.i01

Bayne, E. M., Haché, S., & Hobson, K. A. (2010). Comparing the predictive capability of forest songbird habitat models based on remotely sensed versus ground-based vegetation information. *Canadian Journal of Forest Research*, *40*(1), 65–71. https://doi.org/10.1139/x09-170

Becik, M., Lenda, M., Amano, T., & Skórka, P. (2020). Different response of the taxonomic, phylogenetic and functional diversity of birds to forest fragmentation. *Scientific Reports*, *10*(1), 20320. https://doi.org/10.1038/s41598-020-76917-2

Bergen, K. M., Goetz, S. J., Dubayah, R. O., Henebry, G. M., Hunsaker, C. T., Imhoff, M. L., Nelson, R. F., Parker, G. G., & Radeloff, V. C. (2009). Remote sensing

of vegetation 3-D structure for biodiversity and habitat: Review and implications for lidar and radar spaceborne missions. *Journal of Geophysical Research*, *114*. https://doi.org/10.1029/2008jg000883

Bergeron, Y., & Fenton, N. J. (2012). Boreal forests of eastern Canada revisited: Old growth, nonfire disturbances, forest succession, and biodiversity. *Botany*, *90*(6), 509–523. https://doi.org/10.1139/b2012-034

Blancher, P., & Wells, J. (2005). *The boreal forest region: North America's bird nursery*. Canadian Boreal Initiative.

Boreal Avian Modelling Project. (2018). *Boreal Avian Modelling Project*. http://www.borealbirds.ca/

Bost, D. S., Reilly, M. J., Jules, E. S., DeSiervo, M. H., Yang, Z., & Butz, R. J. (2019). Assessing spatial and temporal patterns of canopy decline across a diverse montane landscape in the Klamath Mountains, CA, USA using a 30-year Landsat time series. *Landscape Ecology*, *34*, 2599–2614. https://doi.org/10.1007/s10980-019-00907-7

Boyce, M. S., Vernier, P. R., Nielsen, S. E., & Schmiegelow, F. K. A. (2002). Evaluating resource selection functions. *Ecological Modelling*, *157*(2-3), 281–300. https://doi.org/10.1016/s0304-3800(02)00200-4

Bradbury, R. B., Hill, R. A., Mason, D. C., Hinsley, S. A., Wilson, J. D., Balzter, H., Anderson, G. Q. A., Whittingham, M. J., Davenport, I. J., & Bellamy, P. E. (2005). Modelling relationships between birds and vegetation structure using airborne LiDAR data: A review with case studies from agricultural and woodland environments. *Ibis*, *147*(3), 443–452. https://doi.org/10.1111/j.1474-919x.2005.00438.x

Bradley, B. A., & Fleishman, E. (2008). Can remote sensing of land cover improve species distribution modelling? *Journal of Biogeography*, *35*(7), 1158–1159. https://doi.org/10.1111/j.1365-2699.2008.01928.x

Brandt, J. P., Flannigan, M. D., Maynard, D. G., Thompson, I. D., & Volney, W. J.

A. (2013). An introduction to Canada's boreal zone: Ecosystem processes, health, sustainability, and environmental issues. *Environmental Reviews*, *21*(4), 207–226. https://doi.org/10.1139/er-2013-0040

Brassard, B. W., & Chen, H. Y. H. (2010). *Stand Structure and Composition Dynamics of Boreal Mixedwood Forest: Implications for Forest Management*. Sustainable Forest Management Network. https://doi.org/https://doi.org/10.7939/R3HR7R

Brawn, J. D., Robinson, S. K., & Thompson III, F. R. (2001). The role of disturbance in the ecology and conservation of birds. *Annual Review of Ecology and Systematics*, *32*(1), 251–276. https://doi.org/10.1146/annurev.ecolsys.32.081501.114031

Bregman, T., Lees, A., MacGregor, H., Darski, B., Moura, N. de, Aleixo, A., Barlow, J., & Tobias, J. (2016). Using avian functional traits to assess the impact of land-cover change on ecosystem processes linked to resilience in tropical forests. *Proceedings of the Royal Society Biological Sciences*, *283*(1844). https://doi.org/10.1098/rspb.2016.1289

Brodie, S. J., Thorson, J. T., Carroll, G., Hazen, E. L., Bograd, S., Haltuch, M. A., Holsman, K. K., Kotwicki, S., Samhouri, J. F., Willis-Norton, E., et al. (2020). Trade-offs in covariate selection for species distribution models: A methodological comparison. *Ecography*, *43*(1), 11–24. https://doi.org/10.1111/ecog.04707

Buckland, S. T., Anderson, D. R., Burnham, K. P., Laake, J. L., Borchers, D. L., Thomas, L., et al. (2001). *Introduction to distance sampling: Estimating abundance of biological populations*. Oxford University Press.

Burnham, K. P., & Anderson, D. R. (2002). *Model selection and multimodel inference: A practical information-theoretic approach* (Vol. 2). Springer, New York.

Burns, P., Clark, M., Salas, L., Hancock, S., Leland, D., Jantz, P., Dubayah, R., & Goetz, S. J. (2020). Incorporating canopy structure from simulated GEDI lidar into bird species distribution models. *Environmental Research Letters*, *15*(9), 095002. https://doi.org/10.1088/1748-9326/ab80ee

Büttner, G. (2014). CORINE land cover and land cover change products. *Land Use and Land Cover Mapping in Europe: Practices & Trends*, 55–74. https://doi.org/10.1007/978-94-007-7969-3_5

Cadotte, M. W., Carscadden, K., & Mirotchnick, N. (2011). Beyond species: Functional diversity and the maintenance of ecological processes and services. *Journal of Applied Ecology*, *48*(5), 1079–1087. https://doi.org/10.1111/j.1365-2664.2011.02048.x

Campos-Cerqueira, M., & Aide, T. M. (2016). Improving distribution data of threatened species by combining acoustic monitoring and occupancy modelling. *Methods in Ecology and Evolution*, *7*(11), 1340–1348. https://doi.org/10.1111/2041-210x.12599

Carrascal, L., & Diaz, L. (2006). Winter bird distribution in abiotic and habitat structural gradients: A case study with Mediterranean montane oakwoods. *Ecoscience*, *13*(1), 100–110. https://doi.org/10.2980/1195-6860(2006)13%5B100:wbdiaa%5D2.0.co;2

Carrillo-Rubio, E., Kéry, M., Morreale, S. J., Sullivan, P. J., Gardner, B., Cooch, E. G., & Lassoie, J. P. (2014). Use of multispecies occupancy models to evaluate the response of bird communities to forest degradation associated with logging. *Conservation Biology*, *28*(4), 1034–1044. https://doi.org/10.1111/cobi.12261

Casey, B., & Bayne, E. (2022a). Predicting avian response to forest harvesting using the Normalized Burn Ratio [Unpublished manuscript]. *University of Alberta*.

Casey, B., & Bayne, E. (2022b). Predicting the effects of forestry on birds using forest resource inventories, LiDAR, and Landsat. *University of Alberta*.

Casey, B., & Bayne, E. (2022c). The influence of time-lag between LiDAR and wildlife survey data on species distribution models [Unpublished manuscript]. *University of Alberta*.

Chan-Mcleod, A. C. A., & Moy, A. (2007). Evaluating residual tree patches as stepping stones and short-term refugia for red-legged frogs. *Journal of Wildlife Management*,

71(6), 1836–1844. https://doi.org/10.2193/2006-309

Chaparro, L., Schmieder, K., & Schurr, F. M. (2022). The value of remotely sensed vs. Field-surveyed habitat structure for predicting bird abundance: A case study in traditional orchards. *Journal of Ornithology*, *163*(3), 723–733. https://doi.org/10.1007/s10336-022-01970-9

Clawges, R., Vierling, K., Vierling, L., & Rowell, E. (2008). The use of airborne lidar to assess avian species diversity, density, and occurrence in a pine/aspen forest. *Remote Sensing of Environment*, *112*(5), 2064–2073. https://doi.org/10.1016/j.rse.2007.08.023

Cohen, W. B., & Goward, S. N. (2004). Landsat's role in ecological applications of remote sensing. *Bioscience*, *54*(6), 535–545. https://doi.org/10.1641/0006-3568(2004)054%5B0535:lrieao%5D2.0.co;2

Cohen, W. B., Yang, Z., Healey, S. P., Kennedy, R. E., & Gorelick, N. (2018). A LandTrendr multispectral ensemble for forest disturbance detection. *Remote Sensing of Environment*, *205*, 131–140. https://doi.org/10.1016/j.rse.2017.11.015

Connor, T., Hull, V., Viña, A., Shortridge, A., Tang, Y., Zhang, J., Wang, F., & Liu, J. (2018). Effects of grain size and niche breadth on species distribution modeling. *Ecography*, *41*(8), 1270–1282. https://doi.org/10.1111/ecog.03416

Coops, N. C., Tompaski, P., Nijland, W., Rickbeil, G. J. M., Nielsen, S. E., Bater, C. W., & Stadt, J. J. (2016). A forest structure habitat index based on airborne laser scanning data. *Ecological Indicators*, *67*, 346–357. https://doi.org/10.1016/j.ecolind.2016.02.057

Cosco, J. A. (2011). *Common Attribute schema (CAS) for forest inventories across Canada*. Boreal Avian Modelling Project; Canadian BEACONs Project.

Craig, A., & Macdonald, S. E. (2009). Threshold effects of variable retention harvesting on understory plant communities in the boreal mixedwood forest. *Forest Ecology and Management*, *258*(12), 2619–2627. https://doi.org/10.1016/j.

foreco.2009.09.019

Crawford, H. S., & Jennings, D. T. (1989). Predation by birds on spruce budworm Choristoneura fumiferana: Functional, numerical, and total responses. *Ecology*, *70*(1), 152–163. https://doi.org/10.2307/1938422

Culbert, P. D., Radeloff, V. C., Flather, C. H., Kellndorfer, J. M., Rittenhouse, C. D., & Pidgeon, A. M. (2013). The influence of vertical and horizontal habitat structure on nationwide patterns of avian biodiversity. *The Auk*, *130*(4), 656–665. https://doi.org/10.1525/auk.2013.13007

Cumming, S., Lefevre, K. L., Bayne, E., Fontaine, T., Schmiegelow, F. K. A., & Song, S. J. (2010a). Toward conservation of Canada's boreal forest avifauna: Design and application of ecological models at continental extents. *Avian Conservation and Ecology*, *5*(2), 8. https://doi.org/10.5751/ace-00406-050208

Cumming, S., Schmiegelow, F., Bayne, E., & Song, S. (2010b). *Canada's forest resource inventories: Compiling a tool for boreal ecosystems analysis and modelling.* Boreal Avian Modelling Project.

Curzon, M. T., Kern, C. C., Baker, S. C., Palik, B. J., & D'Amato, A. W. (2020). Retention forestry influences understory diversity and functional identity. *Ecological Applications*, eap.2097. https://doi.org/10.1002/eap.2097

Davies, A. B., & Asner, G. P. (2014). Advances in animal ecology from 3D-LiDAR ecosystem mapping. *Trends in Ecology and Evolution*, *29*(12), 681–691. https://doi.org/10.1016/j.tree.2014.10.005

Delcourt, C. J., Combee, A., Izbicki, B., Mack, M. C., Maximov, T., Petrov, R., Rogers, B. M., Scholten, R. C., Shestakova, T. A., Wees, D. van, et al. (2021). Evaluating the differenced normalized burn ratio for assessing fire severity using Sentinel-2 imagery in Northeast Siberian Larch Forests. *Remote Sensing*, *13*(12), 2311. https://doi.org/10.3390/rs13122311

Dorazio, R. M. (2014). Accounting for imperfect detection and survey bias in statistical analysis of presence-only data. *Global Ecology and Biogeography*, *23*(12), 1472–

1484. https://doi.org/10.1111/geb.12216

Dubayah, R., Blair, J. B., Goetz, S., Fatoyinbo, L., Hansen, M., Healey, S., Hofton, M., Hurtt, G., Kellner, J., Luthcke, S., Armston, J., Tang, H., Duncanson, L., Hancock, S., Jantz, P., Marselis, S., Patterson, P. L., Qi, W., & Silva, C. (2020). The Global Ecosystem Dynamics Investigation: High-resolution laser ranging of the Earth's forests and topography. *Science of Remote Sensing*, *1*, 100002. https://doi.org/10.1016/j.srs.2020.100002

Edwards, F. A., Edwards, D. P., Hamer, K. C., & Davies, R. G. (2013). Impacts of logging and conversion of rainforest to oil palm on the functional diversity of birds in Sundaland. *Ibis*, *155*(2), 313–326. https://doi.org/10.1111/ibi.12027

Elith, J., & Leathwick, J. R. (2009). Species distribution models: Ecological explanation and prediction across space and time. *Annual Review of Ecology, Evolution, and Systematics*, *40*(1), 677–697. https://doi.org/10.1146/annurev.ecolsys.110308.120159

Elith, J., Leathwick, J. R., & Hastie, T. (2008). A working guide to boosted regression trees. *Journal of Animal Ecology*, *77*(4), 802–813. https://doi.org/10.1111/j.1365-2656.2008.01390.x

Engler, J. O., Stiels, D., Schidelko, K., Strubbe, D., Quillfeldt, P., & Brambilla, M. (2017). Avian SDMs: Current state, challenges, and opportunities. *Journal of Avian Biology*, *48*(12), 1483–1504. https://doi.org/10.1111/jav.01248

Evans, K. L., James, N. A., & Gaston, K. J. (2006). Abundance, species richness and energy availability in the North American avifauna. *Global Ecology and Biogeography*, *15*(4), 372–385. https://doi.org/10.1111/j.1466-822x.2006.00228.x

Evans, K. L., Newson, S. E., Storch, D., Greenwood, J. J., & Gaston, K. J. (2008). Spatial scale, abundance and the species–energy relationship in British birds. *Journal of Animal Ecology*, *77*(2), 395–405. https://doi.org/10.1111/j.1365-2656.2007.01332.x

Falls, J., & Kopachena, J. (2020). White-throated Sparrow (Zonotrichia albicollis),

version 1.0. In *Birds of the World (A. F. Poole, Editor)* (Vol. 1). Cornell Lab of Ornithology.

Farrell, S. L., Collier, B. A., Skow, K. L., Long, A. M., Campomizzi, A. J., Morrison, M. L., Hays, K. B., & Wilkins, R. N. (2013). Using LiDAR-derived vegetation metrics for high-resolution, species distribution models for conservation planning. *Ecosphere*, *4*(3), 42. https://doi.org/10.1890/es12-000352.1

Fedrowitz, K., Koricheva, J., Baker, S. C., Lindenmayer, D. B., Palik, B., Rosenvald, R., Beese, W., Franklin, J. F., Kouki, J., Macdonald, E., Messier, C., Sverdrup-Thygeson, A., & Gustafsson, L. (2014). Can retention forestry help conserve biodiversity? A meta-analysis. *Journal of Applied Ecology*, *51*, 1669–1679. https://doi.org/10.1111/1365-2664.12289

Ferrier, S., Jetz, W., & Scharlemann, J. (2017). Biodiversity modelling as part of an observation system. *The GEO Handbook on Biodiversity Observation Networks*, 239–257. https://doi.org/10.1007/978-3-319-27288-7_10

Ferrier, S., Watson, G., Pearce, J., & Drielsma, M. (2002). Extended statistical approaches to modelling spatial pattern in biodiversity in northeast New South Wales. I. Species-level modelling. *Biodiversity & Conservation*, *11*, 2275–2307.

Ficetola, G. F., Bonardi, A., Mücher, C. A., Gilissen, N. L. M., & Padoa-Schioppa, E. (2014). How many predictors in species distribution models at the landscape scale? Land use versus LiDAR-derived canopy height. *International Journal of Geographical Information Science*, *28*(8), 1723–1739. https://doi.org/10.1080/13658816.2014.891222

Foga, S., Scaramuzza, P. L., Guo, S., Zhu, Z., Dilley, R. D., Jr., Beckmann, T., Schmidt, G. L., Dwyer, J. L., Hughes, M. J., & Laue, B. (2017). Cloud detection algorithm comparison and validation for operational Landsat data products. *Remote Sensing of Environment*, *194*, 379–390. https://doi.org/10.1016/j.rse.2017.03.026

Foody, G. M. (2002). Status of land cover classification accuracy assessment. *Remote Sensing of Environment*, *80*(1), 185–201. https://doi.org/10.1016/s003

4-4257(01)00295-4

Fourcade, Y., Besnard, A. G., & Secondi, J. (2018). Paintings predict the distribution of species, or the challenge of selecting environmental predictors and evaluation statistics. *Global Ecology and Biogeography*, *27*(2), 245–256. https://doi.org/10.1111/geb.12684

Fox, G. A., Negrete-Yankelevich, S., & Sosa, V. J. (2015). *Ecological statistics: Contemporary theory and application*. Oxford University Press, USA.

Franklin, J. (1995). Predictive vegetation mapping: Geographic modelling of biospatial patterns in relation to environmental gradients. *Progress in Physical Geography: Earth and Environment*, *19*(4), 474–499. https://doi.org/10.1177/030913339501900403

Franklin, J. (2010a). *Mapping species distributions: Spatial inference and prediction*. Cambridge University Press.

Franklin, J. (2010b). Moving beyond static species distribution models in support of conservation biogeography. *Diversity and Distributions*, *16*(3), 321–330. https://doi.org/10.1111/j.1472-4642.2010.00641.x

Franklin, J. F., Lindenmayer, D. B., MacMahon, J. A., McKee, A., Magnusson, J., Perry, D. A., Waide, R., & Foster, D. R. (2000). Threads of continuity: Ecosystem disturbances, biological legacies and ecosystem recovery. *Conservation Biology in Practice*, *1*(1), 8–16. https://doi.org/10.1111/j.1526-4629.2000.tb00155.x

French, N. H., Kasischke, E. S., Hall, R. J., Murphy, K. A., Verbyla, D. L., Hoy, E. E., & Allen, J. L. (2008). Using Landsat data to assess fire and burn severity in the North American boreal forest region: An overview and summary of results. *International Journal of Wildland Fire*, *17*(4), 443–462. https://doi.org/10.1071/WF08007

Fritz, A., Li, L., Storch, I., & Koch, B. (2018). UAV-derived habitat predictors contribute strongly to understanding avian species-habitat relationships on the Eastern Qinghai-Tibetan Plateau. *Remote Sensing in Ecology and Conservation*,

4(1, SI), 53–65. https://doi.org/10.1002/rse2.73

Frolking, S., Palace, M. W., Clark, D., Chambers, J. Q., Shugart, H., & Hurtt, G. C. (2009). Forest disturbance and recovery: A general review in the context of spaceborne remote sensing of impacts on aboveground biomass and canopy structure. *Journal of Geophysical Research: Biogeosciences*, *114*(G2). https://doi.org/10.1029/2008jg000911

Furness, R. W., & Greenwood, J. J. (2013). *Birds as monitors of environmental change*. Springer Science & Business Media.

Gagic, V., Bartomeus, I., Jonsson, T., Taylor, A., Winqvist, C., Fischer, C., Slade, E. M., Steffan-Dewenter, I., Emmerson, M., & Potts, S. G. (2015). Functional identity and diversity of animals predict ecosystem functioning better than species-based indices. *Proceedings of the Royal Society B: Biological Sciences*, *282*(1801), 20142620. https://doi.org/10.1098/rspb.2014.2620

Galetto, L., Torres, C., & Martínez Pastur, G. J. (2019). Variable retention harvesting: Conceptual analysis according to different environmental ethics and forest valuation. *Ecological Processes*, *8*(1). https://doi.org/10.1186/s13717-019-0195-3

García-Feced, C., Tempel, D., Forestry, M. K.-. J. of, & 2011, U. (2011). LiDAR as a tool to characterize wildlife habitat: California spotted owl nesting habitat as an example. *Journal of Forestry*, *109*(8), 436–443. https://academic.oup.com/jof/article-abstract/109/8/436/4598973

Gauthier, S., Bernier, P., Kuuluvainen, T., Shvidenko, A. Z., & Schepaschenko, D. G. (2015). Boreal forest health and global change. *Science*, *349*(6250), 819–822. https://doi.org/10.1126/science.aaa9092

Goetz, S. J., Steinberg, D., Betts, M. G., Holmes, R. T., Doran, P. J., Dubayah, R., & Hofton, M. (2010). Lidar remote sensing variables predict breeding habitat of a Neotropical migrant bird. *Ecology*, *91*(6), 1569–1576. https://doi.org/10.1890/09-1670.1

Goetz, S., Steinberg, D., Dubayah, R., & Blair, B. (2007). Laser remote sensing of canopy habitat heterogeneity as a predictor of bird species richness in an eastern temperate forest, USA. *Remote Sensing of Environment*, *108*(3), 254–263. https://doi.org/10.1016/j.rse.2006.11.016

Golding, N., & Purse, B. V. (2016). Fast and flexible Bayesian species distribution modelling using Gaussian processes. *Methods in Ecology and Evolution*, *7*(5), 598–608. https://doi.org/10.1111/2041-210x.12523

Gomes, V. C. F., Queiroz, G. R., & Ferreira, K. R. (2020). An overview of platforms for big earth observation data management and analysis. *Remote Sensing*, *12*(8). https://doi.org/10.3390/rs12081253

Gomez, C., White, J. C., & Wulder, M. A. (2016). Optical remotely sensed time series data for land cover classification: A review. *ISPRS Journal of Photogrammetry and Remote Sensing*, *116*, 55–72. https://doi.org/10.1016/j.isprsjprs.2016.03.008

Gorelick, N., Hancher, M., Dixon, M., Ilyushchenko, S., Thau, D., & Moore, R. (2017). Google Earth Engine: Planetary-scale geospatial analysis for everyone. *Remote Sensing of Environment*, *202*, 18–27. https://doi.org/10.1016/j.rse.2017.06.031

Gotmark, F., Blomqvist, D., Johansson, O. C., & Bergkvist, J. (1995). Nest Site Selection: A Trade-Off between Concealment and View of the Surroundings? *Journal of Avian Biology*, *26*(4), 305. https://doi.org/10.2307/3677045

Gottschalk, T. K., Ekschmitt, K., & Bairlein, F. (2007). A GIS-based model of Serengeti grassland bird species. *Ostrich*, *78*(2), 259–263. https://doi.org/10.2989/ostrich.2007.78.2.22.102

Gottschalk, T. K., Huettmann, F., & Ehlers, M. (2005). Thirty years of analysing and modelling avian habitat relationships using satellite imagery data: A review. *International Journal of Remote Sensing*, *26*(12), 2631–2656. https://doi.org/10.1080/01431160512331338041

Groot, A., Lussier, J.-M., Mitchell, A., & MacIsaac, D. (2005). A silvicultural systems perspective on changing Canadian forestry practices. *The Forestry Chronicle*, *81*(1), 50–55. https://doi.org/10.5558/tfc81050-1

Guisan, A., & Thuiller, W. (2005). Predicting species distribution: Offering more than simple habitat models. *Ecology Letters*, *8*(9), 993–1009. https://doi.org/10.1111/j.1461-0248.2005.00792.x

Guisan, A., Tingley, R., Baumgartner, J. B., Naujokaitis-Lewis, I., Sutcliffe, P. R., Tulloch, A. I., Regan, T. J., Brotons, L., McDonald-Madden, E., Mantyka-Pringle, C., et al. (2013). Predicting species distributions for conservation decisions. *Ecology Letters*, *16*(12), 1424–1435. https://doi.org/10.1111/ele.12189

Guisan, A., & Zimmermann, N. E. (2000). Predictive habitat distribution models in ecology. *Ecological Modelling*, *135*(2-3), 147–186. https://doi.org/10.1016/s0304-3800(00)00354-9

Gustafsson, L., Baker, S. C., Bauhus, J., Beese, W. J., Brodie, A., Kouki, J., Lindenmayer, D. B., Lõhmus, A., Pastur, G. M., Messier, C., Neyland, M., Palik, B., Sverdrup-Thygeson, A., Volney, W. J. A., Wayne, A., & Franklin, J. F. (2012). Retention Forestry to Maintain Multifunctional Forests: A World Perspective. *BioScience*, *62*(7), 633–645. https://doi.org/10.1525/bio.2012.62.7.6

Gustafsson, L., Kouki, J., & Sverdrup-Thygeson, A. (2010). Tree retention as a conservation measure in clear-cut forests of northern Europe: A review of ecological consequences. *Scandinavian Journal of Forest Research*, *25*(4), 295–308. https://doi.org/10.1080/02827581.2010.497495

Halaj, J., Ross, D., & Moldenke, A. (2000). Importance of habitat structure to the arthropod food-web in Douglas-fir canopies. *Oikos (Copenhagen, Denmark)*, *90*(1), 139–152. https://doi.org/10.1034/j.1600-0706.2000.900114.x

Hall, S. A., Burke, I. C., Box, D. O., Kaufmann, M. R., & Stoker, J. M. (2005). Estimating stand structure using discrete-return lidar: An example from low density, fire prone ponderosa pine forests. *Forest Ecology and Management*, *208*(1-3), 189–209. https://doi.org/10.1016/j.foreco.2004.12.001

Halpern, C. B., Halaj, J., Evans, S. A., & Dov Iak, M. (2012). Level and pattern of overstory retention interact to shape long-term responses of understories to timber harvest. *Ecological Applications*, *22*(8), 2049–2064. https://doi.org/10.1890/12-0299.1

Hannon, S., & Schmiegelow, F. (2002). Corridors may not improve the conservation value of small reserves for most boreal birds. *Ecological Applications*, *12*(5), 1457–1468. https://doi.org/10.1890/1051-0761(2002)012%5B1457:cmnitc%5D2.0.co;2

Hanski, I., Henttonen, H., Korpimäki, E., Oksanen, L., & Turchin, P. (2001). Small-rodent dynamics and predation. *Ecology*, *82*(6), 1505–1520. https://doi.org/10.1890/0012-9658(2001)082%5B1505:srdap%5D2.0.co;2

He, K. S., Bradley, B. A., Cord, A. F., Rocchini, D., Tuanmu, M.-N. N., Schmidtlein, S., Turner, W., Wegmann, M., & Pettorelli, N. (2015). Will remote sensing shape the next generation of species distribution models? *Remote Sensing in Ecology and Conservation*, *1*(1), 4–18. https://doi.org/10.1002/rse2.7

Heithecker, T. D., & Halpern, C. B. (2007). Edge-related gradients in microclimate in forest aggregates following structural retention harvests in western Washington. *Forest Ecology and Management*, *248*(3), 163–173. https://doi.org/10.1016/j.foreco.2007.05.003

Hermosilla, T., Wulder, M. A., White, J. C., & Coops, N. C. (2022). Land cover classification in an era of big and open data: Optimizing localized implementation and training data selection to improve mapping outcomes. *Remote Sensing of Environment*, *268*, 112780. https://doi.org/10.1016/j.rse.2021.112780

Hijmans, R. J. (2020). *Raster: Geographic data analysis and modeling* [Manual]. https://CRAN.R-project.org/package=raster

Hijmans, R. J. (2021). *Raster: Geographic data analysis and modeling* [Manual]. https://CRAN.R-project.org/package=raster

Hill, M. O. (1973). Diversity and evenness: A unifying notation and its consequences.

Ecology, *54*(2), 427–432. https://doi.org/10.2307/1934352

Hill, R. A., & Hinsley, S. A. (2015). Airborne lidar for woodland habitat quality monitoring: Exploring the significance of lidar data characteristics when modelling organism-habitat relationships. *Remote Sensing*, *7*(4), 3446–3466. https://doi.org/10.3390/rs70403446

Hill, R., & Thomson, A. (2005). Mapping woodland species composition and structure using airborne spectral and LiDAR data. *International Journal of Remote Sensing*, *26*(17), 3763–3779. https://doi.org/10.1080/01431160500114706

Hinsley, S. A., Hill, R. A., Bellamy, P. E., & Balzter, H. (2006). The application of lidar in woodland bird ecology: Climate, canopy structure, and habitat quality. *Photogrammetric Engineering and Remote Sensing*, *72*(12), 1399–1406. https://doi.org/10.14358/pers.72.12.1399

Hird, J. N., Kariyeva, J., & McDermid, G. J. (2021). Satellite time series and Google Earth Engine democratize the process of forest-recovery monitoring over large areas. *Remote Sensing*, *13*(23). https://doi.org/10.3390/rs13234745

Hislop, S., Jones, S., Soto-Berelov, M., Skidmore, A., Haywood, A., & Nguyen, T. H. (2018). Using landsat spectral indices in time-series to assess wildfire disturbance and recovery. *Remote Sensing*, *10*(3), 460. https://doi.org/10.3390/rs10030460

Hobson, K. A., & Schieck, J. (1999). Changes in Bird Communities in Boreal Mixedwood Forest: Harvest and Wildfire Effects over 30 Years. *Ecological Applications*, *9*(3), 849–863. https://doi.org/10.1890/1051-0761(1999)009%5B0849:cibcib%5D2.0.co;2

Holbrook, J. D., Vierling, K. T., Vierling, L. A., Hudak, A. T., & Adam, P. (2015). Occupancy of red-naped sapsuckers in a coniferous forest: Using LiDAR to understand effects of vegetation structure and disturbance. *Ecology and Evolution*, *5*(22), 5383–5393. https://doi.org/10.1002/ece3.1768

Hopkins, L. M., Hallman, T. A., Kilbride, J., Robinson, W. D., & Hutchinson, R. A.

(n.d.). A comparison of remotely sensed environmental predictors for avian distributions. *Landscape Ecology*. https://doi.org/10.1007/s10980-022-01406-y

Huber, N., Kienast, F., Ginzler, C., & Pasinelli, G. (2016). Using remote-sensing data to assess habitat selection of a declining passerine at two spatial scales. *Landscape Ecology*, *31*(9), 1919–1937. https://doi.org/10.1007/s10980-016-0370-1

Jaeger, B. (2017). *r2glmm: Computes r squared for mixed (multilevel) models* [Manual]. https://CRAN.R-project.org/package=r2glmm

Kennedy, R. E., Townsend, P. A., Gross, J. E., Cohen, W. B., Bolstad, P., Wang, Y. Q., & Adams, P. (2009). Remote sensing change detection tools for natural resource managers: Understanding concepts and tradeoffs in the design of landscape monitoring projects. *Remote Sensing of Environment*, *113*(7), 1382–1396. https://doi.org/10.1016/j.rse.2008.07.018

Kennedy, R. E., Yang, Z., & Cohen, W. B. (2010). Detecting trends in forest disturbance and recovery using yearly Landsat time series: 1. LandTrendr - Temporal segmentation algorithms. *Remote Sensing of Environment*, *114*(12), 2897–2910. https://doi.org/10.1016/j.rse.2010.07.008

Kennedy, R. E., Yang, Z., Gorelick, N., Braaten, J., Cavalcante, L., Cohen, W. B., & Healey, S. (2018). Implementation of the LandTrendr algorithm on Google Earth Engine. *Remote Sensing*, *10*(5), 691. https://doi.org/10.3390/rs10050691

Kerr, J. T., & Ostrovsky, M. (2003). From space to species: Ecological applications for remote sensing. *Trends in Ecology & Evolution*, *18*(6), 299–305. https://doi.org/10.1016/s0169-5347(03)00071-5

Key, C. H., & Benson, N. C. (2006a). Landscape assessment: Ground measure of severity, the composite burn index; and remote sensing of severity, the normalized burn ratio. *In: Lutes, Duncan C.; Keane, Robert E.; Caratti, John F.; Key, Carl H.; Benson, Nathan C.; Sutherland, Steve; Gangi, Larry J. 2006. FIREMON: Fire Effects Monitoring and Inventory System. Gen. Tech. Rep. RMRS-GTR-164-CD. Fort Collins, CO: US Department of Agriculture, Forest Service, Rocky Mountain Research Station. P. LA-1-55*, *164*.

Key, C., & Benson, N. (2006b). *Landscape assessment: Ground measure of severity, the composite burn index; and remote sensing of severity, the normalized burn ratio*. USDA Forest Service.

Knight, E. C., Sòlymos, P., Scott, C., & Bayne, E. M. (2020). Validation prediction: A flexible protocol to increase efficiency of automated acoustic processing for wildlife research. *Ecological Applications*, *30*(7), e02140. https://doi.org/10.1002/eap.2140

Koma, Z., Seijmonsbergen, A. C., Grootes, M. W., Nattino, F., Groot, J., Sierdsema, H., Foppen, R. P. B., & Kissling, D. (2022). Better together? Assessing different remote sensing products for predicting habitat suitability of wetland birds. *Diversity and Distributions*, *28*(4), 685–699. https://doi.org/10.1111/ddi.13468

Kortmann, M., Heurich, M., Latifi, H., Roesner, S., Seidl, R., Mueller, J., Thorn, S., Rösner, S., Seidl, R., Müller, J., & Thorn, S. (2018). Forest structure following natural disturbances and early succession provides habitat for two avian flagship species, capercaillie (Tetrao urogallus) and hazel grouse (Tetrastes bonasia). *Biological Conservation*, *226*(July), 81–91. https://doi.org/10.1016/j.biocon.2018.07.014

Kosicki, J. Z. (2018). Are landscape configuration metrics worth including when predicting specialist and generalist bird species density? A case of the generalised additive model approach. *Environmental Modeling & Assessment*, *23*, 193–202. https://doi.org/10.1007/s10666-017-9575-1

Kuuluvainen, T., & Gauthier, S. (2018). Young and old forest in the boreal: Critical stages of ecosystem dynamics and management under global change. *Forest Ecosystems*, *5*. https://doi.org/10.1186/s40663-018-0142-2

Laliberté, E., & Legendre, P. (2010). A distancebased framework for measuring functional diversity from multiple traits. *Ecology*, *91*(1), 299–305. https://doi.org/10.1890/08-2244.1

Laliberté, E., Legendre, P., & Shipley, B. (2014). *FD: Measuring functional diversity (FD) from multiple traits, and other tools for functional ecology* [Manual]. https:

//CRAN.R-project.org/package=FD

Lang, N., Jetz, W., Schindler, K., & Wegner, J. D. (2022). A high-resolution canopy height model of the Earth. *arXiv Preprint arXiv:2204.08322*.

Lanner, R. M. (1996). *Made for each other: A symbiosis of birds and pines*. Oxford University Press on Demand.

Lavorel, S., Storkey, J., Bardgett, R. D., De Bello, F., Berg, M. P., Le Roux, X., Moretti, M., Mulder, C., Pakeman, R. J., Díaz, S., et al. (2013). A novel framework for linking functional diversity of plants with other trophic levels for the quantification of ecosystem services. *Journal of Vegetation Science*, *24*(5), 942–948. https://doi.org/10.1111/jvs.12083

Leaver, J., Mulvaney, J., Smith, D. A. E., Smith, Y. C. E., & Cherry, M. I. (2019). Response of bird functional diversity to forest product harvesting in the Eastern Cape, South Africa. *Forest Ecology and Management*, *445*, 82–95. https://doi.org/10.1016/j.foreco.2019.04.054

Leeuwen, M. van, & Nieuwenhuis, M. (2010). Retrieval of forest structural parameters using LiDAR remote sensing. *European Journal of Forest Research*, *129*(4), 749–770. https://doi.org/10.1007/s10342-010-0381-4

Lefsky, M. A., Cohen, W. B., Parker, G. G., Harding, D. J., Parker, G. G., & Harding, D. J. (2002). Lidar remote sensing for ecosystem studies. *BioScience*, *52*(1), 19–30. https://doi.org/10.1641/0006-3568(2002)052%5B0019:lrsfes%5D2.0.co;2

Lelli, C., Bruun, H. H., Chiarucci, A., Donati, D., Frascaroli, F., Fritz, Ö., Goldberg, I., Nascimbene, J., Tøttrup, A. P., Rahbek, C., & Heilmann-Clausen, J. (2018). Biodiversity response to forest structure and management: Comparing species richness, conservation relevant species and functional diversity as metrics in forest conservation. *Forest Ecology and Management*, *432*, 707–707. https://doi.org/10.1016/j.foreco.2018.09.057

Lesak, A. A., Radeloff, V. C., Hawbaker, T. J., Pidgeon, A. M., Gobakken, T., & Contrucci, K. (2011). Modeling forest songbird species richness using LiDAR-

derived measures of forest structure. *Remote Sensing of Environment*, *115*, 2823–2835. https://doi.org/10.1016/j.rse.2011.01.025

Leston, L., Bayne, E., & Schmiegelow, F. (2018). Long-term changes in boreal forest occupancy within regenerating harvest units. *Forest Ecology and Management*, *421*, 40–53. https://doi.org/10.1016/j.foreco.2018.02.029

Leston, L., Bayne, E., Toms, J., Mahon, C., Crosby, A., Sólymos, P., Ball, J., Song, S., Schmiegelow, F., Stralberg, D., et al. (2023). Comparing alternative methods of modelling cumulative effects of oil and gas footprint on boreal bird abundance. *Landscape Ecology*, *38*(1), 147–168. https://doi.org/10.1007/s10980-022-01531-8

Li, H., & Wu, J. (2004). Use and misuse of landscape indices. *Landscape Ecology*, *19*(4), 389–399. https://doi.org/10.1023/b:land.0000030441.15628.d6

Li, X., & Wang, Y. (2013). Applying various algorithms for species distribution modelling. *Integrative Zoology*, *8*(2), 124–135. https://doi.org/10.1111/1749-4877.12000

Lim, K., Treitz, P., Wulder, M., St-Onge, B., & Flood, M. (2003). LiDAR remote sensing of forest structure. *Progress in Physical Geography*, *27*(1), 88–106. https://doi.org/10.1191/0309133303pp360ra

Lindberg, E., Roberge, J. M., Johansson, T., & Hjältén, J. (2015). Can airborne laser scanning (ALS) and forest estimates derived from satellite images be used to predict abundance and species richness of birds and beetles in boreal forest? *Remote Sensing*, *7*(4), 4233–4252. https://doi.org/10.3390/rs70404233

Lindenmayer, D. B., Fischer, J., Felton, A., Montague-Drake, R., D. Manning, A., Simberloff, D., Youngentob, K., Saunders, D., Wilson, D., M. Felton, A., et al. (2007). The complementarity of single-species and ecosystem-oriented research in conservation research. *Oikos (Copenhagen, Denmark)*, *116*(7), 1220–1226.

Lindenmayer, D. B., Franklin, J. F., Lõhmus, A., Baker, S. C., Bauhus, J., Beese, W., Brodie, A., Kiehl, B., Kouki, J., Pastur, G. M., Messier, C., Neyland, M.,

Palik, B., Sverdrup-Thygeson, A., Volney, J., Wayne, A., & Gustafsson, L. (2012). A major shift to the retention approach for forestry can help resolve some global forest sustainability issues. *Conservation Letters*, *5*(6), 421–431. https://doi.org/10.1111/j.1755-263x.2012.00257.x

Lindermayer, D. B., & Franklin, J. F. (2002). *Conserving forest biodiversity: A comprehensive multiscaled approach*. Island Press.

MacArthur, R. H., & MacArthur, J. W. (1961). On bird species diversity. *Ecology*, *42*(3), 594–598. https://doi.org/10.2307/1932254

Mackey, B. G., & Lindenmayer, D. B. (2001). Towards a hierarchical framework for modelling the spatial distribution of animals: Modelling the spatial distribution of animals. *Journal of Biogeography*, *28*(9), 1147–1166. https://doi.org/10.1046/j.1365-2699.2001.00626.x

Mahon, C. L., Holloway, G., Sólymos, P., Cumming, S. G., Bayne, E. M., Schmiegelow, F. K. A., & Song, S. J. (2016). Community structure and niche characteristics of upland and lowland western boreal birds at multiple spatial scales. *Forest Ecology and Management*, *361*, 99–116. https://doi.org/10.1016/j.foreco.2015.11.007

Manly, B. F. J., McDonald, L. L., Thomas, D. L., McDonald, T. L., & Erickson, W. P. (2002). *Resource selection by animals: Statistical design and analysis for field studies*. Springer Science & Business Media. https://doi.org/10.1007/0-306-48151-0

Marquis, R. J., & Whelan, C. J. (1994). Insectivorous birds increase growth of white oak through consumption of leaf-chewing insects. *Ecology*, *75*(7), 2007–2014. https://doi.org/10.2307/1941605

Martinuzzi, S., Vierling, L. A., Gould, W. A., Falkowski, M. J., Evans, J. S., Hudak, A. T., & Vierling, K. T. (2009). Mapping snags and understory shrubs for a LiDAR-based assessment of wildlife habitat suitability. *Remote Sensing of Environment*, *113*(12), 2533–2546. https://doi.org/10.1016/j.rse.2009.07.002

Marvin, D. C., Koh, L. P., Lynam, A. J., Wich, S., Davies, A. B., Krishnamurthy,

R., Stokes, E., Starkey, R., & Asner, G. P. (2016). Integrating technologies for scalable ecology and conservation. *Global Ecology and Conservation*, *7*, 262–275. https://doi.org/10.1016/j.gecco.2016.07.002

Mason, N. W., Mouillot, D., Lee, W. G., & Wilson, J. B. (2005). Functional richness, functional evenness and functional divergence: The primary components of functional diversity. *Oikos*, *111*(1), 112–118. https://doi.org/10.1111/j.0030-1299.2005.13886.x

McCarthy, J. (2001). Gap dynamics of forest trees: A review with particular attention to boreal forests. *Environmental Reviews*, *9*(1), 1–59. https://doi.org/10.1139/a00-012

McGaughey, R. J. (2018). *FUSION/LDV: Software for LIDAR data analysis and Visualization*. United States Department of Agriculture, Pacific Northwest Research Station.

McKinnon, E. A., Stanley, C. Q., & Stutchbury, B. J. (2015). Carry-over effects of nonbreeding habitat on start-to-finish spring migration performance of a songbird. *PLoS One*, *10*(11), e0141580. https://doi.org/10.1371/journal.pone.0141580

Meurant, G. (2012). *The ecology of natural disturbance and patch dynamics*. Academic press.

Meynard, C. N., Devictor, V., Mouillot, D., Thuiller, W., Jiguet, F., & Mouquet, N. (2011). Beyond taxonomic diversity patterns: How do alpha, beta and gamma components of bird functional and phylogenetic diversity respond to environmental gradients across France? *Global Ecology and Biogeography*, *20*(6), 893–903. https://doi.org/10.1111/j.1466-8238.2010.00647.x

Miller, J. D., & Thode, A. E. (2007). Quantifying burn severity in a heterogeneous landscape with a relative version of the delta Normalized Burn Ratio (dNBR). *Remote Sensing of Environment*, *109*(1), 66–80. https://doi.org/10.1016/j.rse.2006.12.006

Mori, A. S., & Kitagawa, R. (2014). Retention forestry as a major paradigm for safeguarding forest biodiversity in productive landscapes: A global meta-analysis. *Biological Conservation*, *175*, 65–73. https://doi.org/10.1016/j.biocon.2014.04.016

Morse, D., & Poole, A. (2020). Black-throated Green Warbler (Setophaga virens), version 1.0. In *Birds of the World (P. G. Rodewald, Editor)* (Vol. 1). Cornell Lab of Ornithology.

Moudrý, V., Moudrá, L., Barták, V., Bejek, V., Gdulová, K., Hendrychová, M., Moravec, D., Musil, P., Rocchini, D., astný, K., Volf, O., & álek, M. (2021). The role of the vegetation structure, primary productivity and senescence derived from airborne LiDAR and hyperspectral data for birds diversity and rarity on a restored site. *Landscape and Urban Planning*, *210*, 104064. https://doi.org/10.1016/j.landurbplan.2021.104064

Mouillot, D., Graham, N. A. J., Bastien Villé Ger, S., Mason, N. W. H., & Bellwood, D. R. (2013a). A functional approach reveals community responses to disturbances. *Trends in Ecology & Evolution*, *28*(3). https://doi.org/10.1016/j.tree.2012.10.004

Mouillot, D., Graham, N. A., Villéger, S., Mason, N. W., & Bellwood, D. R. (2013b). A functional approach reveals community responses to disturbances. *Trends in Ecology & Evolution*, *28*(3), 167–177. https://doi.org/10.1016/j.tree.2012.10.004

Müller, J., Moning, C., Bässler, C., Heurich, M., & Brandl, R. (2009). Using airborne laser scanning to model potential abundance and assemblages of forest passerines. *Basic and Applied Ecology*, *10*(7), 671–681. https://doi.org/10.1016/j.baae.2009.03.004

Müller, J., Stadler, J., Brandl, R., Mueller, J., Stadler, J., & Brandl, R. (2010). Composition versus physiognomy of vegetation as predictors of bird assemblages: The role of lidar. *Remote Sensing of Environment*, *114*(3), 490–495. https://doi.org/10.1016/j.rse.2009.10.006

Nakagawa, S., & Schielzeth, H. (2013). A general and simple method for obtaining R2 from generalized linear mixed-effects models. *Methods in Ecology and Evolution*, *4*(2), 133–142. https://doi.org/10.1111/j.2041-210x.2012.00261.x

Natural Regions Committee. (2006). *Natural regions and subregions of Alberta*. Compiled by DJ Downing; WW Pettapiece. Government of Alberta.

Natural Resources Canada. (2017). *The State of Canada's Forests: Annual Report 2017*.

Neumann, W., Martinuzzi, S., Estes, A. B., Pidgeon, A. M., Dettki, H., Ericsson, G., & Radeloff, V. C. (2015). Opportunities for the application of advanced remotely-sensed data in ecological studies of terrestrial animal movement. *Movement Ecology*, *3*(1), 8. https://doi.org/10.1186/s40462-015-0036-7

Niemi, G., Hanowski, J., Helle, P., Howe, R., Mönkkönen, M., Venier, L., & Welsh, D. (1998). Ecological sustainability of birds in boreal forests. *Conservation Ecology*, *2*(2). https://doi.org/10.5751/es-00079-020217

Nieto, S., Flombaum, P., & Garbulsky, M. F. (2015). Can temporal and spatial NDVI predict regional bird-species richness? *Global Ecology and Conservation*, *3*, 729–735. https://doi.org/10.1016/j.gecco.2015.03.005

Northrup, J. M., Rivers, J. W., Yang, Z., & Betts, M. G. (2019). Synergistic effects of climate and landuse change influence broadscale avian population declines. *Global Change Biology*, *25*(5), 1561–1575. https://doi.org/10.1111/gcb.14571

Norton, M. R., & Hannon, S. J. (1997). Songbird response to partial-cut logging in the boreal mixedwood forest of Alberta. *Canadian Journal of Forest Research*, *27*(1), 44–53. https://doi.org/10.1139/x96-149

Odsen, S. G., Pinzon, J., Schmiegelow, F. K. A., Acorn, J. H., & Spence, J. R. (2018). Boreal songbirds and variable retention management: A 15-year perspective on avian conservation and forestry. *Canadian Journal of Forest Research*, *48*(12), 1495–1502. https://doi.org/10.1139/cjfr-2018-0203

Oksanen, J., Blanchet, F. G., Friendly, M., Kindt, R., Legendre, P., McGlinn, D., Minchin, P. R., O'Hara, R. B., Simpson, G. L., Solymos, P., Stevens, M. H. H., Szoecs, E., & Wagner, H. (2020). *Vegan: Community ecology package* [Manual]. https://CRAN.R-project.org/package=vegan

Paillet, Y., Bergès, L., Hjältén, J., Ódor, P., Avon, C., Bernhardt-Römermann, M., Bijlsma, R.-J., De Bruyn, L., Fuhr, M., Grandin, U., Kanka, R., Lundin, L., Luque, S., Magura, T., Matesanz, S., Mészáros, I., Sebastià, M.-T., Schmidt, W., Standovár, T., ... Virtanen, R. (2009). Biodiversity differences between managed and unmanaged forests: Meta-analysis of species richness in Europe. *Conservation Biology*, *24*(1), 101–112. https://doi.org/10.1111/j.1523-1739.2009.01399.x

Pearson, S. M. (1993). The spatial extent and relative influence of landscape-level factors on wintering bird populations. *Landscape Ecology*, *8*(1), 3–18. https://doi.org/10.1007/bf00129863

Pebesma, E. (2020). *Sf: Simple features for r* [Manual]. https://CRAN.R-project.org/package=sf

Petchey, O. L., & Gaston, K. J. (2006). Functional diversity: Back to basics and looking forward. *Ecology Letters*, *9*(6), 741–758. https://doi.org/10.1111/j.1461-0248.2006.00924.x

Pettorelli, N., Ryan, S., Mueller, T., Bunnefeld, N., Jedrzejewska, B., Lima, M., & Kausrud, K. (2011). The normalized difference vegetation index (NDVI): Unforeseen successes in animal ecology. *Climate Research*, *46*(1), 15–27. https://doi.org/10.3354/cr00936

Phillips, S. J., & Dudík, M. (2008). Modeling of species distributions with Maxent: New extensions and a comprehensive evaluation. *Ecography*, *31*(2), 161–175. https://doi.org/10.1111/j.0906-7590.2008.5203.x

Pickell, P. D., Hermosilla, T., Frazier, R. J., Coops, N. C., & Wulder, M. A. (2016). Forest recovery trends derived from Landsat time series for North American boreal forests. *International Journal of Remote Sensing*, *37*(1), 138–149. https://doi.org/10.1080/2150704x.2015.1126375

Pitocchelli, J. (2020). Mourning Warbler (Geothlypis philadelphia), version 1.0. In *Birds of the World (P. G. Rodewald, Editor)* (Vol. 1). Cornell Lab of Ornithology.

Poulin, J., D'Astous, E., Villard, M., Hejl, S. J., Newlon, K. R., McFadzen, M. E., Young, J. S., & Ghalambor, C. K. (2020). Brown Creeper (Certhia americana), version 1.0. In A. Poole (Ed.), *Birds of the World* (Vol. 1). Cornell Lab of Ornithology.

Price, K., Daust, K., Lilles, E., & Roberts, A. M. (2020). Long-term response of forest bird communities to retention forestry in northern temperate coniferous forests. *Forest Ecology and Management*, *462*. https://doi.org/10.1016/j.foreco.2020.117982

R Core Team. (2020). *R: A language and environment for statistical computing* [Manual]. https://www.R-project.org/

Ralston, J., & Kirchman, J. J. (2013). Predicted range shifts in North American boreal forest birds and the effect of climate change on genetic diversity in blackpoll warblers (Setophaga striata). *Conservation Genetics*, *14*, 543–555. https://doi.org/10.1007/s10592-012-0418-y

Randin, C. F., Ashcroft, M. B., Bolliger, J., Cavender-Bares, J., Coops, N. C., Dullinger, S., Dirnboeck, T., Eckert, S., Ellis, E., Fernandez, N., Giuliani, G., Guisan, A., Jetz, W., Joost, S., Karger, D., Lembrechts, J., Lenoir, J., Luoto, M., Morin, X., ... Payne, D. (2020). Monitoring biodiversity in the Anthropocene using remote sensing in species distribution models. *Remote Sensing of Environment*, *239*. https://doi.org/10.1016/j.rse.2019.111626

Regos, A., Gagne, L., Alcaraz-Segura, D., Honrado, J. P., & Domínguez, J. (2019). Effects of species traits and environmental predictors on performance and transferability of ecological niche models. *Scientific Reports*, *9*(1), 4221. https://doi.org/10.1038/s41598-019-40766-5

Renner, S. C., Suarez-Rubio, M., Kaiser, S., Nieschulze, J., Kalko, E. K. V. V., Tschapka, M., & Jung, K. (2018). Divergent response to forest structure of two mobile vertebrate groups. *Forest Ecology and Management*, *415-416*, 129–138. https://doi.org/10.1016/j.foreco.2018.02.028

Rittenhouse, C. D., Pidgeon, A. M., Albright, T. P., Culbert, P. D., Clayton, M. K., Flather, C. H., Huang, C., Masek, J. G., & Radeloff, V. C. (2010). Avifauna response to hurricanes: Regional changes in community similarity. *Global Change Biology*, *16*(3), 905–917. https://doi.org/10.1111/j.1365-2486.2009.02101.x

Robin, X., Turck, N., Hainard, A., Tiberti, N., Lisacek, F., Sanchez, J.-C., & Müller, M. (2011). pROC: An open-source package for R and S+ to analyze and compare ROC curves. *BMC Bioinformatics*, *12*, 77. https://doi.org/10.1186/1471-2105-12-77

Rose, E. T., Simons, T. R., Klein, R., & McKerrow, A. J. (2016). Normalized burn ratios link fire severity with patterns of avian occurrence. *Landscape Ecology*, *31*(7), 1537–1550. https://doi.org/10.1007/s10980-015-0334-x

Rose, R. A., Byler, D., Eastman, J. R., Fleishman, E., Geller, G., Goetz, S., Guild, L., Hamilton, H., Hansen, M., Headley, R., Hewson, J., Horning, N., Kaplin, B. A., Laporte, N., Leidner, A., Leimgruber, P., Morisette, J., Musinsky, J., Pintea, L., … Wilson, C. (2015). Ten ways remote sensing can contribute to conservation. *Conservation Biology*, *29*(2), 350–359. https://doi.org/10.1111/cobi.12397

Rosenvald, R., & Lohmus, A. (2008). For what, when, and where is green-tree retention better than clear-cutting? A review of the biodiversity aspects. *Forest Ecology and Management*, *255*(1), 1–15. https://doi.org/10.1016/j.foreco.2007.09.016

Roy, C., Michel, N. L., Handel, C. M., Van Wilgenburg, S. L., Burkhalter, J. C., Gurney, K. E. B., Messmer, D. J., Princé, K., Rushing, C. S., Saracco, J. F., Schuster, R., Smith, A. C., Smith, P. A., Sólymos, P., Venier, L. A., & Zuckerberg, B. (2019). Monitoring boreal avian populations: How can we estimate trends and trajectories from noisy data? *Avian Conservation and Ecology*, *14*(2), art8. https://doi.org/10.5751/ace-01397-140208

RS-eco. (2021). *Traitdata: Easy access to various ecological trait data* [Manual]. https://github.com/RS-eco/traitdata

Russell, R. E., Saab, V. A., & Dudley, J. G. (2007). Habitat-suitability models

for cavity-nesting birds in a postfire landscape. *Journal of Wildlife Management*, *71*(8), 2600–2611. https://doi.org/10.2193/2007-034

Schaffer-Smith, D., Swenson, J. J., Reiter, M. E., & Isola, J. E. (2018). Quantifying shorebird habitat in managed wetlands by modeling shallow water depth dynamics. *Ecological Applications*, *28*(6), 1534–1545. https://doi.org/10.1002/eap.1732

Schieck, J., & Song, S. J. (2006). Changes in bird communities throughout succession following fire and harvest in boreal forests of western North America: Literature review and meta-analyses. *Canadian Journal of Forest Research*, *36*(5), 1299–1318. https://doi.org/10.1139/x06-017

Schmiegelow, F. K., Machtans, C., & Hannon, S. (1997). Are boreal birds resilient to forest fragmentation? An experimental study of short-term community responses. *Ecology*, *78*(786), 1914–1932. https://doi.org/10.1890/0012-9658(1997)078%5B1914:abbrtf%5D2.0.co;2

Schultz, M., Clevers, J. G., Carter, S., Verbesselt, J., Avitabile, V., Quang, H. V., & Herold, M. (2016). Performance of vegetation indices from Landsat time series in deforestation monitoring. *International Journal of Applied Earth Observation and Geoinformation*, *52*, 318–327. https://doi.org/10.1016/j.jag.2016.06.020

Seavy, N. E., Viers, J. H., & Wood, J. K. (2009). Riparian bird response to vegetation structure: A multiscale analysis using LiDAR measurements of canopy height. *Ecological Applications*, *19*(7), 1848–1857. https://doi.org/10.1890/08-1124.1

Seoane, J., Bustamante, J., & Daz-Delgado, R. (2004). Are existing vegetation maps adequate to predict bird distributions? *Ecological Modelling*, *175*(2), 137–149. https://doi.org/10.1016/j.ecolmodel.2003.10.011

Serrouya, R., & D'Eon, R. (2004). Variable retention forest harvesting: Research synthesis and implementation guidelines. *Sustainable Forest Management Network*.

Sheeren, D., Bonthoux, S., & Balent, G. (2014). Modeling bird communities using unclassified remote sensing imagery: Effects of the spatial resolution and data period. *Ecological Indicators*, *43*, 69–82. https://doi.org/10.1016/j.ecol

ind.2014.02.023

Sherry, T., Holmes, R., Pyle, P., Patten, M., & Rodewald, P. (2020). American redstart (setophaga ruticilla), version 1.0. In *Birds of the World (P. G. Rodewald, Editor)* (Vol. 1). Cornell Lab of Ornithology.

Shirley, S. M., Yang, Z., Hutchinson, R. A., Alexander, J. D., Mcgarigal, K., & Betts, M. G. (2013). Species distribution modelling for the people: Unclassified landsat TM imagery predicts bird occurrence at fine resolutions. *Diversity and Distributions*, *19*, 855–866. https://doi.org/10.1111/ddi.12093

Shmueli, G. (2010). To explain or to predict? *Statistical Science*, *25*(3), 289–310. https://doi.org/10.1214/10-STS330

Simonson, W. D., Allen, H. D., & Coomes, D. A. (2014). Applications of airborne lidar for the assessment of animal species diversity. *Methods in Ecology and Evolution*, *5*(8), 719–729. https://doi.org/10.1111/2041-210x.12219

Sitters, H., Christie, F., Di Stefano, J., Swan, M., Collins, P., & York, A. (2014). Associations between occupancy and habitat structure can predict avian responses to disturbance: Implications for conservation management. *Forest Ecology and Management*, *331*, 227–236. https://doi.org/10.1016/j.foreco.2014.08.013

Skidmore, A. K. (1990). Terrain position as mapped from a gridded digital elevation model. *International Journal of Geographical Information Systems*, *4*(1), 33–49. https://doi.org/10.1080/02693799008941527

Sólymos, P., Matsuoka, S. M., Bayne, E. M., Lele, S. R., Fontaine, P., Cumming, S. G., Stralberg, D., Schmiegelow, F. K. A., & Song, S. J. (2013). Calibrating indices of avian density from non-standardized survey data: Making the most of a messy situation. *Methods in Ecology and Evolution*, *4*(11), 1047–1058. https://doi.org/10.1111/2041-210x.12106

Stralberg, D., Matsuoka, S., Hamann, A., Bayne, E., Sólymos, P., Schmiegelow, F., Wang, X., Cumming, S., & Song, S. (2015). Projecting boreal bird responses to climate change: The signal exceeds the noise. *Ecological Applications*, *25*(1),

52–69. https://doi.org/10.1890/13-2289.1

Survey, U. S. G. (2018). *Landsat 4-7 Surface Reflectance (Ledaps) Product Guide*. Department of the Interior, U.S. Geological Survey.

Swanson, M. E., Franklin, J. F., Beschta, R. L., Crisafulli, C. M., DellaSala, D. A., Hutto, R. L., Lindenmayer, D. B., & Swanson, F. J. (2011). The forgotten stage of forest succession: Early-successional ecosystems on forest sites. *Frontiers in Ecology and the Environment*, *9*(2), 117–125. https://doi.org/10.1890/090157

Swatantran, A., Dubayah, R., Goetz, S., Hofton, M., Betts, M. G., Sun, M., Simard, M., & Holmes, R. (2012). Mapping migratory bird prevalence using remote sensing data fusion. *PLoS ONE*, *7*(1). https://doi.org/10.1371/journal.pone.0028922

Syphard, A. D., & Franklin, J. (2009). Differences in spatial predictions among species distribution modeling methods vary with species traits and environmental predictors. *Ecography*, *32*(6), 907–918. https://doi.org/10.1111/j.1600-0587.2009.05883.x

Tattoni, C., Rizzolli, F., & Pedrini, P. (2012). Can LiDAR data improve bird habitat suitability models? *Ecological Modelling*, *245*(October), 103–110. https://doi.org/10.1016/j.ecolmodel.2012.03.020

Tewkesbury, A. P., Comber, A. J., Tate, N. J., Lamb, A., & Fisher, P. F. (2015). A critical synthesis of remotely sensed optical image change detection techniques. *Remote Sensing of Environment*, *160*, 1–14. https://doi.org/10.1016/j.rse.2015.01.006

Tews, J., Brose, U., Grimm, V., Tielbörger, K., Wichmann, M. C., Schwager, M., & Jeltsch, F. (2004). Animal species diversity driven by habitat heterogeneity/diversity: The importance of keystone structures. *Journal of Biogeography*, *31*(1), 79–92. https://doi.org/10.1046/j.0305-0270.2003.00994.x

Thuiller, W., Araujo, M., & Lavorel, S. (2004). Do we need land-cover data to model species distributions in Europe? *Journal of Biogeography*, *31*(3), 353–361. https:

//doi.org/10.1046/j.0305-0270.2003.00991.x

Turner, W., Spector, S., Gardiner, N., Fladeland, M., Sterling, E., & Steininger, M. (2003). Remote sensing for biodiversity science and conservation. *Trends in Ecology and Evolution*, *18*(6), 306–314. https://doi.org/10.1016/s0169-5347(03)00070-3

Twedt, D. J. (2020). Influence of forest harvest severity and time since perturbation on conservation of North American birds. *Forest Ecology and Management*, *458*, 117742. https://doi.org/10.1016/j.foreco.2019.117742

USGS. (2020). *Landsat normalized difference vegetation index*. https://www.usgs.gov/land-resources/nli/landsat/landsat-normalized-difference-vegetation-index?qt-science_support_page_related_con=0#qt-science_support_page_related_con

Valbuena, R., O'Connor, B., Zellweger, F., Simonson, W., Vihervaara, P., Maltamo, M., Silva, C. A., Almeida, D. R., Danks, F., & Morsdorf, F. (2020). Standardizing ecosystem morphological traits from 3D information sources. *Trends in Ecology & Evolution*, *35*(8), 656–667. https://doi.org/10.1016/j.tree.2020.03.006

Van Balen, J. H. (1973). A comparative sudy of the breeding ecology of the great tit Parus major in different habitats. *Ardea*, *55*(1–2), 1–93.

Vanagas, G. (2004). Receiver operating characteristic curves and comparison of cardiac surgery risk stratification systems. *Interactive CardioVascular and Thoracic Surgery*, *3*(2), 319–322. https://doi.org/10.1016/j.icvts.2004.01.008

Vanderwell, M. C., Malcolm, J. R., & Mills, S. C. (2007). A meta-analysis of bird responses to uniform partial harvesting across North America. *Conservation Biology*, *21*(5), 1230–1240. https://doi.org/10.1111/j.1523-1739.2007.00756.x

Vaughn, I. P., & Ormerod, S. J. (2003). Improving the quality of distribution models for conservation by addressing shortcomings in the field collection of training data. *Conservation Biology*, *17*(6), 1601–1611. https://doi.org/10.1111/j.1523-1739.2003.00359.x

Venier, L. A., Dalley, K., Goulet, P., Mills, S., Pitt, D., Cowcill, K., Pitta, D., & Cowcill, K. (2015). Benefits of aggregate green tree retention to boreal forest birds. *Forest Ecology and Management*, *343*, 80–87. https://doi.org/10.1016/j.foreco.2015.01.024

Venier, L. A., Thompson, I. D., Fleming, R., Malcolm, J., Aubin, I., Trofymow, J. A., Langor, D., Sturrock, R., Patry, C., Outerbridge, R. O., Holmes, S. B., Haeussler, S., Grandpré, L. D., Chen, H. Y. H., Bayne, E., De Grandpré, L., Chen, H. Y. H., Bayne, E., Arsenault, A., & Brandt, J. P. (2014). Effects of natural resource development on the terrestrial biodiversity of Canadian boreal forests. *Environmental Reviews*, *22*(4), 457–490. https://doi.org/10.1139/er-2013-0075

Venier, L., & Pearce, J. (2007). Boreal forest landbirds in relation to forest composition, structure, and landscape: Implications for forest management. *Canadian Journal of Forest Research*, *37*(7), 1214–1226. https://doi.org/10.1139/x07-025

Venier, L., Pearce, J., Fillman, D., McNicol, D., & Welsh, D. (2009). Effects of spruce budworm (Choristoneura fumiferana (Clem.)) outbreaks on boreal mixed-wood bird communities. *Avian Conservation and Ecology*, *4*(1). https://doi.org/10.5751/ace-00296-040103

Veraverbeke, S., Harris, S., & Hook, S. (2011). Evaluating spectral indices for burned area discrimination using MODIS/ASTER (MASTER) airborne simulator data. *Remote Sensing of Environment*, *115*(10), 2702–2709. https://doi.org/10.1016/j.rse.2011.06.010

Veraverbeke, S., Lhermitte, S., Verstraeten, W. W., & Goossens, R. (2012). Evaluation of pre/post-fire differenced spectral indices for assessing burn severity in a Mediterranean environment with Landsat Thematic Mapper. *International Journal of Remote Sensing*, *32*(12), 3521–3537. https://doi.org/10.1080/01431161003752430

Verbesselt, J., Hyndman, R., Newnham, G., & Culvenor, D. (2010). Detecting trend and seasonal changes in satellite image time series. *Remote Sensing of Environment*, *114*(1), 106–115. https://doi.org/10.1016/j.rse.2009.08.014

Vernier, P. R., Schmiegelow, P. K. A., & Cumming, S. G. (2002). Modeling bird abundance from forest inventory data in the boreal mixed-wood forests of Canada. *Predicting Species Occurrences: Issues of Accuracy and Scale*, 559–571\r868.

Vierling, K. T., Swift, C. E., Hudak, A. T., Vogeler, J. C., & Vierling, L. A. (2014). How much does the time lag between wildlife field-data collection and LiDAR-data acquisition matter for studies of animal distributions? A case study using bird communities. *Remote Sensing Letters*, *5*(2), 185–193. https://doi.org/10.1080/2150704x.2014.891773

Vierling, K. T., Vierling, L. A., Gould, W. A., Martinuzzi, S., & Clawges, R. M. (2008). Lidar: Shedding new light on habitat characterization and modeling. *Frontiers in Ecology and the Environment*, *6*(2), 90–98. https://doi.org/10.1890/070001

Villeger, S., Mason, N. W. H., & Mouillot, D. (2008). New multidimensional functional diversity indices for a multifaceted framework in functional ecology. *Ecology*, *89*(8), 2290–2301. https://doi.org/10.1890/07-1206.1

Virkkala, R., & Lehikoinen, A. (2014). Patterns of climate-induced density shifts of species: Poleward shifts faster in northern boreal birds than in southern birds. *Global Change Biology*, *20*(10), 2995–3003. https://doi.org/10.1111/gcb.12573

Vogeler, J. C. J. C., Hudak, A. T. A. T., Vierling, L. a. L. A., Evans, J., Green, P., & Vierling, K. T. K. T. (2014). Terrain and vegetation structural influences on local avian species richness in two mixed-conifer forests. *Remote Sensing of Environment*, *147*, 13–22. https://doi.org/10.1016/j.rse.2014.02.006

Vogeler, J. C., Hudak, A. T., Vierling, L. A., & Vierling, K. T. (2013). Lidar-Derived Canopy Architecture Predicts Brown Creeper Occupancy of Two Western Coniferous Forests. *The Condor*, *115*(3), 614–622. https://doi.org/10.1525/cond.2013.110082

Weisberg, P. J., Dilts, T. E., Becker, M. E., Young, J. S., Wong-Kone, D. C., Newton, W. E., & Ammon, E. M. (2014). Guild-specific responses of avian species richness to LiDAR-derived habitat heterogeneity. *Acta Oecologica*, *59*, 72–83. https://

doi.org/10.1016/j.actao.2014.06.002

White, B., Ogilvie, J., Campbell, D. M. H., Hiltz, D., Gauthier, B., Chisholm, H. K., Wen, H. K., Murphy, P. N. C., & Arp, P. A. (2012). Using the cartographic depth-to-water index to locate small streams and associated wet areas across landscapes. *Canadian Water Resources Journal*, *37*(4), 333–347. https://doi.org/10.4296/cwrj2011-909

White, J. C., Saarinen, N., Kankare, V., Wulder, M. A., Hermosilla, T., Coops, N. C., Pickell, P. D., Holopainen, M., Hyyppä, J., & Vastaranta, M. (2018). Confirmation of post-harvest spectral recovery from Landsat time series using measures of forest cover and height derived from airborne laser scanning data. *Remote Sensing of Environment*, *216*, 262–275. https://doi.org/10.1016/j.rse.2018.07.004

Wilman, H., Belmaker, J., Simpson, J., Rosa, C. de la, Rivadeneira, M. M., & Jetz, W. (2014). EltonTraits 1.0: Species-level foraging attributes of the world's birds and mammals. *Ecology*, *95*(7), 2027–2027. https://doi.org/10.1890/13-1917.1

Wilson, S. J., & Bayne, E. M. (2018). Use of an acoustic location system to understand how presence of conspecifics and canopy cover influence Ovenbird (Seiurus aurocapilla) space use near reclaimed wellsites in the boreal forest of Alberta. *Avian Conservation & Ecology*, *13*(2). https://doi.org/10.5751/ACE-01248-130204

Wulder, M. A., White, J. C., Goward, S. N., Masek, J. G., Irons, J. R., Herold, M., Cohen, W. B., Loveland, T. R., & Woodcock, C. E. (2008). Landsat continuity: Issues and opportunities for land cover monitoring. *Remote Sensing of Environment*, *112*(3), 955–969. https://doi.org/10.1016/j.rse.2007.07.004

Wulder, M. A., White, J. C., Nelson, R. F., Næsset, E., Ørka, H. O., Coops, N. C., Hilker, T., Bater, C. W., & Gobakken, T. (2012). Lidar sampling for large-area forest characterization: A review. *Remote Sensing of Environment*, *121*, 196–209. https://doi.org/10.1016/j.rse.2012.02.001

Yip, D. A., Knight, E. C., HaaveAudet, E., Wilson, S. J., Charchuk, C., Scott, C. D., Sólymos, P., & Bayne, E. M. (2019). Sound level measurements from audio recordings provide objective distance estimates for distance sampling wildlife

populations. *Remote Sensing in Ecology and Conservation*, rse2.118. https://doi.org/10.1002/rse2.118

Zellweger, F., Morsdorf, F., Purves, R. S., Braunisch, V., & Bollmann, K. (2014). Improved methods for measuring forest landscape structure: LiDAR complements field-based habitat assessment. *Biodiversity and Conservation*, *23*(2), 289–307. https://doi.org/10.1007/s10531-013-0600-7

Zhu, Z. (2017). Change detection using landsat time series: A review of frequencies, preprocessing, algorithms, and applications. *ISPRS Journal of Photogrammetry and Remote Sensing*, *130*, 370–384. https://doi.org/10.1016/j.isprsjprs.2017.06.013

Zhu, Z., & Woodcock, C. E. (2014). Continuous change detection and classification of land cover using all available Landsat data. *Remote Sensing of Environment*, *144*, 152–171. https://doi.org/10.1016/j.rse.2014.01.011

Zielewska-Buettner, K., Heurich, M., Mueller, J., & Braunisch, V. (2018). Remotely sensed single tree data enable the determination of habitat thresholds for the three-toed woodpecker (Picoides tridactylus). *Remote Sensing*, *10*(12). https://doi.org/10.3390/rs10121972